Humboldt-Universität zu Berlin

Dissertation

The Hippocampal Mossy Fiber Synapse: Transmission, Modulation and Plasticity

Zur Erlangung des akademischen Grades

doctor rerum naturalium

im Fach Biologie

Mathematisch-Naturwissenschaftliche Fakultät I

Frau Dipl.-Biol. Anja Gundlfinger

geboren am 11. Juni 1976 in Aachen

Dekan: Prof. Dr. Christian Limberg

Gutachter: 1. Prof. Dr. Andreas V.M. Herz

2. Prof. Dr. Dietmar Schmitz

3. Prof. Dr. Andreas Draguhn

eingereicht: 22. Oktober 2007

Datum der Promotion: 3. April 2008

Zusammenfassung

Synapsen sind die spezialisierten subzellulären Kontaktstellen im Gehirn, die die Kommunikation zwischen einzelnen Nervenzellen, den Neuronen, auf elektrischem oder chemischem Weg ermöglichen. Anatomisch und physiologisch sind Synapsen jedoch erstaunlich divers, unter anderem abhängig von der untersuchten Hirnregion, der Identität der prä- und postsynaptischen Neurone, den präsynaptisch ausgeschütteten Neurotransmittern und postsynaptischen Rezeptorsystemen. Generell kann die Effektivität oder Stärke synaptischer Übertragung durch unterschiedliche Mechanismen beeinflusst werden. Hier werden nun Mechanismen, Ausprägung und funktionelle Relevanz von Neuromodulation, Kurzzeit- und Langzeit-Plastizität der Stärke der synaptischen Übertragung an der hippokampalen Moosfaser-Synapse erarbeitet. Die vorgestellten Daten konnten mit Hilfe von *in vitro* experimentellen Ansätzen an der hippokampalen Formation von Mäusen gewonnen werden und durch Analysen und Simulationen aus dem Bereich der theoretischen Biologie bestätigt und erweitert werden.

Abstract

Chemical synapses are key elements for the communication between nerve cells. This communication can be regulated on various time scales and through different mechanisms affecting synaptic transmission. Amongst these are slow and long-lasting adjustments by endogenous neuromodulators, instantaneous and reversible activity-dependent regulation by short-term plasticity and persistent activity-dependent changes by long-term plasticity. Within this thesis, we have investigated several aspects of modulation of synaptic transmission and its functional relevance at the example of the hippocampal mossy fiber synapse. The presented results were acquired through electrophysiological and microfluorometric experiments at the hippocampal formation of mice and could be verified and substantiated through theoretical analyses, simulations and computational modelling.

Schlagwörter:

Hippokampus, Moosfaser-Synapse, Neuromodulation, Plastizität

Keywords:

Hippocampus, Mossy Fiber Synapse, Neuromodulation, Plasticity

Table of Contents

About this Thesis

Seahorses (genus Hippocampus) are unique members of the class of ray-finned fish. The male and female form a strong monogamous relation, where the male stays in their home territory pregnant with their eggs, while the female wanders freely around. Hippocampi do not look like other fish either, a feature which they owe their catching name from (after the Greek hippo, horse, and kampos, sea monster, worm). The following question has therefore arisen amongst ichthyologists: What can we learn about fish in general by studying the highly specialized genus of seahorses as a model system?

The mammalian hippocampus is the seat of learning and memory formation. This unique subcortical network structure is highly conserved throughout the mammalian species with specialized synaptic connections from one cellular stage to the other. From early on, neuroscientists were eager to use the hippocampal formation and its synaptic systems as a model system for studying a panoply of crucial topics, ranging from basic synaptic physiology up to behavioral task solving. Still, the question remains the same as in fish hippocampi: What can we learn about principles of synaptic transmission, its plasticity and functioning, from studying the highly specialized hippocampal formation?

Synapses are not mere relay stations but remarkably diverse. This diversity is partially based on numerous mechanisms to regulate and alter the efficacy of synaptic communication. The functional role of a synaptic connection between two cell types in a neuronal network will, however, crucially be dependent on its physiological characteristics. And the same holds true for the relevance of the network as a whole. We should thus turn the initial, critical question around and make it a strong and positive demand: We do need to study the intricate and specialized details of all the underlying substructures (including its synapses) before being able to comprehensively learn about the function of a larger neuronal network. In the course of this thesis, the reader will therefore gradually be guided through different aspects of synaptic functioning at the example of the hippocampal mossy fiber onto CA3 pyramidal cell synapse. We will cover topics from presynaptic regulation of transmission, over the relation of temporal presynaptic input to postsynaptic response amplitude distributions, to finally the functional role of short-term plasticity of synaptic efficacy. The level of investigation will also gradually evolve from subcellular mechanisms, over cellular plasticity to a network phenomenon.

As an introduction, Chapter 1 will begin the excursion with a broad overview of general working principles of chemical synaptic transmission in the central nervous system. Common morphological and physiological properties of synapses will be highlighted, followed by means and phenomenology of modulation of synaptic transmission on various timescales.

In Chapter 2, we will present the hippocampal mossy fiber synapse onto CA3 pyramidal cells and elucidate its most distinguished morphological and physiological features. Basic principles of mossy fiber synaptic transmission, its modulation and plasticity are discussed.

Chemical transmission at the hippocampal mossy fiber synapse is regulated by a variety of neuromodulatory systems, including adenosine. In Chapter 3, the intracellular mechanism underlying adenosine-mediated inhibition of synaptic transmission will be covered. Using electrophysiological and optical recording techniques, we will present the

signalling cascade from adenosine receptor activation downstream towards modulation of transmitter release.

Adenosine-mediated inhibition of transmission mediates a low basal probability of transmitter release at mossy fiber synapses, leading to large short-term plasticity of synaptic response amplitudes. In Chapter 4, this remarkable short-term plasticity will be described using experimental and modelling techniques. With this combined approach, we will also investigate the interdependence of short- and long-term plasticity of mossy fiber synaptic responses.

Short-term plasticity of synaptic transmission results in dynamical modulation of postsynaptic response amplitudes. In Chapter 5, the relation between such dynamical modulation of synaptic currents and the action potential output sequence of neurons is investigated. We will introduce a mechanism how short-term synaptic plasticity in combination with subthreshold membrane potential oscillations can generate a temporal spike code. Technical and methodological details are finally summarized in the Appendices.

1 Synapses - Communication Between Neurons

Synapses are key elements for signal transduction and plasticity in the brain. They are specialized structures, which chemically or electrically connect neurons in the central nervous system. In the human brain, there are about 10^{15} synapses, allowing for communication between the roughly 10^{12} neurons in a diverse and specific manner. Over the course of the last century, the peculiar anatomy and physiology of the manifold types of synapses in the brain have been extensively studied and described. These distinct modes of action of synapses throughout the central nervous system and the possibility of dynamically modulating them provide the basis for a variety of computational properties found in neuronal networks.

In this Chapter, we will introduce the general working principles of chemical synapses. We will start with a historical introduction into how the concept of synapses as we know it today has evolved over several decades. Then we will present common morphological and physiological properties of synapses in the central nervous system, followed by means and phenomenology of modulation of synaptic transmission on various timescales. This introductory Chapter will give the reader the necessary conceptual background for the following more detailed approaches to study synaptic properties in the rest of this thesis.

1.1 How the Synapse Became a Synapse

It has not always been clear that nerve cells are independent elements, which communicate with each other through specialized structures, the synapses. In the second half of the 19th century there was a vigorous debate between proponents of the reticular theory, who believed that neurons built up a continuous syncytium, interconnected by protoplasmic bridges, and those who thought of neurons as independent units, which transfer information by a means distinct from direct electrical propagation. As early as 1856, Claude Bernard demonstrated that the toxin curare, commonly used as dart poison, causes muscle paralysis not by direct action on the muscle but on the nerve fiber. Hence, there seemed to be a physiological cleft between nerve and effector cell.

Anatomically, this controversially discussed hypothesis could not readily be confirmed. After having developed a new impregnation technique to visualize individual neurons, today known as the ‘Golgi stain’, Camillo Golgi set new standards in describing different types of nerve cells in 1886. His morphological data, however, still left room for interpreting the nature of the finest neuronal processes and he joined the reticularist camp arguing for direct cytoplasmic connections between neighboring nerve cells. It was on Ramón y Cajal to lead neuroscience to its modern view. Using Golgi’s technique, he vigorously studied manifold nervous structures, including cerebellar stellate and Purkinje cells, and finally proposed a first version of the Neuron Doctrine in 1889, stating that

nerve cells are independent elements[1] . In the end, both Golgi and Cajal were awarded the Nobel Prize for Medicine or Physiology in 1906 for the development of the novel staining technique (Golgi) and utilizing it to perfection for the description of different nerve cell types (Cajal). Even in his acceptance speech, Golgi still defended the reticular theory, while Cajal put forward the today accepted neuron doctrine. Not until the development of electron microscopical techniques to visualize the separated neuronal structures, however, could this controversy finally be resolved.

Following Cajal's example, other neuroanatomists confirmed his basic findings and subsequently introduced the basic terminology for nerve cells and their structural properties that is still in use today. Nerve cells were recognized under the cell theory and named neurons. The shorter and largely branched processes from the cell body were referred to as dendrites, the longer fibers were called axons. Based on his earlier studies on spinal reflexes, the neurophysiologist Charles Sherrington in 1897 proposed that if sensory nerves terminate in free endings, as shown by Cajal, these endings must be associated with activity transfer and its properties (Sherrington, 97). He then was the first to suggest the nomenclature synapse, to describe these free endings between nerve cell and their target structure [2]. His proposal combined the anatomical and functional relevance of the synaptic structures. Owing to his systemic approach, Sherrington also provided the conceptual basis for interpreting synaptic contacts as the crucial building blocks for understanding neural mechanisms underlying behavior.

Over the following decades, many of the details of synaptic transmission could be unravelled by numerous neuroscientists, including several recipients of the Nobel Prize for Physiology or Medicine, whose work can be related to work on synaptic systems: Charles Sherrington (1932) as the founding father of the terminology of synapses; Henry Dale and Otto Loewi (1936) for their work on the requirement of neurotransmitters in the transmission of nerve impulses; John Eccles, who had been a student of Charles Sherrington, together with Alan Hodgkin and Andrew Huxley (1963) for the discovery of the ionic mechanisms of inhibition and excitation along nerves; Bernard Katz, Ulf von Euler and Julius Axelrod (1970) for their groundbreaking work on neurotransmitters. Finally, Bert Sakmann and Erwin Neher were awarded the Nobel Prize for their development of a technical breakthrough for studying nervous functioning, the Patch-Clamp method (1991). To date, patch-clamp recordings have become one of the most-used techniques for studying electrophysiologically single-cell properties and evoked synaptic responses.

All of these achievements helped advancing our knowledge of the composition and functioning of synapses to the picture we have today. Interestingly, the century-old controversy on whether neurons are independent units or are also electrically connected

---

[1] The German neuroanatomist von Waldeyer-Hartz is sometimes also credited with formulating the Neuron Doctrine, although he did not contribute personal observations in this research area (Guillery, 05), much to Cajal's annoyance.

[2] More accurately, it was one of Sherrington's students, John Fulton, who proposed the term *synapse* from *syn*, together, and *haptein*, to fasten, as opposed to Sherrington's original suggestion *syndesm*. Fulton had consulted a friend of his, Pace Verrall, who, being a Euripidean scholar, found *synapse* to be more appropriate as it more actively describes the functional connection between cells and yields a better adjectival form. Sherrington, however, is always cited as the originator of the term synapse, since it first appeared in his chapter on the nervous system in a newly edited version of the ‚Textbook of Physiology' (Shepherd und Erulkar, 97).

has over the years been challenged again. While at the beginning of the modern neuroscience aera, believers in Cajal and therefore later also in the sole existence of chemical synapses were in the lead, the discovery and description of electrical synapses also proved the other side to be correct. In the following, however, we will restrict our presentation of the basic concepts of the current understanding of synapses on chemical synaptic transmission. To this end, we will first elucidate what a basic chemical synapse is composed of and how it can be described, both at an anatomical level as well as at a functional and physiological level.

1.2 Chemical Synaptic Transmission

The patterns of cellular connections found in the central nervous system are highly complex. Some neurons make contacts with neurons nearby, while others project their axons into rather distant regions. This diversity in network structure is also reflected in the morphology and physiology of synapses. The basic synaptic unit, however, consists of the following features.

1.2.1 Synapse Morphology

Anatomically, a synaptic complex is composed of a presynaptic end terminal or an en passant bouton, and the postsynaptic target, which can be the cell body, a dendritic structure or even the axon of a neuron (Figure 1A). An axon terminal can be as large as 7-8 µm (Calyx of Held giant synapse), but most are between 1 and 2 µm in diameter. All presynaptic terminals contain almost the same structural elements, including endoplasmic reticulum, mitochondria, synaptic and other vesicles, and thickened membrane specializations at the apposition zone between the pre- and postsynaptic membrane termed active zones. Presynaptically, they consist of protein complexes that are associated with the transmitter release machinery at the release sites. Postsynaptically, the target membrane also appears to be thickened with an electron-dense substance adhering to it including the neurotransmitter receptors, called the postsynaptic density (PSD). The presynaptic and postsynaptic cell membranes are separated by a space called the synaptic cleft. Typically, the synaptic cleft is wider (~20-40 nm) than the adjacent intercellular space and continuous with the extracellular fluid. More recently, the role of neighboring glial cells in synaptic transmission has been highlighted, for instance in removal of neurotransmitter from the synaptic cleft. These advances point to a ‘tripartite’ synapse, consisting of the presynapse, postsynapse and glia cells (Rollenhagen und Lubke, 06).

1.2.2 Synapse Physiology

Chemical synaptic transmission can be broken down into the following steps (Figure 1B): Incoming action potentials into the presynaptic terminal trigger the influx of calcium through voltage-dependent calcium channels, mostly N- and P/Q-type. This calcium influx will then activate intracellular calcium sensors, which induce the exocytosis of vesicles, leading to the spread of neurotransmitter into the synaptic cleft. On the postsynaptic side, the neurotransmitter then binds to specific neurotransmitter receptor systems, leading to the opening of ion channels and influx of charge-carrying ions. These in the end induce the postsynaptically detectable hyper- or depolarizing deflections of the neuronal membrane potential (Jessell und Kandel, 93).

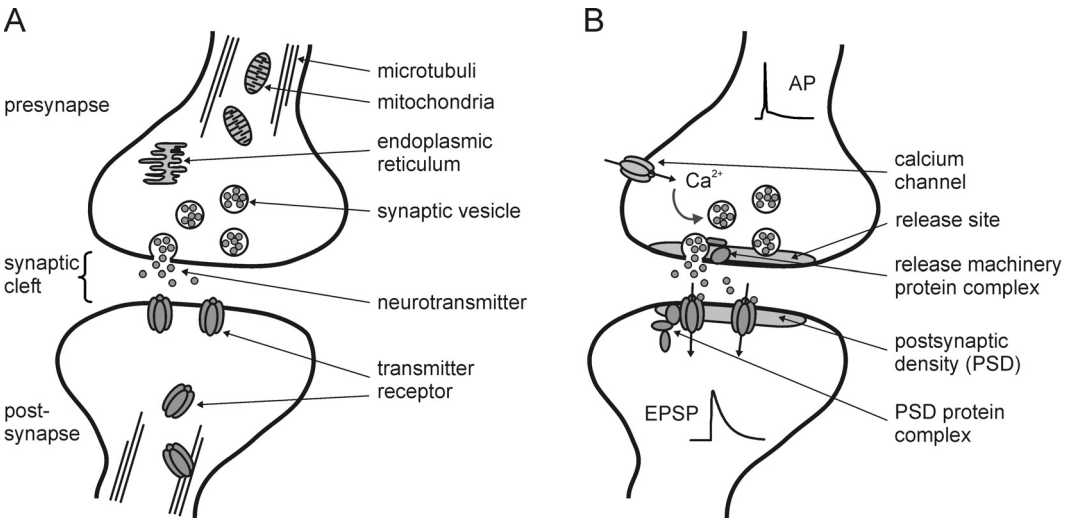

Figure 1: Scheme of the anatomy of a basic synaptic unit and the physiology of synaptic transmission. (A) Synapses are subdivided into presynapse, synaptic cleft and postsynapse. Presynaptically, neurotransmitter is released from vesicles at release sites into the synaptic cleft. Several types of synaptic vesicles may be detectable in synaptic terminals. Postsynaptically, neurotransmitter binds at transmitter receptors. (B) Upon cellular activity, an action potential invades the presynaptic terminal leading to activation of voltage-dependent calcium channels. Inflowing calcium will trigger docking of primed vesicles to the release machinery protein complex. Neurotransmitter is released from the vesicles into the synaptic cleft and postsynaptically binds to its respective receptors. This triggers opening of conductances which translates the chemical signal back into an electrical signal.

Neurotransmitter exert either excitatory or inhibitory effects in the postsynaptic cell. In general, excitatory neurotransmitters such as glutamate or acetylcholine open postsynaptic Na^+ and/or Ca^{2+} channels, leading to an influx of positively charged cations and depolarization of the postsynaptic membrane. Inhibitory neurotransmitters such as GABA or glycine, on the other hand, typically induce the opening of Cl^- channels, leading to an influx of negatively charged anions and hyperpolarization of the postsynaptic membrane. This inhibition is, however, critically dependent on the reversal potential of the respective ions, which can developmentally be regulated, as recently demonstrated for GABA: Early during postnatal development, GABA still poses an excitatory effect due to modulated intracellular chloride concentration (Ben Ari, 02; Gulledge und Stuart, 03). Through diffusion in the synaptic cleft, neurotransmitters can also bind to presynaptic autoreceptors, thereby modulating intrinsic conductances in the terminal and modulate synaptic transmission.

In addition to ‘ionotropic’ actions (i.e. the direct binding to and opening of ion channels), released neurotransmitters can also exert ‘metabotropic’ effects, that is binding to metabotropic or G-protein-coupled receptors, which will then activate intracellular second messenger cascades. The excitatory amino acid transmitter glutamate, for instance, can activate 3 classes of ionotropic receptors (AMPA-, kainate and NMDA-type glutamate receptors) composed of distinct receptor subunits, and bind to metabotropic glutatamate receptors, which are subdivided into currently 8 groups (mGluR1-8). Ionotropic and metabotropic receptors can be found both pre- and postsynaptically, so that released neurotransmitter may influence both the pre- and postsynaptic cell. In summary, the type of neurotransmitter released from presynaptic vesicles and the corresponding postsynaptic receptor systems activated by this transmitter determine the physiological functioning of a synaptic complex.

1.2.3 Formal Description of Synaptic Strength

The strength or efficacy of a chemical synaptic connection determines the reliability of information transmission between two neurons. This strength is highly variable between different cell and synapse types, with very strong connections resulting in so-called 'teacher synapses' (e.g. the hippocampal mossy fiber onto CA3 pyramidal cell synapse), where even one synapse can drive the postsynaptic neuron into firing, and weak synapses, where the summation of coincident input from many synapses is needed for a supra-threshold postsynaptic response.

Synaptic strength can be described by three quantal parameters: (1) The number of release sites (or units) available for exocytosis of transmitter is given by n, with only a single release occuring at each site. Synapses can consist of more than one release site. (2) The probability of release of transmitter p is extremely small but finite in quiescent periods of no presynaptic action potential activity, and greatly increases to values up to 1 upon activation. The probability of release is determined by the amount of calcium available at the calcium sensor responsible for triggering vesicle release (being dependent on the distance between calcium channels and sensor and the activity and availability of calcium binding proteins) and the sensitivity of the trigger to induce vesicle release. Typically, one treats p to be uniform over different release sites. (3) The quantal content q reflects the amount of postsynaptic neurotransmitter receptors available given that the vesicle content is constant over repetitive activation of the presynapse as classically assumed (FATT und KATZ, 52; Wang et al., 03; Gandhi und Stevens, 03). In a solely descriptive scheme of synaptic strength, the measurable postsynaptic response amplitude A can thus be determined by

$$A = n \cdot p \cdot q \tag{1}$$

with n and p reflecting presynaptic and q reflecting postsynaptic features.

The basal quantal parameters of a specific synapse are usually constant over time as long as the contextual conditions remain the same. There are, however, a number of conditions which lead to modulation of one or several parameters and therefore change the resulting synaptic strength: Structural reorganization of the presynaptic terminal can induce an increase or decrease in the number of release sites n. Modulation of the presynaptic calcium influx triggering transmitter release will be reflected by a change in the probability of transmitter release p. Insertion or endocytosis of postsynaptic transmitter receptors might change the quantal content q. These exemplary changes occur on different timescales and are caused by distinct physiological stimuli. In the following paragraphs, we will discuss conditions and underlying intracellular mechanisms of how synaptic efficacy is known to be modulated.

1.3 Neuromodulation of Transmission

In contrast to the rapid and synapse-specific chemical synaptic transmission, 'neuromodulation' refers to a broader and long-lasting mechanism to modulate the strength of synaptic connections and alter intrinsic properties of a larger number of network neurons (Marder und Thirumalai, 02; LeBeau et al., 05). Neuromodulation can be achieved by numerous amines, neuropeptides and sometimes also classical neurotransmitters, including dopamine, serotonin, glutamate, GABA, acetylcholine and adenosine, that are released or co-released from synaptic terminals.

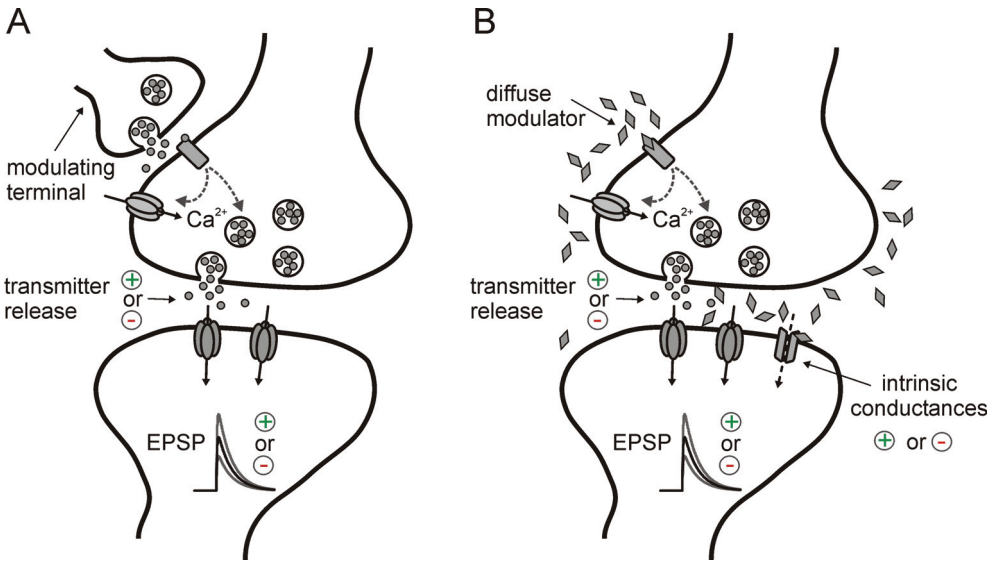

Figure 2: Neuromodulation of synaptic transmission. (A) Neurotransmitter release can be altered by direct targeting of a modulator-releasing terminal to the presynapse, causing presynaptic inhibition (e.g. through changing calcium influx) or facilitation (e.g. through depolarization of the presynaptic terminal). (B) A diffuse modulator can act on pre- and/or postsynaptic receptors, influencing transmitter release or intrinsic conductances. The signalling cascades involved in this modulation are diverse and synapse-specific.

The effects of neuromodulators on synaptic transmission can be subdivided according to their functional mechanisms into 4 groups: On the one hand, (1) heterosynaptic facilitation and (2) presynaptic inhibition denote the action of a neuromodulator or transmitter released directly from a synaptic terminal onto the terminal under investigation, with the first leading to facilitation and the latter to inhibition of transmitter release (Figure 2A). On the other hand, a diffusely released neuromodulator can act on (3) presynaptic receptors, again modulating transmitter release, or (4) on postsynaptic receptors and activate or inhibit intrinsic conductances (Figure 2B). Physiologically, neuromodulators are released during specific behavioral states, such as arousal or the sleep-wake cycle. Most importantly, slow neuromodulation regulates the gain of fast chemical transmission and thereby provides a means to globally adjust the excitability and response characteristics of a neuronal network.

1.3.1 GTP-binding Proteins Mediate Neuromodulation

Intracellularly, neuromodulation of synaptic and network parameters is achieved by activation of ionotropic or metabotropic receptor systems. While only a subset of synapses expresses presynaptic ionotropic receptors, virtually all synaptic terminals in the central nervous system are modulated by metabotropic receptors. These metabotropic receptors are coupled via GTP-binding proteins (Hille, 01), or G proteins, to various targets such as Ca^{2+} channels, K^+ channels, various second messenger signalling cascades or the exocytotic release machinery downstream of Ca^{2+} influx. All G proteins are heterotrimeric molecules composed of Gα, Gβ and Gγ subunits, which are associated with the cell membrane on the cytoplasmic side by hydrophobic anchors. In their resting state, G proteins carry GDP bound in a pocket of their α subunit. Upon receptor-agonist-activation, the GDP is liberated, a cytoplasmic GTP takes its position and the G protein dissociates into two membrane-associated parts, Gα-GTP and the Gβγ dimer, which are the activated forms of the G protein, capable of signaling to specific effectors such as

enzymes or ion channels. Eventually, Gα-GTP inactivates itself through the intrinsically activating GTPase by hydrolizing the bound GTP to GDP and rejoins a Gβγ subunit to form an inactive heterotrimer again.

1.3.2 Signalling Cascades of Neuromodulation

The intracellular action of G protein coupled receptors depends on which G proteins they can activate. Although there are at least 15 genes only encoding for different Gα subunits, G protein complexes can be subdivided into 4 broad classes based on their modes of action: G_s (for stimulating), $G_{i/o}$ (for inhibitory), and G_q. G_s stimulates adenylyl cyclase, leading to cAMP production and a resulting activation of protein kinase A (PKA). This cascade depends on the classical second messenger cAMP, which is known to be involved in for example augmentation of heart muscle calcium currents through β-adrenergic activation or the activation of the hyperpolarization-activated cation channel I_h. $G_{i/o}$ on the other hand inhibits adenylyl cyclase via $G_{\alpha i}$ or acts on phospholipase C (PLC) via Gβγ, leading to modulation of Ca^{2+} release via IP3. Finally, PLC can also be activated by G_q via the Gα subunit.

More recently, Gβγ subunits of G_i proteins have also been shown to directly modulate voltage-dependent calcium channels by a 'membrane-delimited' mechanism, i.e. the Gβγ message remains bound to the membrane and no intermediate messenger is needed for the calcium channel modulation (Herlitze et al., 96; Ikeda und Dunlap, 99; Takahashi et al., 98). The direct modulation of calcium channels by Gβγ is voltage-dependent and reversible by a strong depolarization. Functionally, inhibition of calcium channels by Gβγ can be characterized by a positive shift in the channel voltage-dependence (typically referred to as a shift from the 'willing' into the 'reluctant' state of the channel), a slowing of channel activation and a less steep voltage-dependence of activation. This direct action of Gβγ was first identified in cultured cell lines (Herlitze et al., 96), but shortly after also described as being the main mechanism for $GABA_B$-mediated inhibition of transmitter release at the Calyx of Held giant synaptic terminal (Kajikawa et al., 01). There, activation of presynaptic $GABA_B$ or mGluR receptors led to the inhibition of P/Q-type calcium channels which mediate transmission. Thus, it may present a powerful means to modulate synaptic transmission also at other synaptic systems directly by interfering with the initial trigger of vesicle exocytosis - the calcium influx into the presynaptic terminal.

Summarizing, G protein mediated neuromodulatory mechanisms rely on the activation or inhibition of a manifold variety of intracellular signalling pathways but in the end lead to a slow (i.e. in the range of seconds to minutes) modulation of chemical synaptic transmission. Importantly, under physiological conditions, synapses are always regulated by a combination of several neuromodulatory substances, which in the end provides the synaptic terminal (in combination with intrinsic features) with its specific response characteristics in the neuronal network.

1.4 Short-Term Plasticity of Synaptic Transmission

In addition to the slow effect of neuromodulation, synaptic transmission is also instantaneously regulated in an activity-dependent manner. During repetitive presynaptic stimulation, as for example found in irregular or burst-like in vivo activity, synaptic efficacy can be rapidly increased or decreased. This dynamical modulation of synaptic

transmission is referred to as ‘short-term plasticity’ or STP (for review see (Zucker und Regehr, 02).

Short-term plasticity can be either facilitating or depressing, in that repetitive activation of a synapse leads to an increase or decrease of the measurable response amplitude, respectively. These increases or decreases can occur on various timescales, so that one subdivides short-term enhancement of responses in facilitation (~100 of ms), augmentation (~5-10 s after high-frequency stimuli) and post-tetanic potentiation (30 s - several minutes after high-frequency stimuli). In a most basic approach, STP is tested by applying pairs of stimulating inputs in so-called ‘paired-pulse’ paradigms, where one determines the ratio of the response amplitudes to the second stimulus to the response amplitude to the first stimulus, the paired-pulse ratio (PPR). This ratio then qualitatively (larger than 1: facilitating, smaller than 1: depressing) and quantitatively (the absolute amount of modulation) describes the short-term plasticity properties of the synapse.

STP characteristics such as the sign and amount of plasticity are dependent on a combination of various factors, including the type of synapse, the identity of pre- and postsynaptic cells, and the temporal characteristics of the presynaptic input. Neocortical connections in layer 2/3 (Varela et al., 97) and the Calyx of Held giant synapse (Xu und Wu, 05; Taschenberger et al., 05), for instance, predominantly exhibit short-term depression of their response amplitudes, while hippocampal mossy fiber onto CA3 pyramidal cell (Toth et al., 00) and cerebellar parallel fiber onto Purkinje cell synapses (Dittman et al., 00) typically show short-term facilitation of their response amplitudes. STP is even target-cell specific, in that synapses stemming from the same presynaptic cell can exhibit opposing short-term plasticity characteristics depending on the postsynaptic target cell, as for instance found in mossy fiber synaptic connections onto CA3 pyramidal cells and interneurons (Toth et al., 00). Thus, the short-term plasticity features may contribute to the distinct functional roles of synapses in their specific neural network.

1.4.1 Mechanisms of Short-Term Plasticity

In the above introduced formal description of synaptic efficacy, the response amplitude of a synapse following presynaptic stimulation is determined by the presynaptic factors p (probability of transmitter release) and n (number of release sites) and the postsynaptically allocated factor q (quantal size). Modulation of any of these factors will result in measurable short-term plasticity of the synaptic responses. The precise mechanism of STP, however, depends on the quality of its expression. A number of parameters have been demonstrated to contribute to short-term plasticity characteristics in a highly synapse-specific manner (Figure 3).

Short-term facilitation is generally mediated by presynaptic factors as follows: Incoming action potential waveforms can be broadened through a change in K^+ channel kinetics leading to larger depolarization in the presynaptic terminal (Geiger und Jonas, 00). Furthermore, calcium channel kinetics may be altered leading to a changed calcium influx. The intraterminal calcium concentration is highly critical to short-term plasticity, with ‘residual calcium’, that is the accumulation of calcium due to repetetive invasion of action potentials in the presynaptic terminal, being responsible for facilitation of release (Zucker und Regehr, 02). This residual calcium may be modulated by intrinsic mechanisms such as buffering proteins or mitochondria. Saturation of such buffer proteins like calbindin or parvalbumin has also been shown to mediate short-term plasticity (Blatow et al., 03). Also, the trigger for vesicle fusion with the presynaptic membrane can be altered leading to a changed probability of release. Finally, ionotropic

or metabotropic autoreceptors may influence the membrane potential in the presynaptic terminal by opening or closing of intrinsic conductances, or act on calcium channels themselves.

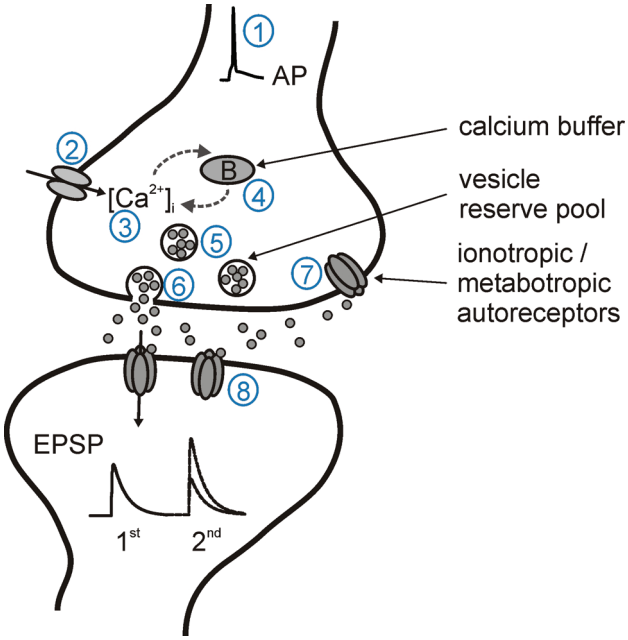

Figure 3: Mechanisms of short-term plasticity. Short-term synaptic plasticity may be regulated by the following parameters: Broadening of the action potential waveform (1) through K^+ channel modulation; changed Ca^{2+} channel conductance (2); intra-terminal calcium concentration $[Ca^{2+}]_i$ (3); regulation of residual calcium through intrinsic calcium buffers (4) such as calbindin or mitochondria; size of the vesicle reserve pool (5); modulation of the trigger for vesicle fusion and transmitter release (6); action of ionotropic or metabotropic autoreceptors (7); and postsynaptic receptor desensitization (8).

Short-term depression, on the other hand, can be due to either a presynaptic or postsynaptic use-dependent modulation of transmission. The most widespread mechanism for depression appears to be a depletion of the pool of releasable vesicles (Zucker und Regehr, 02), where higher levels of transmission are associated with larger depression. Additionally, a dynamical decrease in synaptic strength can result from the release of modulatory substances by the activated presynaptic terminals or postsynaptic cells, or from desensitization of the postsynaptic ligand-gated receptors, making the target less sensitive to neurotransmitter release.

Summarizing, it remains to be highlighted that synapses which intrinsically exhibit a low probability of transmitter release p will tend to express short-term facilitation, while synapses with a high probability of release usually express short-term depression (Dobrunz und Stevens, 97). Dynamical facilitation and depression are both instantaneous, short-lasting (typically tens to hundreds of milliseconds) alterations of synaptic efficacy, that are usually fully reversible. Hence, they only represent the most recent input history and do not influence later synaptic transmission.

1.4.2 Functional Implications of Short-Term Plasticity

A number of different roles have been proposed for short-term plasticity in various synaptic systems. One focus of attention has been a potential filtering function of STP for information encoded in spike trains (Abbott und Regehr, 04; Dittman et al., 00; Klyachko

und Stevens, 06a), with short-term depression imposing low-pass filter characteristics in favor of onset detection and inducing attenuation of responses during high-frequency presynaptic activity. This mechanism appears to be employed during the behavioral adaptation to repetitive whisker deflection in rodents, which is caused by depression of transmission in thalamocortical synapses (Chung et al., 02). In addition, short-term depression has been shown to equalize postsynaptic response amplitudes to changes in the firing frequency in neocortical layer 4 to layer 2/3 synapses and thus serves as a mean of gain control (Sen et al., 96). Short-term facilitation, on the other hand, imposes high-pass filtering characteristics, which increases the reliability of information transmission during periods of high-frequency input as for example found during bursts of activity.

Short-term plasticity characteristics can also be used as an experimental tool to determine the locus of action of for instance an intrinsic neuromodulator or externally applied drug. As short-term plasticity, in particular facilitation, is exclusively attributed to presynaptic mechanisms, any notable change in STP during modulation of synaptic efficacy will indicate a presynaptic mechanism of action. In the same lines, however, this also results in short-term plasticity itself being a rather variable, dynamical process. Every modulation of a synapse's basic features, such as long-term potentiation of transmission (see below), neuromodulation by autoreceptors, or even the accessibility of calcium will lead to indirect changes in STP. Thus, a description of short-term plasticity characteristics of a synapse can only be given under known fixed conditions.

1.5 Long-Term Plasticity of Synaptic Transmission

As early as the description of structure and functioning of nerve cells and the existence of synapses by Ramon y Cajal and Sherrington, it was hypothesized that long-lasting, activity-dependent changes in synaptic transmission should underly the storage of experiences and memory traces. Not until the early 1970s could this claim experimentally be supported when Bliss and Lømo demonstrated that repetitive activation of perforant path synapses onto dentate gyrus granule cells in the hippocampus (the brain region known to be essential for memory formation) resulted in an increase in synaptic efficacy for hours (Bliss und Collingridge, 93; Bliss und Lomo, 73). Since then, long-term potentiation and also long-term depression of synaptic transmission has been found and described at manifold glutamatergic synaptic systems in the central nervous system (Malenka und Nicoll, 99; Martin et al., 00).

1.5.1 Basic Features of Long-Term Potentiation

Long-term potentiation (LTP) refers to a rapidly induced (usually via high-frequency presynaptic activation) increase in synaptic efficacy, that lasts for hours to days. Hereby, one can differentiate between early (up to 1 hour) and late (several hours) phases of LTP, but the exact time-windows for this distinction are not consistently agreed upon. Late phase LTP is dependent on an alteration in gene expression. The characteristics, induction and expression mechanisms of early phase LTP will be discussed below.

Literature on the induction and expression mechanisms of long-term potentiation is vast and sometimes overwhelming. Again, persistent modulation of the presynaptic factors n or p, or the postsynaptic quantal size q could in principle account for long-lasting changes in synaptic efficacy. Contradictory literature is mostly due to the variety of mechanisms found at different synapses, with distinct transduction pathways,

mediators, stimulating patterns and kinetics, but also results from a long and fierce debate on the locus of expression of long-term potentiation triggered by controversial data (Malenka und Nicoll, 99). Two forms of potentiation can, however, be seen as exemplary model types of LTP found at several synapses: the one involving modulation of the postsynaptic density, the other one expressed through presynaptic modulation of transmitter release.

1.5.2 LTP through Postsynaptic Modulation of Strength

Most excitatory, glutamatergic synapses exhibit a form of LTP initially described at hippocampal CA1 and dentate gyrus synapses, and later also found throughout the mammalian brain, including the cerebral cortex (for review see (Bliss und Collingridge, 93; Bear und Malenka, 94; Malenka und Bear, 04). Here, long-term potentiation is dependent on the activation of postsynaptic NMDA-type glutamate receptors. At resting membrane potential, NMDA receptors are voltage-dependently blocked by magnesium ions, which are only released from the channel pore upon depolarization of the postsynaptic membrane. When activated, NMDA-receptors allow for local influx of Ca^{2+} as well as Na^{+} into the dendritic spine, with the rise in calcium being the local trigger for subsequent intracellular signalling leading to long-term potentiation. When the calcium concentration threshold for LTP is reached, α-calcium-calmodulin-dependent proteinkinase II (CaMKII) is activated and remains active long after the calcium signal has decayed due to its autophosphorylating property. One proposed model implies that CaMKII can directly phosphorylate the AMPA-receptor subunit GluR1 leading to a higher conductance, which has been shown to occur after the induction of LTP. In addition, CaMKII has been shown to influence the subsynaptic localization of AMPA receptors, such that more AMPA receptors are delivered to the postsynaptic membrane. This trafficking process can also occur at synapses which prior to potentiation were "silent", that is they did not express any measurable AMPA receptors. Summarizing, the most commonly found form of NMDA-receptor dependent LTP involves exclusively postsynaptic changes in synaptic strength.

1.5.3 LTP through Presynaptic Modulation of Strength

In contrast to these postsynaptic changes of synaptic strength after potentiation, also NMDA-receptor independent, presynaptically expressed forms of LTP have been described. Hippocampal mossy fiber onto CA3 pyramidal cell (Zalutsky und Nicoll, 90; Nicoll und Schmitz, 05), corticothalamic (Castro-Alamancos und Calcagnotto, 99) and cerebellar parallel fiber (Salin et al., 96a) synapses could be shown to potentiate in synaptic efficacy by presynaptic changes. Here, increases in transmitter release are obtained in that the release probability *p* is enhanced, new release sites are recruited and formerly silent synapses are activated (Tong et al., 96; Nicoll und Schmitz, 05). A more detailed description of such presynaptic LTP will be given in Chapter 2 at the example of the hippocampal mossy fiber synapse.

1.5.4 Functional Implications of LTP

Long-lasting changes in the strength of connections between neurons have long been discussed to underlie the storage of memory traces in the central nervous system (Bliss und Collingridge, 93; Malenka und Nicoll, 99; Martin et al., 00). Although there is still an ongoing controversy about the absolute validity of this hypothesis, several key features of long-term potentiation argue in favor of it. Long-term potentiation is usually synapse-specific, i.e. when expressed at one set of synapses by activation, the increase in

efficacy does not occur at neighboring synapses. This specificity is thought to greatly increase the storage capacity of neurons, as it minimizes redundancy in information. Also, changes in synaptic strength have been found to be persistent over days to even months (Reymann und Frey, 07; Sajikumar und Frey, 04). This persistency would be a key requisite for long-lasting storage of information. Further on, NMDA-receptor dependent LTP is usually associative, i.e. potentiation of one set of synapses will facilitate LTP at an independent, but neighboring set of synapses onto the same postsynaptic cell. This associativity is often thought of as a cellular correlate of associative or classical conditioning and thus presents another computational feature essential for learning and memory formation. Finally, recent studies have presented evidence that behaviorally testable learning, such as fear conditioning or motor learning, lead to modulation in synaptic strength in the underlying neuronal networks (Rumpel et al., 05).

In contrast to NMDA-receptor dependent forms of LTP, the functions of presynaptic forms of LTP are much less understood. The classic concept of associativity, for instance, cannot be fullfilled in this case, as only presynaptic activity is involved in modulation of synaptic strength. In this context, we will propose a new functional consequence of presynaptic, NMDA-receptor independent long-term potentiation at the hippocampal mossy fiber synapse in Chapter 4 of this thesis. Summarizing, however, there is cumulating evidence for the validity of the 'synaptic-plasticity-memory' hypothesis, which will have to be tested further experimentally and theoretically in the future.

1.6 Diversity and Specificity of Synapses

In this Chapter, the basic properties of anatomy, physiology and modifiability of synapses were introduced. Although there are common features found at synapses throughout the nervous system, diversity amongst synapses is immense. Most synaptic properties such as size, complexity, short-term and long-term plasticity are very specific for the type of synapse under investigation. In order to gain knowledge about the functions of the nervous system as a whole, one therefore has to understand its individual building blocks first. There is no one "model synapse" from which neuroscientists can deduce all the details of synaptic transmission, its modulation and plasticity.

In the remainder of this thesis we will thus focus our investigations on one particular synapse: the hippocampal mossy fiber synapse onto CA3 pyramidal cells. We will introduce its basic mechanisms of transmission and plasticity, elucidate how synaptic strength is regulated by neuromodulators, describe its marked short-term plasticity and how this is changed after long-term potentiation, and finally propose how these synaptic properties might contribute to the role of the synapse on downstream signalling in the hippocampal network. And we will always keep in mind the very specificity of our findings as already perceived by Bernard Katz early on during his work on synaptic physiology:

> *"The more one finds out about properties of different synapses, the less grows ones's inclination to make general statements about their mode of action"* (Bernard Katz, 1966 in Nerve, Muscle and Synapse.)

2 Anatomy and Physiology of Hippocampal Mossy Fiber Synapses

As elaborated in the last Chapter, synapses are remarkably diverse in structure and function, specialized for their distinct roles in the neuronal network. One of the most heavily studied regions in the central nervous system is the hippocampal formation, which has attracted anatomists and physiologists likewise due to its highly structured network, clear connectivity pathways and functionally different cell types. The hippocampal formation bears a large number of distinct synaptic projections, connecting neurons in the entorhinal cortex via the dentate gyrus with the cornu ammonis region and further on through the subicular region looping back to the entorhinal cortex.

The manifold types of synapses found in the hippocampus differ remarkably in size, number, efficacy and plasticity. This diversity is dependent on the identity of the pre- and post-synaptic cells, the area within the hippocampus and also the developmental stage of the organism studied. In this Chapter, we will introduce the hippocampal mossy fiber synapse, the second step in the classical trisynaptic hippocampal excitatory circuit, and highlight its most remarkable morphological and physiological features by discussing the relevant literature and presenting first own experimental data.

2.1 The Hippocampal Formation

The hippocampal formation is located deep within the medial temporal lobe of the brain and is composed of the dentate gyrus, hippocampus, subiculum and entorhinal cortex. The basic layout of cells and fiber pathways of the hippocampal formation is highly conserved in all mammals, which makes it an ideal candidate for studying basic questions in the neurosciences. A panoply of research areas have greatly profitted from investigating the hippocampal formation, ranging from psychology interested in learning, synapse physiology investigating basic principles of synaptic transmission, to computational neuroscience concerned with modeling of neural networks. Functionally, the hippocampal formation could be shown to be crucially involved in memory formation, spatial navigation and also the pathophysiological conditions of epilepsy and Alzheimer's disease. In order to fully understand the underlying mechanisms of these phenomena, one will have to elucidate the cellular and synaptic components making up the hippocampal formation.

The classical hippocampal trisynaptic circuit consists of glutamatergic connections onto the three types of principal neurons of the hippocampus: granule cells in the dentate gyrus, pyramidal neurons in area CA3, and pyramidal neurons in area CA1 (Figure 4A). First, dentate gyrus granule cells receive excitatory input from layer 2 pyramidal cells of the entorhinal cortex. Granule cells then connect to CA3 pyramidal cells via their axonal projections, termed 'mossy fibers' (MF). CA3 pyramidal cells themselves provide input to CA1 pyramidal cells via the Schaffer collaterals, which in turn project to the subiculum and back to the entorhinal cortex. In addition to this trisynaptic circuit, CA3 and CA1 pyramidal neurons receive direct input from the entorhinal cortex and CA3 neurons are strongly connected to each other via 'associational-commissural' recurrent collaterals.

Finally, a large variety of interneurons are found throughout the hippocampus, providing the network with local, feedforward and feedback inhibitory regulation.

The hippocampal mossy fiber synapse as the second step in the excitatory trisynaptic circuit will be the main focus for the remainder of this thesis. Various aspects of mossy fiber synaptic transmission, its modulation and plasticity will be elucidated in Chapters 3 to 5, using electrophysiological, microfluorometric and modelling techniques. To give the reader the necessary conceptual background, we will present the basic anatomical and physiological properties of hippocampal mossy fiber synapses in the following paragraphs.

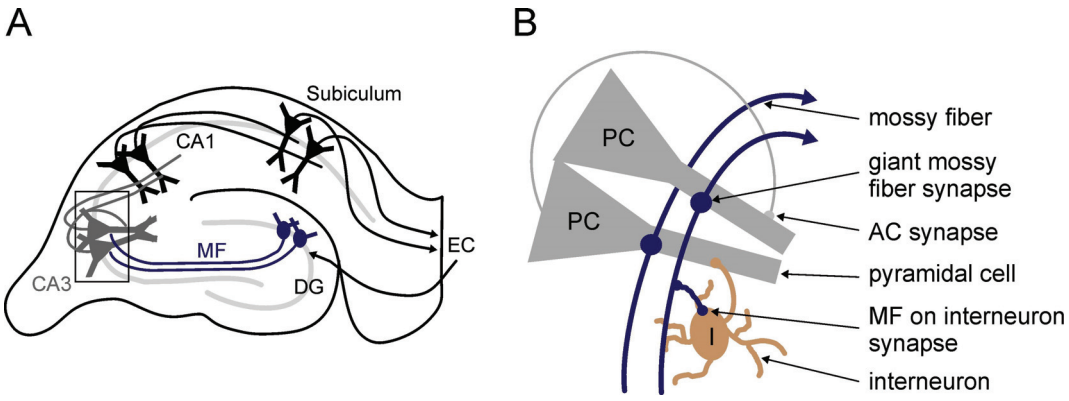

Figure 4: Hippocampal Circuitry. (A) Schematic overview of a parasaggital cut through the hippocampal formation. The excitatory trisynaptic circuit is depicted with input from the entorhinal cortex (EC), dentate gyrus (DG) granule cells, CA3, CA1 and subicular pyramidal cells (PC). (B) Microcircuitry in the CA3 region including pyramidal cells, local interneurons and the various synaptic connections onto and between these. In blue, mossy fiber (MF) projections from DG granule cells are shown, synapsing onto PCs and interneurons via giant synapses, filopodial extensions and en passant synapses.

2.2 Anatomy of the Mossy Fiber Synaptic Pathway

In the rat dentate gyrus, each granule cell gives rise to a single, unmyelinated mossy fiber axon with an approximate diameter of 1 µm and total length of on average ~3300 µm (Acsady et al., 98). On their way to the CA3 region, mossy fibers form 4 types of synapses with distinct postsynaptic cells (for review see (Henze et al., 00). Already in the hilar region, the mossy fiber axons make contact to (1) polymorphic and basket cell interneurons via thin collaterals and (2) glutamatergic mossy cells via large boutons, while the main axons project on through the CA3 region in a narrow, visually identifiable band, termed 'stratum lucidum'. The stratum lucidum corresponds to the proximal 100 µm of the apical dendrites of CA3 pyramidal cells and and was named after its bright, as practically soma-free, appearance in light microscope pictures. In area CA3, the mossy fibers make contact with (3) CA3 excitatory principal cells via 'giant' boutons and (4) inhibitory interneurons via filopodial extensions from the giant boutons. The individual synapses onto these 4 cell types are morphologically distinct and some of their functional differences can already be derived from their structure. We will, however, focus our presentation by contrasting the properties of the giant mossy fiber boutons on CA3 pyramidal cells and the filopodial contacts on CA3 interneurons, as they will play a further role in the upcoming chapters.

The hippocampal mossy fiber pathway was first named after its unusual morphological appearance. The large varicosities and filamentous extensions reminded Ramón y Cajal of moss, as had the mossy fibers in the cerebellum before. The different types of mossy fiber synapses bear distinct structural properties which impose them with differential physiological potential (Urban et al., 01):

The most prominent synaptic component of the hippocampal mossy fibers are the characteristic large boutons onto CA3 pyramidal cell proximal dendrites in stratum lucidum (Figure 2 1B). These mossy fiber terminals are unusually large with a diameter of ~2 to 10 µm (Henze et al., 00; Rollenhagen und Lubke, 06; Bischofberger et al., 06) and are found arranged in either an en passant fashion or attached via a short process to the main axon. In adult MF boutons in the hippocampus, the number of transmitter bearing vesicles is estimated between 11,000 and 25,000, consisting of mostly small clear vesicles and a minority of large, dense-core vesicles. These vesicles cluster in multiple (up to 40) active zones in the presynaptic terminal, which completely envelopes a large, multi-headed spine on the proximal postsynaptic dendrite. On average, each CA3 pyramidal cell is contacted by 50 large MF boutons. Thus, due to the large number of active zones per bouton and their near proximity to the cell soma, even the relatively small number of granule cell terminals bears the potential for strong excitatory input onto CA3 pyramidal neurons. It should be noted, however, that CA3 pyramidal cells additionally receive input from layer II stellate cells in the entorhinal cortex via the perforant path (~4,000 synapses per CA3 cell) and neighbouring CA3 pyramidal neurons via the associational-commissural collaterals (~12,000 synapses). The relative strengths of these different types of synapses, their influence on CA3 pyramidal firing and the impact of the sparse connectivity of granule cells onto CA3 pyramidal cells is still under debate.

In contrast to the MF boutons onto CA3 pyramidal neurons and hilar mossy cells, the MF interneuron-associated boutons are small, typically form only one or a few active zones, and the synapses are either en passant or at the ends of synaptic filopodia, which extend from the giant bouton. Each hilar or CA3 interneuron receives about ten times more synapses from MFs than do principal neurons, with a single MF innervating typically 40-50 inhibitory targets in CA3 alone (Acsady et al., 98; Lawrence und McBain, 03). The MF innervated interneurons themselves then make inhibitory synaptic contact to CA3 pyramidal neurons, which presents part of the MF pathway as a classical feedforward inhibitory circuit.

2.3 Basal Mossy Fiber Synaptic Physiology

Basic properties describing the physiology of every synapse, including probability of release, average quantal content and kinetics, vary remarkably between neural systems. The MF-CA3 pyramidal cell synapse was one of the first synapses studied in in vitro slices; still, an acurate and complete description of the basic aspects of its neurotransmission is missing. In the following paragraphs, we are going to consider the various difficulties in studying MF synaptic features, introduce already known properties from several measuring techniques, and present own recordings describing basic physiological properties of MF synaptic transmission.

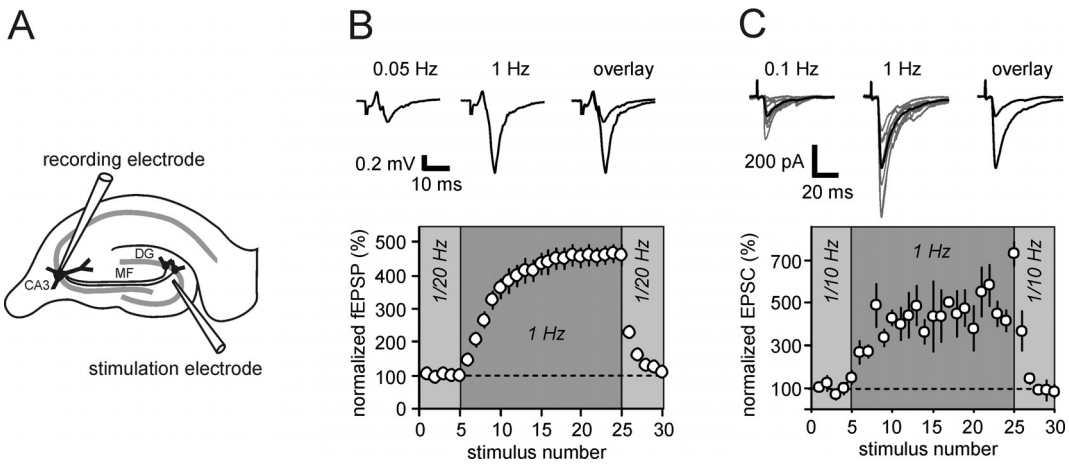

Figure 5: Mossy fiber stimulation criteria - frequency facilitation. (A) In electrophysiological recordings, mossy fibers were extracellularly stimulated with an electrode positioned in the granule cell layer or hilus of the dentate gyrus. (B) In field potential recordings, response amplitudes were always increased to more than 400 % of control values by frequency facilitation paradigm, i.e. switching stimulation frequency from 0.05 to 1 Hz (n = 15). Upper traces depict averages of 10 sweeps each of a single example experiment. (C) In whole-cell recordings, mean response amplitudes were largely increased by switching the stimulation frequency from 0.1 to 1 Hz (n = 6), similar to fEPSP experiments. Upper traces depict overlays of 10 single sweeps (grey) and their mean responses (black) each of a single example experiment (last 10 responses under frequency facilitation).

2.3.1 Studying Mossy Fiber Synaptic Responses

As introduced in paragraph 2.1, CA3 pyramidal neurons receive excitatory and inhibitory input from several presynaptic structures. In combination with the sparse connectivity between dentate gyrus granule cells and CA3 pyramidal neurons, this presents serious complications for investigating MF synaptic response properties: First, the probability of stimulating presynaptic mossy fibers, which actually project to the postsynaptically recorded CA3 cell, is low when using bulk stimulation, and second, the postsynaptically recorded responses might in part or whole be generated by inputs other than the mossy fiber.

There are two main criteria, which help to optimize the reliability of studying a 'pure' MF synaptic response in CA3 pyramidal cells: (1) Mossy fiber synapses exhibit an unusually large facilitation of response amplitudes of up to 1000 % when repeatedly stimulated (Salin et al., 96b). This phenomenon is termed "frequency facilitation", as it is most obvious when the stimulus input is changed from low (~0.05 Hz) to moderate (1 Hz) frequencies (Figure 5). Neighboring synapses show no or very little facilitation (~140 %). (2) Mossy fiber synapses selectively express group II metabotropic glutamate receptors (mGluR2) as presynaptic autoreceptors, which completely inhibit synaptic transmission upon activation (Castillo et al., 97; Yoshino et al., 96; Sanabria et al., 04). Thus, mGluR2 agonists like LCCG1 and DCGIV are successfully used to identify pure MF responses, preferably at the end of experiments. Postsynaptic mossy fiber response amplitudes should be completely blocked upon application of DCGIV, with the incidence of transmission failures in whole-cell recordings of CA3 pyramidal cells significantly increased (Figure 6). In contrast, recorded responses stemming from neighboring A/C synapses are not affected by application of DCGIV.

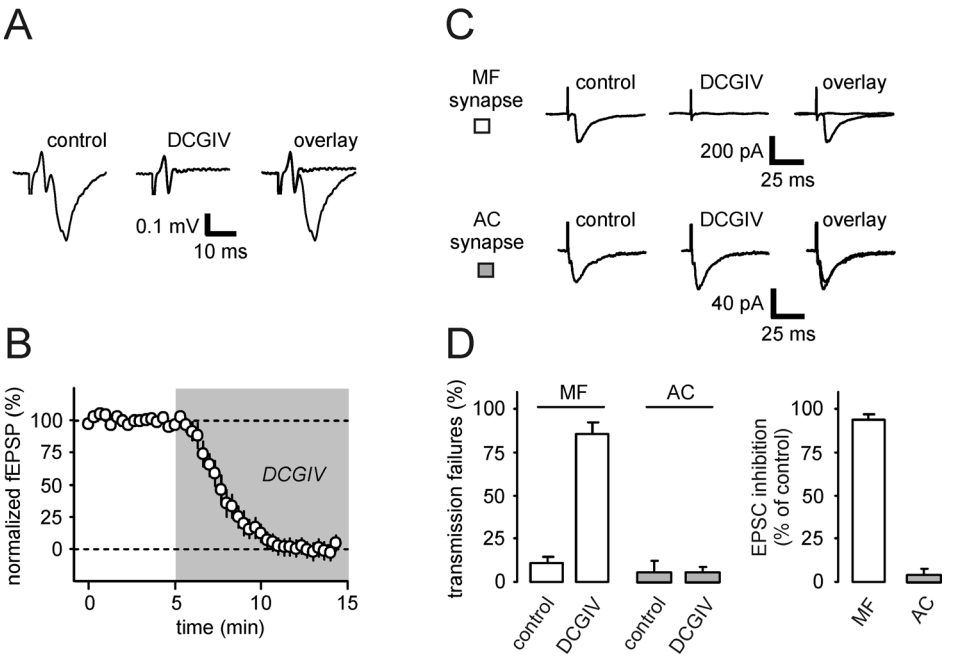

Figure 6: Mossy fiber stimulation criteria - DCGIV sensitivity. (A,B) In mossy fiber field potential recordings, application of the mGluR2 agonist DCGIV (0.5 1 µM) led to complete blockage of fEPSP repsonses (n = 15). Upper traces depict averages of 10 sweeps each of a single example experiment. (C,D) In whole-cell recordings of CA3 pyramidal cells, synaptic responses are differentially affected by application of DCGIV. In mossy fiber (MF) synaptic responses (white bars), DCGIV significantly increased the relative occurence of synaptic transmission failures and reduced the mean response amplitude by 95 % (n = 6). In A/C synaptic responses (grey bars), application of DCGIV did not alter the occurrence of failures, nor did it lead to an inhibition of EPSC amplitudes (n = 4). Upper traces depict mean responses of 20 sweeps each.

In addition to these criteria concerning plasticity and pharmacology of the mossy fiber synapse, also the specific kinetics of MF synaptic responses have been used to argue for selective stimulation of mossy fibers. It has been suggested that MF excitatory postsynaptic currents (EPSCs) should exhibit relatively fast rising phase kinetics due to the close electrotonic location of the synapses to CA3 cell somata (<1-3 ms for the 10-90 % rising time; see (Jonas et al., 93; Henze et al., 00; Toth et al., 00). Furthermore, the response should not show any inflected rising or decay phases, as this might reflect polysynaptic recruitment or anti-orthodromic activation of MF hilar collaterals (Xiang und Brown, 98). Although these parameters give useful additional information about the origin of the recorded responses, using them too restrictively might also lead to arbitrary exclusion of subsets of mossy fiber responses. Therefore, all electrophysiological data presented in this thesis are based on experiments which comply with the criteria as presented above in (1) frequency facilitation and (2) mGluR2-agonist sensitivity.

2.3.2 Quantal Properties of the Mossy Fiber Synapse

Despite the difficulties mentioned in the last paragraph, the most important quantal parameters of mossy fiber synaptic transmission have been described. Due to the sparse connectivity it has proved to be intractable to establish simultaneous paired recordings of presynaptic granule cells and postsynaptic CA3 pyramidal neurons. Thus, most information is based on using minimal stimulation techniques.

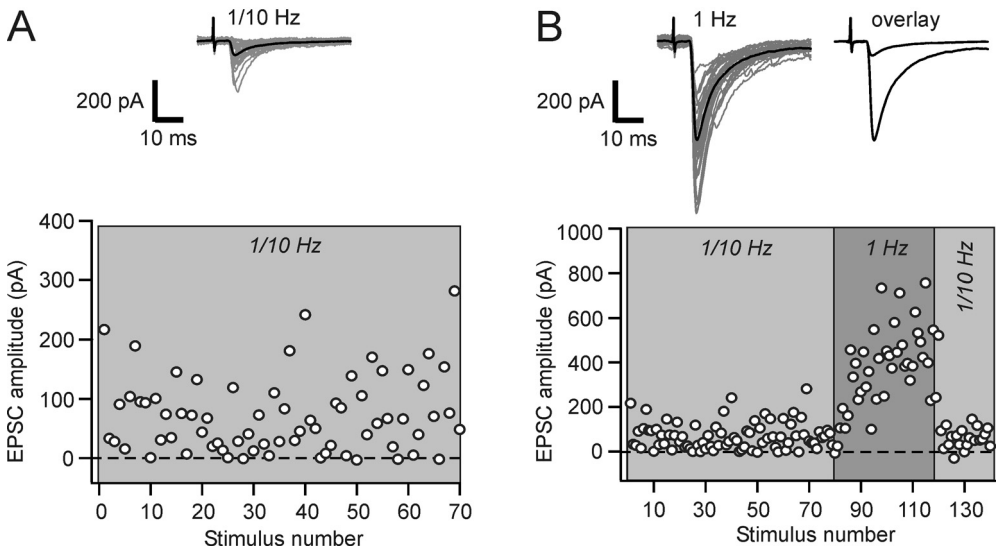

Figure 7: High variability in mossy fiber synaptic response amplitudes. (A) In an examplary whole-cell recording, EPSC amplitudes ranged between 0 (failures of transmission) and 280 pA at a constant stimulation frequency of 0.1 Hz. The mean response was 68 pA and the coefficient of variation of the distribution of response 0.89. (B) In the same cell, increasing the stimulation frequency to 1 Hz led to an increase in mean response amplitude to 431 pA and a reduction in the CV to 0.35. Upper traces show an overlay of 20 individual sweeps (grey) and their mean response (black).

Hereby, focal stimulation of preferably individual granule cells with extracellular stimulus electrodes at low intensity leads to activation of single fibers. Measuring such evoked responses, Jonas et al. (1993) found mossy fiber synapses to exhibit unitary conductances of up to 1 nS and an average quantal conductance of 133 pS. The average rising phase of evoked responses was 0.6 ms, although it has to be noted that the pool of analyzed data was specifically chosen for its fast kinetics (Toth et al., 00). Additionally, again imposing the fast kinetics criterium, spontaneously occuring miniature EPSCs were found to be relatively large and widely distributed in amplitude, with an apparent mean conductance of 251 pS. Similar values had been found earlier with focal application of glutamate to the dentate gyrus cells for selectively stimulating single granule cells (Yamamoto et al., 91). Using variance-mean analysis, Lawrence et al. (2003) could demonstrate a relatively low probability of transmitter release at MF-CA3 pyramidal cell synapses, even under conditions of high extracellular Ca^{2+}. Summarizing these and other complementary studies, the hippocampal mossy fiber synapse can be described by the following estimates of quantal parameters: The number of release sites was morphologically and functionally quantified as n = 7-40, the release probability for each release site calculated as p = 0.01-0.05 and the quantal amplitude found to range between q = 9-12 pA (for review see (Henze et al., 00; Lawrence und McBain, 03).

As discussed in section 2.1, the giant mossy fiber synapse is morphologically complex with a high number of individual active zones. Physiologically, this phenomenon provides the synapse with a unique feature: When an action potential travels along the mossy fiber axon and invades the presynaptic terminal, the up to 40 release sites will independently become activated, and with a certain probability p the neurotransmitter glutamate is released into the synaptic cleft via exocytosis. This probability is low, but still several release sites can concurrently be active in response to one presynaptic stimulus. Consequently, the measurable postsynaptic response will be variable in

amplitude depending on the current number of active release sites. This basic phenomenon of MF synaptic transmission can be seen in an example recording in Figure 7A. Postsynaptic EPSC response amplitudes upon constant stimulation at 0.1 Hz showed a large variability ranging from 0, indicating complete failures of transmission, to ~300 pA. This variability in amplitude can also be expressed in the coefficient of variation (CV), here 0.89, which is remarkably large compared to other described synapses (Dobrunz und Stevens, 99; Klyachko und Stevens, 06a). For obtaining the mean mossy fiber synaptic response, we averaged over several (in this case 30) trials, yielding a mean response amplitude of 68 pA. The variability and mean response amplitudes will also be modulated by a change in stimulation frequency (Figure 7B). For judging experimental data involving single cell MF synaptic responses it is crucial to always keep this broad amplitude distribution in mind.

2.3.3 Regulation of Transmission at the Mossy Fiber Synapse

The hippocampal mossy fiber synapse is a glutamate-releasing excitatory synapse, postsynaptically expressing AMPA- and, to a lesser extent, NMDA-type glutamate receptors (Figure 8). Activation of postsynaptic AMPA receptors upon binding of glutamate thus constitutes the main component of the measurable mossy fiber synaptic responses in CA3 pyramidal cells. Additionally, the MF synapse expresses kainate receptors pre- and postsynaptically and, as already mentioned above, metabotropic glutamate receptors presynaptically. Presynaptically localized receptors hereby appear to act as autoregulators, modulating transmitter release in response to heightened levels of glutamate.

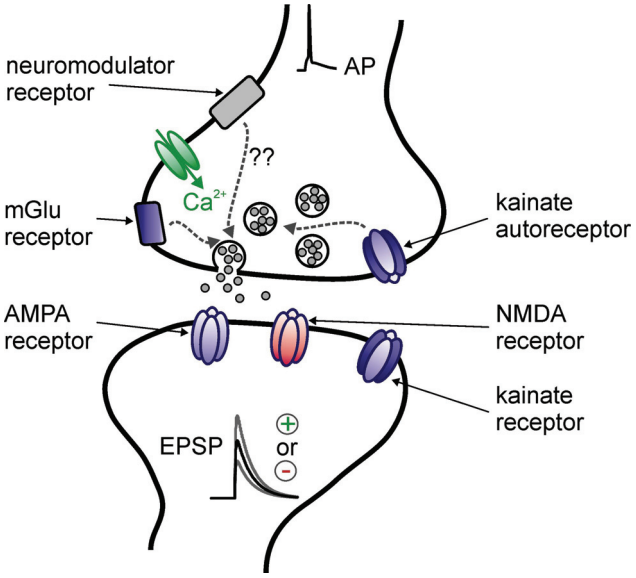

Figure 8: Scheme of receptor and signalling systems at the hippocampal mossy fiber synapse. On the presynaptic side, the incoming action potential (AP) induces calcium influx via voltage-dependent calcium channels and thereby triggers glutamate release. Transmitter release at the MF synapse can be modulated by various presynaptic signalling mechanisms, as a number of neuromodulator receptors are expressed. These can modulate release in several, partly unknown ways. Also presynaptic kainate receptors can influence transmission acting as autoreceptors. On the postsynaptic side, a depolarizing excitatory postsynaptic current is elicited by Na^+ influx largely through AMPA-type glutamate channels. This current can be increased or decreased by neuromodulatory action on the presynaptic side.

In addition to the direct effect of the released transmitter glutamate, several types of neuromodulators have been shown to regulate synaptic efficacy. The mossy fiber synapse presynaptically expresses various other G-protein coupled metabotropic receptor systems, including $GABA_B$, opioid and adenosine receptors. These receptor systems precisely control synaptic transmission via distinct intracellular signalling cascades. The exact mechanism of how the neuromodulator adenosine regulates mossy fiber synaptic transmission will be presented and discussed in detail in Chapter 3.

2.4 Short-Term Plasticity at the Mossy Fiber Synapse

The hippocampal mossy fiber synapse exhibits remarkably pronounced short-term plasticity (Salin et al., 96b; Nicoll und Schmitz, 05). In contrast to most other synapses, STP occurs over a rather broad temporal range with timeconstants of tens of seconds. Here, one can distinguish between two facilitatory short-term plasticity phenomena found at the mossy fiber synapse: paired-pulse facilitation (PPF) and 'frequency facilitation'.

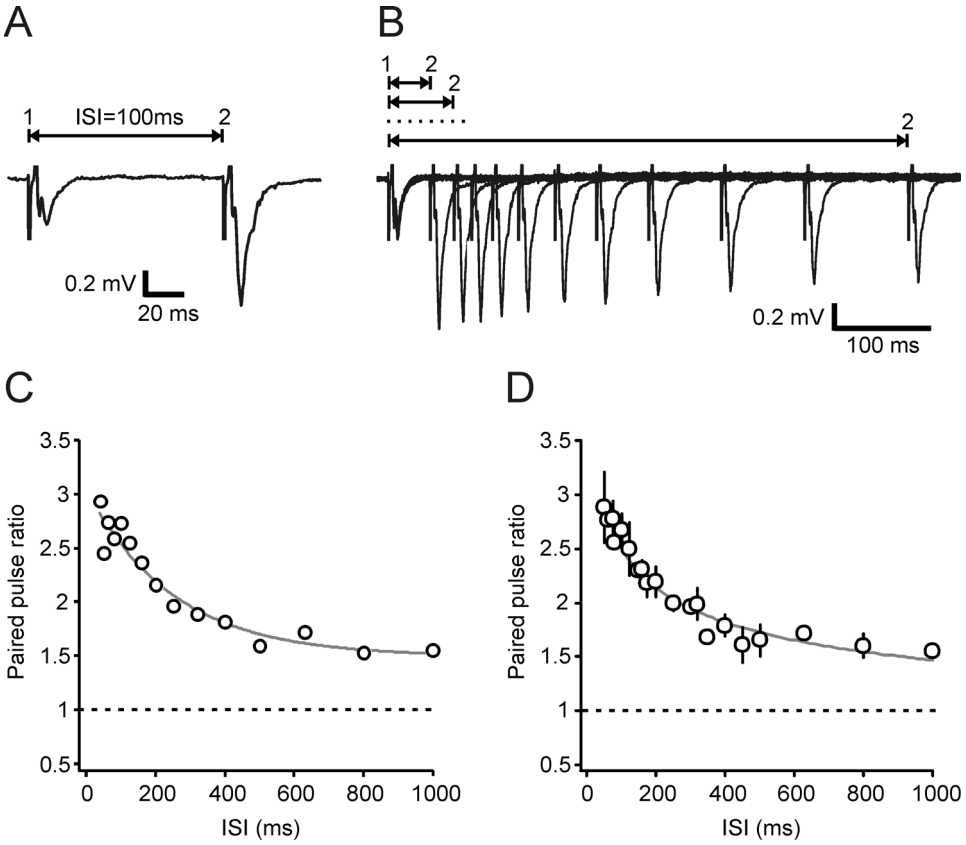

Figure 9: Paired-Pulse facilitation at the mossy fiber synapse. (A) Applying a pair of presynaptic stimuli with an interstimulus interval (ISI) of 100 ms leads to a pronounced facilitation of MF synaptic response. (B) The absolute amount of facilitation depends on the ISI. Succesive trials with varying ISIs from 50 to 500 ms are shown in this overlay. Traces depict averages of 10 sweeps each. (C) The paired-pulse ratio (PPR, i.e. amplitude ratio of 1st to 2nd response) depends on the inter-stimulus interval, with small ISIs triggering larger PPRs. Response distribution of example experiment from A and B is shown. (D) Comparable paired-pulse ratios were measured in n = 6 fEPSP experiments. Grey lines are monoexponential fits to data.

2.4.1 Paired-Pulse Facilitation

The hippocampal mossy fiber synapse exhibits remarkably large short-term plasticity with a highly facilitatory paired-pulse ratio of 2-4, depending on recording conditions. In an exemplary fEPSP recording of mossy fiber synaptic responses (Figure 9A), the PPR was 2.8 at an inter-stimulus interval of 100 ms. At most synapses, paired-pulse plasticity is largest at ISIs of 50-100 ms and exponentially decays at increasing inter-stimulus intervals with a time constant of a few hundred milliseconds reflecting the time course of residual calcium clearance in the presynaptic terminal. Paired-pulse facilitation at the MF synapse, however, is still notably large at higher inter-stimulus intervals. As depicted in Figure 9 B and C for the same experiment, the PPR initially decays from a maximum value of 2.9 with increasing ISIs but stabilizes around 1.6 with ISIs larger than 500 ms. This phenomenon is a general characteristic of mossy fiber STP as can be seen in a summary of n = 6 experiments (Figure 9D). The extended time window of ISIs that can elicit robust paired-pulse facilitation is a first hint at an additional, mossy fiber synapse specific form of short-term plasticity with a much longer time constant.

2.4.2 Frequency Facilitation

Mossy fiber synaptic responses undergo frequency faciliation, in which increases in the frequency of stimulation from low (e.g. 1/20 Hz) to moderate (e.g. 1 Hz) values lead to manifold increases in synaptic efficacy (compare Figure 5B). As mentioned above, this STP property is routinely used to identify the specificity of mossy fiber stimulation at the beginning of an experiment. The relative amount of increase in response amplitude is hereby dependent on the exact stimulation frequency. In an exemplary fEPSP recording of MF synaptic responses, a set of 7 increasing stimulus frequencies (1/80, 1/40, 1/20, 1/10, 1/5, 1/3 and 1 Hz) was applied via extracellular stimulation of the mossy fiber tract (Figure 10A and B). Increasing stimulus frequencies hereby led to steadily increasing mean response amplitudes. As depicted in the summary of n = 5 such experiments where values are normalized to a basal response amplitude during stimulation with 1/20 Hz, fEPSP amplitudes stabilized at a frequency-specific value during each stimulus train (Figure 10C). Moreover, they were fully reversed to baseline values when the input frequency was switched back to 1/20 Hz. Frequency facilitation therefore endows the mossy fiber synapse with the ability to encode its recent input history, as the presynaptic temporal statistics are reflected in the postsynaptic response amplitudes.

Still, this commonly used quantification of STP based on constant frequency stimulation paradigms is rather simplistic, if not deficient, as the physiological in vivo firing statistics of dentate gyrus granule cells is much more irregular: Extended periods of low-frequency firing are interspersed with bursts of high-frequency activity reflecting the behavioral state of the animal. In Chapter 4 we are going to present a new and convenient approach to characterize short-term plasticity at the mossy fiber synapse using irregular stimulus trains and a computational model to extract the underlying processes. Specifically we are going to reveal the exact interdependence of STP and LTP, which leads us to a hypothesis about the functional significance of mossy fiber long-term potentiation.

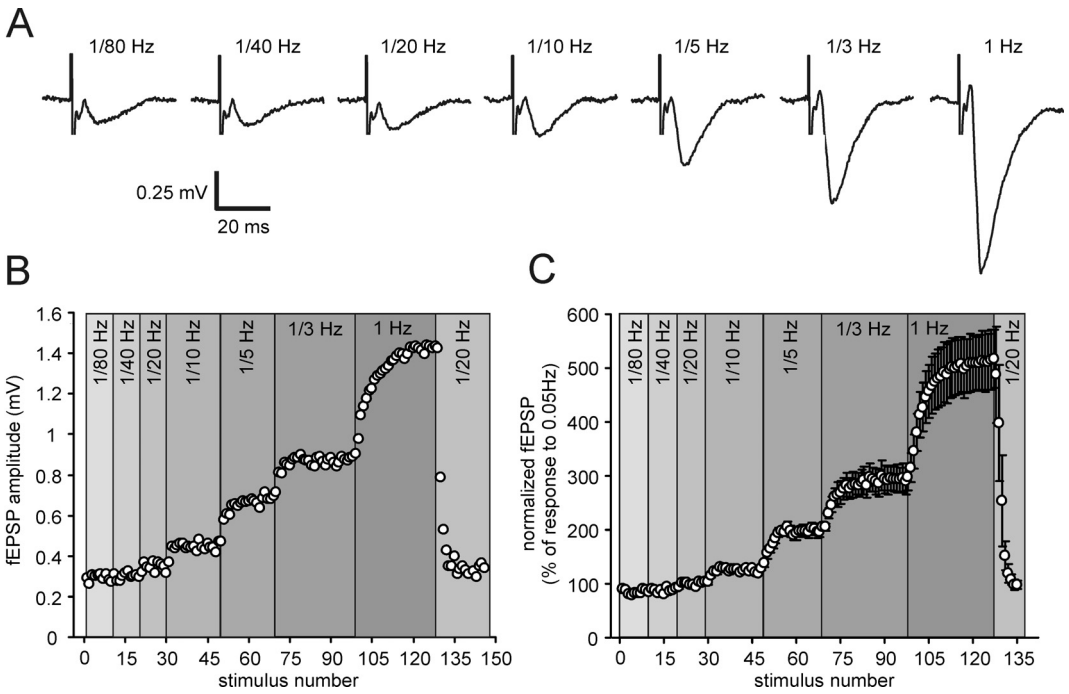

Figure 10: Frequency facilitation at the mossy fiber synapse. (A) Constant stimulation of mossy fibers at increasing frequencies leads to increasing fEPSP amplitudes. Responses are facilitated from initially 0.3 mV at 1/80 Hz up to 1.5 mV at 1 Hz stimulation frequency. Traces depict averages of 10 sweeps each. (B) Timecourse of experiment in A. Facilitation of response amplitudes is fully reversed upon switching the stimulation frequency back to 1/20 Hz. (C) Similar dynamics were measured in n = 5 such experiments. Shown are mean values ± SEM, values are normalized to response at 1/20 Hz.

2.4.3 Physiological Basis and Regulation of Mossy Fiber STP

In general, the amount and sign of short-term plasticity of a synapse mainly depends on its basal transmitter release probability *p*. If *p* is low, synapses tend to exhibit facilitation due to presynaptic accumulation of calcium. In contrast, if *p* is already high, synapses tend to exhibit depression mainly due to a depletion of the presynaptic readily releasable pool of vesicles. As discussed above, the giant mossy fiber synapse is characterized by a rather low probability of transmitter release at each active zone (Hallermann et al., 03; Lawrence und McBain, 03). Thus, its large facilitatory STP follows the formal prediction. The physiological basis of a low transmitter release probability *p* is synapse specific and may rely on regulation of presynaptic calcium influx, calcium buffering, calcium channel location and/or intrinsic conductances as discussed above. For the hippocampal mossy fiber synapse the following critical parameters underlying short-term plasticity were found:

Recently, a major determinant of the low *p* at the mossy fiber synapse could be unravelled (Moore et al., 03). It was proposed that basal MF synaptic transmission is modulated by tonic activation of inhibitory $Gi_{/o}$-proteins. This tonic inhibition of transmission is mediated by A_1-receptors, which are activated by an ambient level of adenosine specifically at the mossy fiber synapse. Antagonizing either the $G_{i/o}$-protein or A_1-receptor activity pharmacologically or by knock-out hereby led to a significantly enhanced basal synaptic transmission and consequently a dramatically reduced short-term

plasticity. Although still controversially discussed (Dietrich et al., 03), but see (Fedele et al., 05), regulation of transmitter release by adenosine appears to critically shape the STP behavior of MF synapses. In Chapter 3 of this thesis we are going to present the intracellular signalling cascade by which adenosine downregulates transmitter release and therewith imposes the hippocampal mossy fiber synapse with its specific short-term dynamics.

Additionally, presynaptically expressed kainate receptors have been shown to contribute to the remarkable mossy fiber facilitatory short-term plasticity (Schmitz et al., 01; Lauri et al., 01; Lerma, 03). Low concentrations of kainate cause an increase in presynaptic fiber excitability and enhance synaptic transmission. As the presynaptic kainate receptors can be activated by synaptically released glutamate, they act as autoregulators of synaptic efficacy and take part in facilitation of synaptic response during repetetive stimulation of mossy fibers.

Finally, a recent technical devolopment made it possible to monitor presynaptic intrinsic conductances by direct patch-clamp recordings of the giant mossy fiber bouton (Bischofberger et al., 06; Geiger et al., 02). Using this technique, it could be shown that presynaptic Ca^{2+} influx is dynamically regulated during high-frequency stimulation by fast inactivation of K^+ conductances (Geiger und Jonas, 00). During repetitive stimulation the presynaptic action potential waveform is increasingly widened and amplified, which leads to enhanced calcium influx and consequently to an increase in synaptic efficacy. Furthermore, the specific properties of Na^+ channels at the giant mossy fiber terminal, such as rapid activation and inactivation kinetics and high density, also amplify the presynaptic action potential and enhance calcium influx (Engel und Jonas, 05).

Summarizing, mossy fiber synaptic short-term plasticity is based on and regulated by a manifold combination of distinct intracellular mechanisms. All of them contribute to the most remarkable feature of MF synaptic physiology with its large facilitation of synaptic transmitter release on an extensive range of timescales from tens of milliseconds to tens of seconds.

2.5 Long-Term Plasticity at the Mossy Fiber Synapse

The hippocampal mossy fiber synapse not only exhibits pronounced short-term plasticity but also experiences longer-lasting changes in synaptic efficacy. These can be induced either activity-dependently with specific stimulus paradigms or chemically by pharmacologically stimulating the respective intracellular transduction pathways. Mossy fiber synapses onto CA3 pyramidal cells can undergo both long-term potentiation (LTP) as well as long-term depression (LTD). In the following paragraphs, we are going to present the phenomenology of these bidirectional regulations of synaptic strength by elucidating their induction and expression mechanisms and giving an outlook on their functional significance.

2.5.1 Long-Term Potentiation

Long-term potentiation at the hippocampal Schaffer collateral synapse onto CA1 pyramidal cells is the most commonly studied form of long-lasting synaptic plasticity. Here, high-frequency repetitive stimulation of the fiber tract leads to an enhancement of synaptic transmission due to an increased insertion of AMPA-type glutamate receptors in the postsynaptic membrane. This potentiation is dependent on the concurrent presynaptic action potential activity and postsynaptic activation of NMDA-type glutatamate receptors

and is therefore thought to be ‘associative’ in a Hebbian sense. Mossy fiber LTP, however, differs from this classical view of LTP in both its induction and expression mechanisms.

Phenomenologically, extracellular tetanic stimulation of the mossy fiber pathway with high frequencies also leads to a robust increase in postsynaptic responses. In an examplary fEPSP recording (Figure 11A and B), application of 3 closely timed 125 pulse trains at 25 Hz potentiated response amplitudes to ~220 %, with a robust increase still apparent after 20 min of recording. The initial post-tetanic potentiation (PTP) is generally large at MF synapses (here: about 500 %) and quickly decays in the first minutes after LTP induction. The paired pulse ratio with an ISI of 50 ms was reduced after LTP from ~3 to 2.3. What are now the exact mechanisms of induction and expression of mossy fiber long-term potentiation?

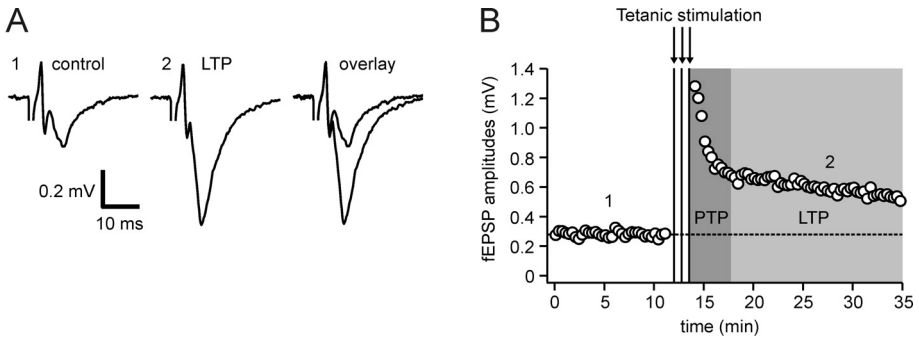

Figure 11: Long-term potentiation at the mossy fiber synapse. (A) Mossy fiber synaptic responses can undergo long-term changes in synaptic strength. Traces depict averages of 10 sweeps each from experiment in B. (B) Tetanic stimulation of the mossy fiber tract (3x bursts of 125 stimuli each at 25 Hz stimulation frequency) led to a pronounced, long-lasting increase in fEPSP amplitude as compared to the stable baseline response, with the mossy fiber specific large amount of post-tetanic stimulation (PTP).

In clear contrast to Schaffer collateral LTP, long-term potentiation at the mossy fiber synapse was shown to be independent of NMDA-receptor activity: Application of the NMDA-receptor specific antagonists such as AP-V did not block the expression of long-term potentiation (Harris und Cotman, 86; Zalutsky und Nicoll, 90). This independence might be due to the lower expression of NMDA-receptors at mossy fiber synapses (compare 2.2.3). Moreover, MF synapses might even lack the appropriate downstream intracellular machinery for expressing NMDA-R dependent LTP via AMPA-receptor trafficking (Kakegawa et al., 02). It is still controversially discussed whether the induction of mossy fiber LTP requires or is modulated by a rise in postsynaptic Ca^{2+} through an alternative pathway other than calcium permeable NMDA-receptors, such as release from intracellular stores or entry through voltage-dependent calcium channels (Yeckel et al., 99). Additionally, a number of studies aimed at elucidating the role of presynaptic metabotropic glutamate and kainate receptors in the induction of MF LTP. Both these receptor groups appear to play a modulatory role in the induction phase, but are not essential. Recently, presynaptically expressed R-type calcium channels were shown to regulate the induction of MF-LTP by lowering its threshold (Breustedt et al., 03; Dietrich et al., 03). This is a surprising finding since R-type calcium channels do not participate in basal synaptic transmission. Still, it suggests that calcium influx through this type of Ca^{2+}-channels has preferential access to adenylyl cyclase, which plays an

important role in the expression of MF LTP. In summary, the mechanisms involved in the induction of mossy fiber long-term potentiation are still under debate.

Opposed to the much unresolved issue of induction, the mechanisms behind the expression of mossy fiber LTP are quite well known and agreed upon. It is unanimously accepted that MF LTP is due to an enhancement of neurotransmitter release. This exclusively presynaptic locus of expression could be demonstrated by a number of different experimental and analytical techniques. These include quantal analysis studies using coefficient of variation (CV) analysis, failure analysis and the recording of miniature excitatory postsynaptic currents (mEPSCs), which led to conclude that MF-LTP is characterized by an increase in transmitter release probability *p* (Nicoll und Schmitz, 05). Moreover, mossy fiber STP could be shown to change quantitatively after the induction of LTP, which again reflects a presynaptic locus of expression (Salin et al., 96b; Toth und McBain, 00). The exact intracellular steps that lead to an enhanced neurotransmitter release after LTP could be described as follows (Figure 12):

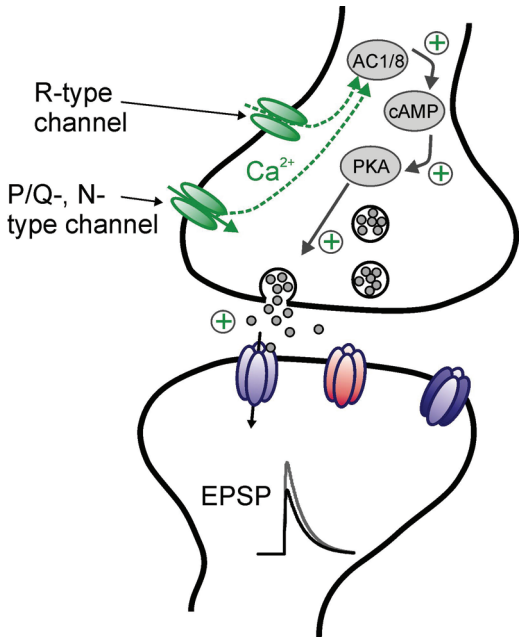

Figure 12: Expression of long-term potentiation at the mossy fiber synapse. Calcium influx through R-type, α1E containing Ca2+ channels leads to activation of adenylyl cyclase 1/8 and enhancement of the downstream signalling cascade. LTP is expressed as an increase in release of the neurotransmitter glutamate.

During LTP induction, Ca^{2+} necessary for activation of the following cascade enters through voltage-dependent calcium channels. Likely candidates are the R-type calcium channels. Then, the signalling cascade involving adenylyl cyclase (AC) protein kinase A (PKA) cAMP was found to be crucial for the expression of LTP (Weisskopf und Nicoll, 95). Pharmacologically activating adenylyl cyclase with forskolin or increasing cAMP concentrations mimick MF LTP (see also Chapter 3), whereas blocking PKA pharmacologically or through genetic mutations prevents LTP (Huang et al., 95). At mossy fiber terminals, the two isoforms AC_1 and AC_8 are expressed and both of them are Ca^{2+}-activated. Up to this point, the expression pathway for MF-LTP is described in detail. The downstream mechanisms of how an increase in PKA activity leads to an increase in neurotransmitter release are, however, less well understood (Nicoll und Schmitz, 05). Studies of synaptic vesicle and release machinery proteins could

demonstrate the requirement of the vesicle protein Rab3A and the active zone protein RIM1α for mossy fiber LTP. RIM1α binds to Rab3A and is a substrate for PKA, so that it might be the next link in the downstream signalling cascade for LTP expression. Yet, in KO mice for these two proteins, application of forskolin for increasing AC activity still leads to an enhancement in neurotransmitter release, which questions their absolute requirement for LTP. Together with controversial findings that presynaptic hyperpolarization- and cyclic nucleotide-activated (HCN) channels might play a role in the expression of potentiation, these studies contribute to the still lively discussion about the exact mechanisms of mossy fiber LTP.

Taken together, there is a growing consensus that Ca^{2+} entry into the presynaptic terminal during tetanic stimulation activates $AC_{1/8}$, and that the subsequent increase in intracellular cAMP concentration is necessary and sufficient for mossy fiber LTP. Long-term potentiation at the mossy fiber synapse is thus expressed through an increase in its release probability *p*. Exactly how an increase in PKA activity can accomplish such a change still needs to be clarified.

2.5.2 Long-Term Depression

Mossy fiber synapses onto CA3 pyramidal cells not only show long-lasting increases in synaptic strength, but also activity-dependent depression of synaptic response amplitudes. Similar to other synapses, this long-term depression (LTD) can be induced by low-frequency stimulation (e.g. 1 Hz for 15 min) and seems to be a reversal of the processes involved in long-term potentiation. Mossy fiber LTD is induced by activation of presynaptic mGluR2 and expressed as a reduction in neurotransmitter release (Kobayashi et al., 96; Yokoi et al., 96). This mGluR2 activation has to be coupled to a presynaptic rise in Ca^{2+}, which again is accomplished by the synaptic activation. Analog to the expression of LTP, mGluR2 activation modulates the same signalling cascade by reducing PKA activity (Tzounopoulos et al., 98). Thus, the mossy fiber CA3 pyramidal cell synapse exhibits bidirectional long-lasting plasticity, which provides the synapse with flexible modulation of its efficacy dependent in response to varying environmental and behavioral circumstances.

3 How Adenosine Modulates Mossy Fiber Synaptic Transmission

Synaptic communication between neurons is precisely and specifically regulated according to behavioral states. In general, this modulation of synaptic transmission is mediated by a wide range of neuromodulators with distinct intracellular effects. Neuromodulation is hereby synapse-specific in that the type of neuromodulators and therewith activated signalling cascades vary remarkably between different types of synapses. The hippocampal mossy fiber synapse presynaptically expresses ionotropic (Min et al., 98; Ruiz et al., 03; Alle und Geiger, 07) as well as several G-protein coupled receptor systems, including opioid, GABAB, mGluRs, and adenosine receptors, (Scanziani et al., 92; Kamiya und Ozawa, 99; Kamiya und Ozawa, 98), which impose mostly inhibitory effects on the synapse upon activation. Some of these modulatory systems have already been studied in detail and their underlying signalling cascades unravelled. Although its direct effect on mossy fiber transmission is well described, the specific intracellular signalling pathway of adenosine receptor mediated inhibition of transmission is not completely understood yet.

In this Chapter, we are going to identify and describe the signalling cascade activated by adenosine at the mossy fiber synapse using electrophysiological and microfluorometric measurements. We will start with an overview of the actions of the neuromodulator adenosine in general, discuss recent findings of its role in mossy fiber synaptic short-term plasticity, before presenting our own data [3].

3.1 Adenosine as a Ubiquitous Regulator of Excitability

The purinergic messenger adenosine is widespread throughout the body and regulates numerous physiological processes in excitable tissues such as the heart and the brain. Many of the actions of adenosine either exert global inhibitory effects, e.g. by slowing the heart rate or reducing neuronal excitability, or increase the delivery of metabolic substrates to highly active tissue, e.g. by vasodilation. Consequently, adenosine appears to couple the rate of energy expenditure to the energy supply in both physiological and pathological conditions (for review see (Dunwiddie und Masino, 01).

Specifically in neuronal physiology, adenosine regulates sleep and arousal states (Porkka-Heiskanen et al., 97; Porkka-Heiskanen et al., 02), acts as a messenger for feedback regulation of transmitter release, and provides a mechanism for coupling the energy demand to the cerebral blood flow (O'Regan, 05). These neuromodulatory actions could be demonstrated by direct measurements of adenosine through microdialysis and behavioral studies, basic pharmacological studies and the use of knock-out animals to

[3] The results presented in this Chapter are based on the manuscript "Adenosine modulates transmission at the hippocampal mossy fibre synapse via direct inhibition of presynaptic Ca2+ channels" by A. Gundlfinger, J. Bischofberger, F.W. Johenning, M. Torvinen, D. Schmitz* and J. Breustedt* (2007). *J Physiol.* 2007 Jul 1;582(Pt1):263-77.

delete specific adenosine receptor subtypes. The most obvious central effect of adenosine in every-day life is that systemic use of the adenosine receptor antagonist caffeine promotes wakefulness and disrupts normal sleep. In the same lines, it could be shown that the endogenous adenosine level progressively increases during prolonged wakefulness and decreases again during subsequent sleep in the basal forebrain of cats.

In addition, adenosine is implicated in a number of neuropathological conditions, where it often excerts an acute protective role under conditions of hyperexcitability, ischemia or hypoxia. Its primary role hereby seems to be the limitation of calcium concentration in cells to reduce excitotoxicity and subsequent damage to the tissue. In several models of epilepsy, adenosine also exhibits anticonvulsant effects. Here, exogeneously administered adenosine agonists reduce seizure activity, while antagonists show proconvulsive effects. Clinically, however, the peripheral sideeffects of adenosine agonists outweigh the therapeutical potential of targeting adenosine receptors for any sort of neuroprotection.

3.2 Regulation of Extracellular Adenosine

There are two primary mechanisms how adenosine can reach the extracellular space in the nervous system: First, via metabolic dephosphorylation of any adenine nucleotides (ATP, ADP, cAMP) via 5'-AMP by ecto-nucleotidases to adenosine (Zimmermann und Braun, 99), and second, by direct release of adenosine from neighbouring cells via diffusion transporters. ATP, for example, is co-released into the extracellular space during release of neurotransmitters such as actylcholine, dopamine, serotonin, and norepinephrin. This ATP is then available for rapid (<1 second) conversion into adenosine, as the necessary ecto-enzymes are highly expressed in the brain and are often present in close physical proximity to adenosine receptors (Cunha et al., 98; Sebastiao et al., 99). In addition to this acute provision of adenosine, the ambient concentration of adenosine in neural systems is equilibrated by passive facilitated diffusion nucleoside transporters. Under normal conditions, adenosine concentration inside cells are low, so that the net flux through the transporters is inwardly directed.

Physiological stimuli that lead to the release, respectively metabolic conversion of adenosine include regulation of the key enzymes in adenine nucleotide metabolism, excess neural activity, and a large increase in energy requirements. In many systems, however, the basal extracellular adenosine concentrations are already sufficient to tonically activate a substantial fraction of the high-affinity subclasses of adenosine receptors (A_1 and A_{2A}), which poses a persistent inhibitory drive onto these synaptic systems. This basal inhibitory tone differs markedly from brain region to brain region and will be discussed for the hippocampal mossy fiber synapse separately later.

3.3 Receptor Subtypes and Signalling Cascades

The various and in part antagonistic effects of adenosine are due to several subclasses of adenosine receptors in the brain, which are linked to a variety of downstream transduction mechanisms (for review see (Fredholm et al., 01). To date, four different adenosine receptor subtypes have been cloned: A_1, A_{2A}, A_{2B}, and A_3. All adenosine receptors belong to the family of metabotropic, seven transmembrane domain, G protein-coupled receptors. They express their neuromodulatory effects by activating

several signalling cascades (for review see (Phillis und Wu, 81; Dunwiddie und Masino, 01).

A_1 receptors are found relatively widespread in the nervous system and exhibit the highest affinity to their endogenous agonist adenosine. They activate the G_i and G_o protein subtypes and thereby inhibit adenylyl cyclase and Ca^{2+} channels on the one hand, and activate GIRKs and phospholipase C on the other hand. These actions pose a general inhibitory effect by inhibiting transmitter release and hyperpolarizing neurons. A_{2A} receptors seem to be more sparesly distributed in the brain and primarily found in the striatum, olfactory tubule and the nucleus accumbens. Conversely to the A_1 receptor, A_{2A} receptor activation leads to stimulation of G_s protein, which activates adenylyl cyclase and inhibits Ca^{2+} channels. Depending on the underlying synaptic system, this either facilitates or decreases transmitter release, which leaves a more diverse effect of adenosine activity. A_{2B} and A_3 receptors are again widespreadly found throughout the nervous system, but exhibit a 50-100 times lower affinity to adenosine. A_{2B} receptors hereby couple to the G_s protein and increase cAMP concentrations by activating adenylyl cyclase and phospholipase C. A_3 receptors are linked to G_i and G_q proteins, which inhibit adenylyl cyclase, increase intracellular Ca^{2+}, and appear to uncouple and desensitize A_1 receptors.

Due to these diverse and contrary actions of adenosine receptor activation, the exact effect of adenosine on a neural system critically depends on its specific expression pattern of the different receptor subclasses. In order to test and critically interpret the actions of adenosine at the hippocampal mossy fiber synapse, we will present known facts about receptor distribution, net effect and functional implications of adenosine receptors in this particular synaptic system in the next section.

3.4 Adenosine at the Hippocampal Mossy Fiber Synapse

Similar to many other systems, activation of adenosine receptors at the hippocampal mossy fiber synapse has been shown to effectively inhibit synaptic transmission (Scanziani et al., 92; Moore et al., 03; Kukley et al., 05; Fedele et al., 05). Postsynaptic response amplitudes are reduced and the frequency of spontaneous transmitter release, as measured in mEPSC recordings, is diminished under acute bath-application of adenosine, while mEPSC amplitudes remain constant.

Recently however, it has been proposed that adenosine not only poses an acute inhibitory effect on mossy fiber synaptic transmission, but there prevails a tonic activation of A_1 receptors (Moore et al., 03). Ambient adenosine thereby leads to persistently reduced postsynaptic responses by activation of $G_{i/o}$ proteins. Removal of the adenosine tone by inactivating A_1 receptor activity using the specific antagonist DPCPX, A_1 receptor knock-out mice and adenosine-degrading enzymes led to a significant increase in mossy fiber synaptic transmission. Most importantly, adenosine receptor activation seems to play a critical role in shaping the unusual short-term plasticity properties of the mossy fiber synapse. The tonic inhibition of synaptic responses by adenosine contributes to the low basal release probability and enables the prominently large range of facilitation as described in Chapter 2. Additionally, removing the A_1 receptor activation significantly impairs mossy fiber LTP expression as seen in pharmacological and knock-out experiments. Although these findings have been confirmed by another group (Fedele et al., 05), a recent study (Kukley et al., 05) found

only minor effects of A_1 receptor antagonism on mossy fiber synaptic transmission. These discrepancies still need to be resolved.

Interestingly, the described effects of a tonic ambient tone of adenosine are highly specific for the mossy fiber synapse and cannot be found even at directly neighboring associational-commissural synapses. There, A_1-receptor antagonism did not lead to a significant increase in synaptic transmission, nor did it change short-term plasticity. Possible explanations for this pronounced difference include specific receptor distributions, locally enhanced adenosine release or metabolism (which could be explained by highly specific expression of ecto-nucleosidases in stratum lucidum) and differences in coupling of the adenosine receptor to its downstream signalling cascades.

Summarizing, the study by Moore et al. elucidated the functional effects of physiologically present tonic adenosine receptor activation. What remains to be clarified is the exact subcellular mechanism how adenosine receptors regulate mossy fiber synaptic transmission. What is the downstream intracellular signalling cascade that in the end leads to the reduced postsynaptic responses and alters short- and long-term plasticity?

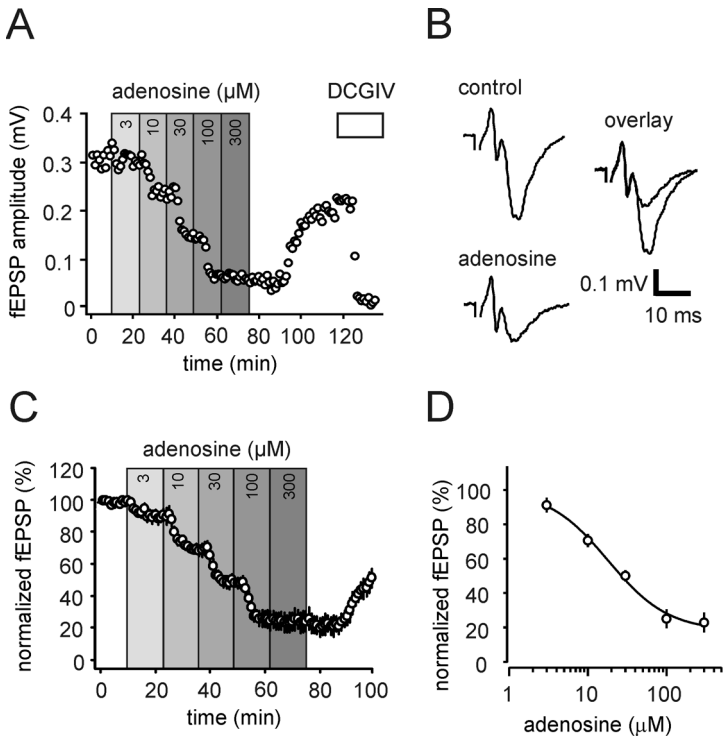

Figure 13: Adenosine inhibits mossy fiber synaptic transmission. (A) Adenosine decreases the response amplitude in an examplary fEPSP recording of mossy fiber synaptic responses in a dose-dependent manner. Saturation of inhibition is reached at 100 µM adenosine and the inhibitory effect is partially reversible upon washout. Application of DCGIV (1µM) leads to complete depression of synaptic responses, verifying mossy fiber origin of response. (B) Average traces of 10 sweeps each for control and adenosine condition from experiment in A. (C) Summary of n = 5 analog experiments as in A. (D) Fitting the underlying dose-response curve with a logistic equation (see Appendix A) yielded an apparent EC_{50} of 18 µM extracellular adenosine for inhibition of mossy fiber synaptic response amplitudes.

3.5 Adenosine Decreases Mossy Fiber Synaptic Transmission via A_1- Receptors

First, we needed to determine the exact impact of adenosine on postsynaptic response amplitudes. To this end, we selectively stimulated mossy fibers with an extracellular electrode and recorded the evoked field excitatory postsynaptic potentials (fEPSPs) in stratum lucidum of area CA3. As depicted in Figure 13A and B, application of adenosine decreased the fEPSP amplitude in a dose-dependent and reversible manner. Mossy fiber origin of the synaptic responses could be verfied by a complete depression of the fEPSP amplitude under application of DCGIV at the end of the experiment. In a summary of n = 5 experiments, the maximal suppression of the response amplitudes was obtained with a concentration of 100 to 300 µM adenosine, reducing the fEPSP to 25.0 ± 5.5 % and 22.8 ± 5.9 % of control values respectively (Figure 13C). We were able to determine an EC50 of 18 µM for adenosine action at the mossy fiber synapse by fitting the dose-response curve with a logistic equation (Figure 13D).

The adenosine receptor subtypes A_1, A_{2A} and A_3 have been shown to be expressed in the hippocampus (Fredholm et al., 01). To identify the subtype responsible for the inhibition of mossy fiber synaptic transmission, we tested the effects of specific adenosine receptor agonists. Application the A_1 receptor agonist CPA (300 nM) reduced fEPSP amplitudes to 24.5 ± 2.9 % of controls (n = 6; Figure 14A), whereas application of the A_{2A} receptor agonist CGS (200 nM) or the A_3-selective agonist IB-MECA (200 nM) did not result in a significant suppression of synaptic transmission (Figure 14B; CGS: 94.6 ± 5.6 %, n = 5; IB-MECA: 84.6 ± 4.9 %, n = 4). Conversely, and as has been reported before (Moore et al., 03; Fedele et al., 05); but see (Kukley et al., 05), application of the specific A_1 receptor antagonist DPCPX led to a large increase in synaptic transmission (Figure 14C). As can be seen in Figure 14D, the enhancement on mossy fiber synaptic transmission by DPCPX was consistently reproducible over slices with concentrations of both 30 and 200 nM, which increased response amplitudes to 298.2 ± 39.9 % (n = 4) and 403.3 ± 54.7 % (n = 5) of control values, respectively.

Additionally, under the influence of DPCPX, the inhibitory effect of adenosine was fully blocked, which further confirms the A_1 receptor specificity (Figure 14C and D). Thus, so far we could establish that inhibition of synaptic transmission by adenosine can be entirely explained by activation of the A_1 receptor subtype, since the application of CPA mimicked and treatment with DPCPX blocked the effect of adenosine.

3.6 Adenosine Acts through a Presynaptic Mechanism

In the last paragraph, we could show that adenosine decreases mossy fiber synaptic transmission both when applied acutely and due to the action of a persistent ambient tone of extracellular adenosine. This observed reduction of fEPSP amplitudes by adenosine could be caused by (1) a presynaptic reduction of transmitter release, (2) a postsynaptic effect, e.g. through hyperpolarization of the postsynaptic membrane, or (3) both (Proctor und Dunwiddie, 87). A presynaptic decrease in transmitter release probability will result in a reduced postsynaptic response but is also predicted to increase short-term facilitation (Zucker und Regehr, 02). To discriminate between these scenarios we performed the following sets of experiments.

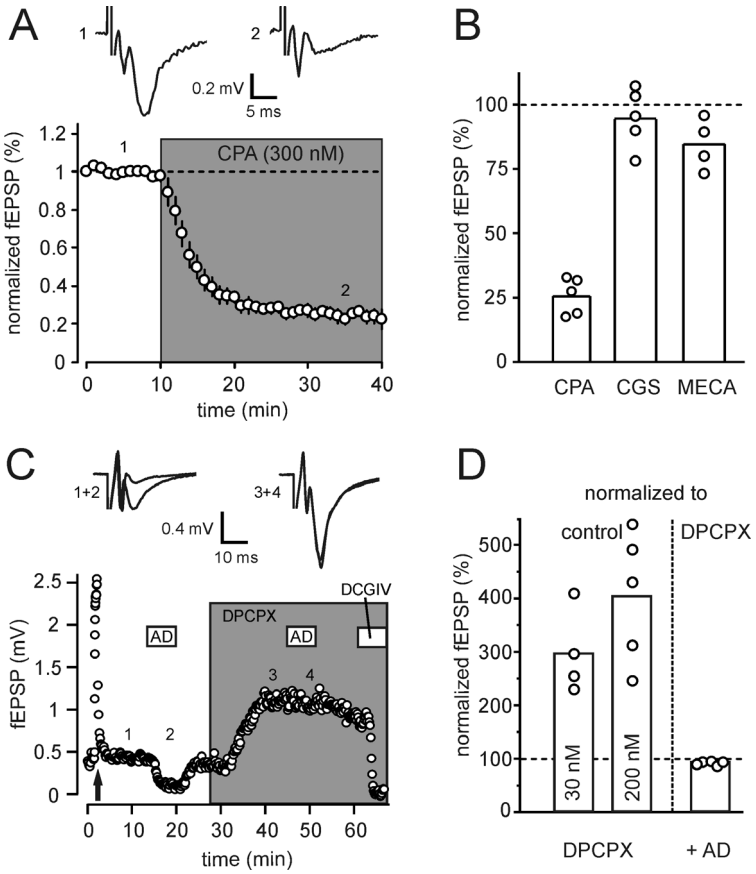

Figure 14: Adenosine inhibits mossy fiber synaptic transmission via A1-receptors. (A) Application of the selective A1-receptor agonist robustly inhibits synaptic transmission to ~25 % of control values (n = 6). Upper traces show mean responses in control and adenosine of 10 sweeps of an examplary experiment, each. (B) Summary of pharmacological experiments using the A_1-, A_{2A}- and A_3-receptor specific agonists CPA, CGS (n = 5), and IB-MECA (n = 4). Only application of CPA leads to a significant inhibition of synaptic responses. (C) The inhibitory effect of adenosine is blocked by pre-application of the A_1-receptor antagonist DPCPX (200 nM). Mossy fiber origin in this exemplary experiment was verified by induction of frequency facilitation (arrow) and complete blockage of response under DCGIV (1 µM). Upper traces are mean responses of 10 sweeps each. (D) DPCPX robustly leads to a pronounced increase in synaptic response amplitudes at concentrations of both 30 (n = 4) and 200 nM (n = 5). Preapplication of DPCPX blocks the inhibitory action of adenosine (n = 5).

Typically, short-term plasticity is tested by synaptic stimulation with two closely timed pulses evoking paired-pulse facilitation or depression. In our case, however, paired pulses (ISIs of 50-100 ms) were not the appropriate measure for short-term plasticity, as reduction of extracellular Ca^{2+} did not result in consistent changes in the paired-pulse ratio (data not shown). Therefore, we recorded mossy fiber fEPSP responses to short stimulus trains of 5 pulses each with inter-stimulus intervals of 50 ms (Toth et al., 00). Similar to paired-pulse paradigms, the amplitude ratio between the 5th and the 1st response is hereby indicative of the short-term facilitatory behavior of the synapse and any changes in this ratio are interpreted as indications for a presynaptically mediated effect. We tested the sensitivity of this measure with a purely presynaptic manipulation by lowering the external Ca^{2+} concentration to 1.0 mM (Figure 15A). The response ratio significantly increased from 3.5 ± 0.3 under control conditions to 6.1 ± 0.8 in the low Ca^{2+} condition

(n = 5; $p < 0.05$, paired t-test). Similarly, application of 300 µM adenosine led to a significant increase in the 5th to 1st response ratio from 4.4 ± 0.5 to 6.2 ± 1.1 (n = 5; $p < 0.05$). This change in short-term plasticity thus hints at a presynaptic locus of adenosine action.

Mechanistically, a change in the presynaptic action potential (AP) waveform could also pose a direct influence on transmitter release (Sabatini und Regehr, 97; Qian und Saggau, 99) by changing calcium influx into the presynaptic terminal. The fiber volley, i.e. the extracellularly measurable potential stemming from passively propagated APs in the presynaptic fibers, is a sensitive measure of these AP waveforms. In our experiments, however, application of adenosine did not lead to any changes in this parameter. Fiber volley amplitude and kinetics were unchanged (Figure 15B and C), arguing against an adenosine-mediated change of the presynaptic AP waveform.

As another measure for the location of action, a reduction in presynaptic transmitter release is expected to result in a higher incidence of synaptic failures, i.e. presynaptic stimulation without successful synaptic transmission. Therefore, we obtained whole-cell recordings from CA3 pyramidal neurons while applying low-intensity extracellular stimulation of mossy fibers (Figure 16A). As typical for mossy fiber synapses, response amplitudes were highly variable with a mean EPSC amplitude of ~129 pA. Subsequent application of adenosine (100 µM) led to a clear and reversible reduction in evoked mean EPSC amplitude to ~31 pA. Already obvious from this single example is the increase in synaptic failures in the presence of adenosine. Reconfirmingly, in n = 6 experiments, the rate of transmission failures was significantly increased from 11.7 ± 2.9 % under control conditions to 60.8 ± 10.8 % under the influence of adenosine (Figure 16B, $p < 0.005$, paired t-test).

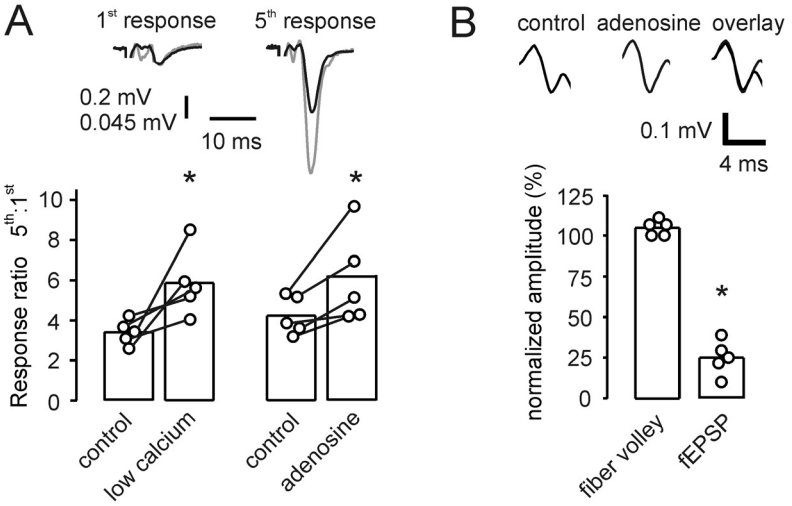

Figure 15: Changes in short-term plasticity and stable fiber volley parameters. (A) Lowering neurotransmitter release probability by decreasing extracellular Ca2+ concentration from 2.5 to 1 mM leads to a significantly increased response ratio of 5th to 1st response in a 5-pulse stimulus train (n = 5). Upper traces show averages of 10 sweeps each of an examplary experiment for control (black line) and low calcium (grey line) condition. Note that responses are scaled to 1st response under control condition. Similarly, application of adenosine (100 µM) also increases the response ratio (n = 5). (B) Application of adenosine leaves the presynaptic fiber volley unchanged, while the postsynaptic response amplitude is significantly decreased (n = 5)

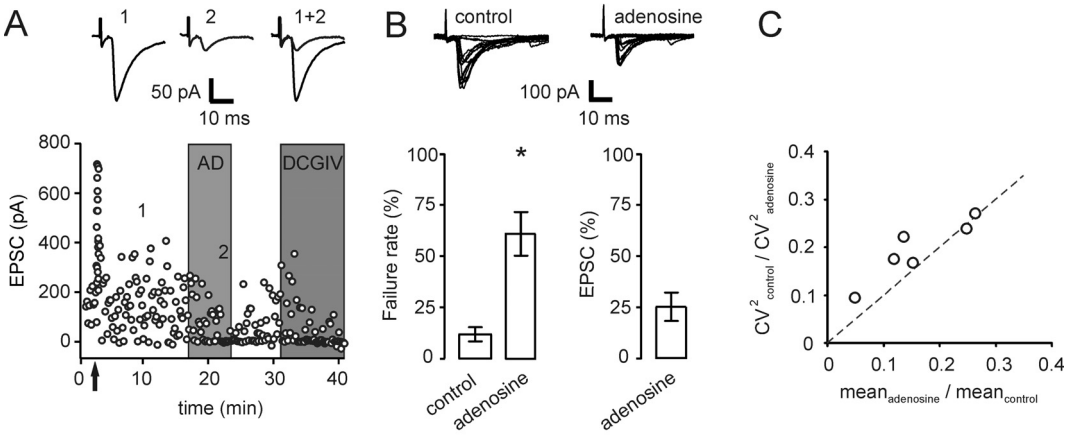

Figure 16: Whole-cell recordings from CA3 pyramidal cells further argue for a presynaptic locus of adenosine action. (A) In an exemplary recording of mossy fiber synaptic responses, application of adenosine (100 µM) leads to a reduction in EPSC amplitude and an increase in the number of synaptic failures of transmission. The effect is reversible upon washout. Upper traces show mean responses of 20 sweeps each for control and adenosine condition. Frequency facilitation (arrow) and inhibition of response under DCGIV point to selective mossy fiber stimulation. (B) Summary of n = 6 experiments as in A. The incidence of failures of transmission is significantly increased under the influence of adenosine and the mean response amplitude is decreased to ~25 %. Upper traces show 10 individual sweeps under control and adenosine condition. (C) Analysis of the coefficient of variation shows a linear relation between the changes in mean response amplitude and CV^2

As derived from the same set of experiments, the ratio of the coefficient of variance ($CV^2_{control}$ / $CV^2_{adenosine}$) scaled linearly with the change of the mean response in adenosine ($mean_{adenosine}$ / $mean_{control}$) (Figure 16C). According to a simple binomial model of a synaptic connection between two neurons, it is predicted that the CV of the EPSC amplitude is strongly dependent on the presynaptic parameters *n* (number of release sites) and *p* (probability of release) and mostly independent of the postsynaptic quantal size *q*. An altered CV therefore also argues for a presynaptic locus of action (Faber und Korn, 91).

Importantly, all whole-cell recordings were performed using cesium- and QX314-based intracellular solution to block ion flow through postsynaptic GIRK channels, which could have contributed to the reduction in response amplitude (Trussell und Jackson, 85; Proctor und Dunwiddie, 87). As we did not find any significant changes in the postsynaptic holding current (-6.8 ± 3.1 pA in adenosine compared to control values) and the reduction of response amplitudes was comparable to data from the fEPSP measurements, we rule out a significant contribution of postsynaptic GIRKs in the action of adenosine. From the cumulative evidence presented above we therefore conclude that adenosine decreases mossy fiber synaptic transmission through presynaptically localized receptors.

3.7 The cAMP-PKA Signalling Cascade is not Required for the Effects of Adenosine

As indicated in paragraph 3.4, adenosine receptors in general and also the A_1 receptor in particular can be coupled to different signal transduction cascades and effector mechanisms in different neural systems (Dunwiddie und Masino, 01). At the mossy

fiber–pyramidal cell synapse, the cAMP-PKA signalling pathway has been reported to mediate some of the neuromodulatory effects of glutamate via mGluR-activation (Kamiya und Yamamoto, 97; Maccaferri et al., 98). We therefore aimed to elucidate the direct involvement of the cAMP-PKA signalling cascade in the inhibitory effects of adenosine on mossy fiber synaptic transmission. To this end, we made use of occlusion experiments, which are based on the assumption that if two measurable effects are mediated by one common underlying mechanism, modulating one effect will have a direct influence on the other. We used several pharmacological tools to modulate the activity of the cAMP-PKA signalling cascade and monitor their cross-effects with the effectivity of adenosine.

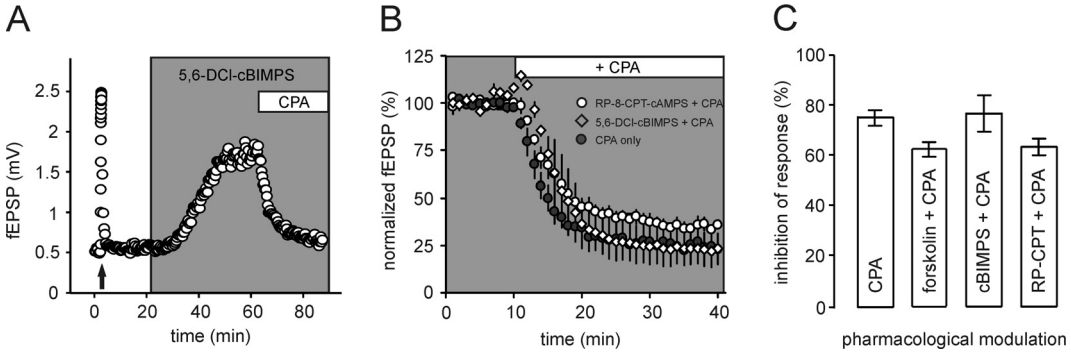

Figure 17: Inhibition of mossy fiber synaptic transmission by adenosine is not mediated by modulation of the cAMP-PKA pathway. (A) Preapplication of the membrane-permeable cAMP analogue 5,6-DCl-cBIMPS (100 µM) does not occlude CPA-mediated inhibition of fEPSP amplitudes. Arrow points to frequency facilitation. (B) Several experiments as in (A) demonstrate comparable effectivity of A1 receptor agonism by CPA under preapplication of either 5,6-DCl-cBIMPS (n = 4) or preincubation with the PKA-inhibitor RP-8-CPT-cAMPS (100 µM, n = 5). (C) Summary of results from (B) and similar experiments with preapplication of forskolin (25 µM, n = 8) activating adenylyl cyclase. No significant difference in inhibition was found between control values with CPA application alone and the three experimental groups exposed to the different pretreatments (1-way ANOVA with Dunnett's multiple comparison post-test, p > 0.05 for all groups).

In our experiments, application of the cAMP analogue Sp-5,6-DCl-cBIMPS (100 µM) led to a strong enhancement of mossy fiber response amplitudes (Figure 17A), confirming the pathway's importance in basal synaptic transmission (see Chapter 2). However, subsequent addition of the A1-receptor agonist CPA (300 nM) with the cAMP analogue still present led to a significant reduction of the fEPSP amplitude. This tendency could be confirmed in n = 4 similar experiments, where synaptic response amplitudes were decreased to on average 37.9 ± 3 % with CPA, while activity of the cAMP-PKA cascade was still elevated by cBIMPS (Figure 17B). This relative value is normalized to the fEPSP amplitude in the presence of cBIMPs alone for setting a reference point.

The same holds true for initial application of the adenylyl cyclase activator forskolin (25 µM), where CPA reduced response amplitudes to 23.4 ± 7.3 % (n = 8). Finally, when we first incubated the slices with the PKA-antagonist RP-8-CPT-cAMPS (100 µM, 3-7 hours incubation) and subsequently added CPA, the fEPSP was again reduced to 36.8 ± 3.3 % (n = 5, Figure 17B). As a positive control, we could verify the competetive effectiveness of RP-8-CPT-cAMPS by a significantly reduced impact of forskolin on mossy fiber synaptic transmission in preincubated slices compared to a control group. Forskolin increased response amplitudes to 386.1 ± 73 % in controls and to only 201.2 ± 11 % in preincubated slices (n = 4). There was no significant difference

between the reduction of fEPSP amplitudes by CPA alone and in the presence of the cAMP-PKA modulators (Figure 17C, ANOVA with Dunnett's multiple comparison test).

Summarizing, as increasing or decreasing PKA activity did not interefere with the ability of CPA to depress response amplitudes, we conclude that the cAMP-PKA signalling cascade is not required for the effects of adenosine on mossy fiber synaptic transmission.

3.8 Adenosine Reduces Presynaptic Calcium Influx

A fundamental parameter determining transmitter release is the amount of calcium influx into presynaptic terminals. At the hippocampal mossy fiber synapse, both basal transmitter release and the induction of LTP critically depend on presynaptic calcium channels. Thus, we tested whether a reduction of calcium influx into the presynaptic terminal is responsible for the adenosine-mediated modulation of transmission at the mossy fiber synapse.

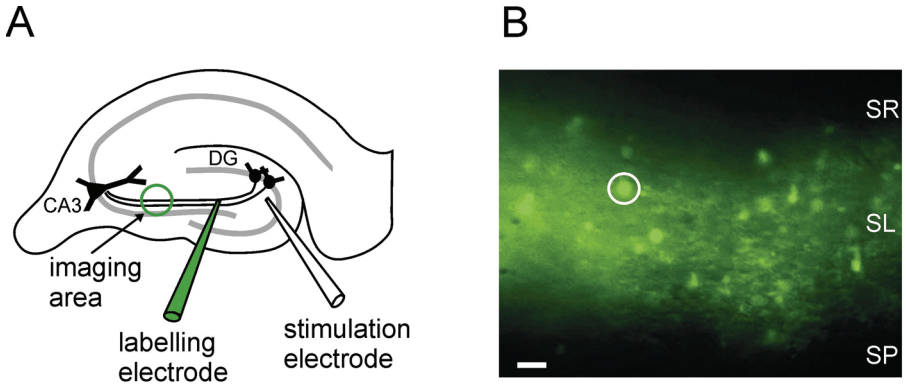

Figure 18: Optical imaging of calcium influx in the mossy fiber band. (A) Scheme of bulk labelling mossy fibers with fluorescent calcium indicator dye. The calcium indicator is transported in the fibers to the imaging area > 400 µm away from the labelling spot. (B) Using this technique, we were able to visually identify individual boutons (white circle) and record a sum response of the fiber tract corresponding to calcium influx in a large number of mossy fiber terminals upon presynaptic stimulation. Visually identifiable are SR = stratum radiatum, SL = stratum lucidum and SP = stratum pyramidale. Image was taken using epiflourescence detected with a CCD camera.

To probe this question, we first made use of an optical recording technique to monitor calcium transients (Regehr und Tank, 91; Breustedt et al., 03). In this approach, mossy fibers, projecting from the dentate into the CA3 region, are selectively labelled with a fluorescent calcium indicator dye (Figure 18). Action potentials are then elicited by extracellular stimulation in the hilar region of the dentate gyrus and the resulting calcium influx into mossy fiber terminals can be detected as the stimulus-locked change in fluorescence intensity. Using this method, we were able to record stable calcium transients over prolonged periods of time. The fluorescence intensity reflecting acute calcium influx is hereby expressed as $\Delta F/F$, i.e. the change of intensity in relation to the basal fluorescence intensity without external stimulation. After establishing a stable baseline response, application of adenosine (100 µM) or CPA (300 nM) reduced the calcium influx significantly (Figure 19A). Calcium transients were inhibited to 74 ± 5 % of control values by adenosine (Figure 3-7B, n = 14) and to 76 ± 3 % by CPA (n = 6).

Similar to the fEPSP experiments, adenosine decreased presynaptic calcium entry in a dose-dependent manner, as depicted in the dose-response curve with increasing concentrations of 3, 10, 30 and 100 µM adenosine (Figure 19C). The absolute amount of the reduction of presynaptic calcium influx was, however, smaller than the reduction of postsynaptic response amplitudes. This non-linear dependency will be discussed later.

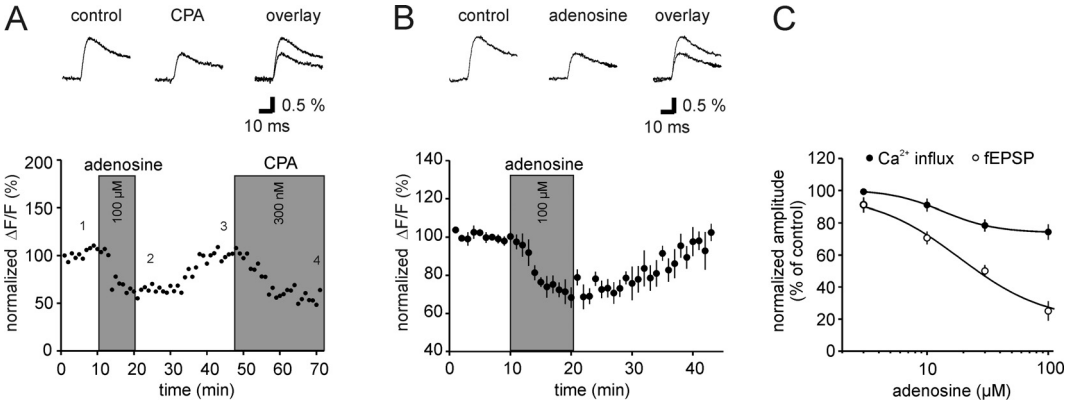

Figure 19: Adenosine reduces calcium transients in presynaptic terminals. (A) Application of adenosine (100 µM) reversibly reduces calcium influx as measured in an exemplary optical imaging experiment. Subsequent application of the A1-receptor agonist CPA (300 nM) leads to comparable reduction in calcium influx. Upper traces depict averages of 5 sweeps each under control and CPA condition. (B) Summary of n = 7 experiments demonstrating the inhibition of calcium influx by adenosine. Upper traces depict averages of 5 sweeps each for control and adenosine condition from experiment in A. (C) Dose-response curves of reduction in calcium influx (black circlecs) and fEPSP amplitude (open circles) for increasing concentrations of adenosine.

The former experiments were performed using a single photodiode, which enables one to monitor changes in calcium influx on a relatively high time resolution. The photodiode, however, lacks spatial resolution, as it detects the summed fluorescence intensity of its region of interest. Therefore, we additionally recorded calcium transients with a Nipkow spinning-disc confocal system in identified single mossy fiber boutons.

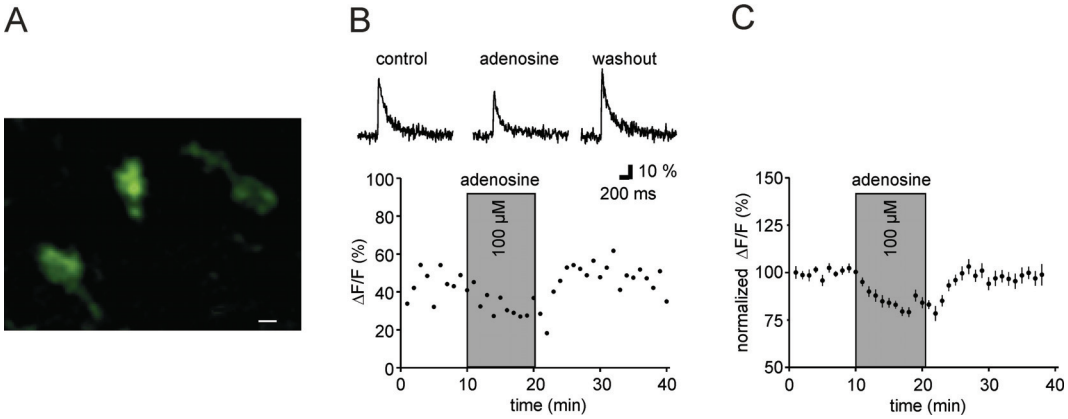

Figure 20: Adenosine decreases calcium transients in single bouton calcium imaging. (A) Picture of three visually identified individual mossy fiber boutons in stratum lucidum. Fibers were labelled with the calcium indicator dye Oregon Green BAPTA-1 AM. Scale bar corresponds to 1µM. (B) Application of adenosine reduces calcium influx in single mossy fiber terminals. Upper traces show averages of 5 sweeps each under control, adenosine and washout condition. (C) Summary of n = 19-22 bouton recordings as in B.

Individual synaptic terminals could be readily identified with this approach (Figure 20A). Moreover, the small laser power per illuminated spot makes it especially suitable for long-term recordings, a necessity for stable pharmacological experiments. Again, application of adenosine (100 µM) reduced the calcium transients in mossy fiber boutons to 82 ± 1 % of control values (Figure 20BC) in good agreement with the photodiode measurements. Also, calcium transients completely recovered to initial values upon wash-out of adenosine.

Taken together, in this paragraph we could demonstrate that adenosine effectively reduces presynaptic calcium influx. This finding could be verified using different approaches to monitor calcium transients, which all led to the same qualitative and quantitative results. Extending this basic descriptive finding, we will continue to elucidate the exact mechanisms of how adenosine modulates presynaptic calcium channels.

3.9 Adenosine Modulates Presynaptic Ca^{2+} Channel Gating

At hippocampal mossy fiber terminals, transmitter release is mediated by voltage-dependent P/Q- and N-type calcium channels, but not by L- and R-type channels (Castillo et al., 94; Kamiya und Ozawa, 98; Breustedt et al., 03); but see (Gasparini et al., 01). In general, N- and P/Q-type calcium channels can be regulated through multiple G-protein-coupled pathways (Ikeda und Dunlap, 99; Hille, 01). Inhibition of Ca^{2+} channel activity is hereby typically caused by a positive shift in the voltage dependence and a slowing of channel activation. In reduced experimental systems (i.e. transfected cell lines), it could be shown that the G protein βγ-subunit acts as the primary regulator of presynaptic calcium channels. We, therefore, performed direct patch-clamp recordings of calcium currents from visually identified mossy fiber boutons (Figure 21A, (Bischofberger et al., 06; Geiger und Jonas, 00) to test whether adenosine inhibits calcium influx through direct modulation of the G-protein subunits βγ (Gβγ).

We were able to evoke large Ca^{2+} currents in single mossy fiber boutons by applying rectangular, depolarizing voltage pulses with a duration of 30 ms from a holding potential of -80 mV to 0 mV in whole-cell voltage-clamp mode (Figure 21B). These calcium currents exhibited an amplitude of 114.5 ± 17.9 pA on average (n = 5 boutons), similar to what was previously described. Application of adenosine (100 µM) significantly reduced the current amplitude to 91.5 ± 1.6 % of control values (Figure 21E, $p < 0.01$, n = 5). This result further confirms the reduction of calcium entry into presynaptic mossy fiber terminals by the action of adenosine as described above by different techniques.

One of the hallmarks of G protein mediated inhibition of Ca^{2+} channels is a pronounced slowing of their activation rate during a depolarizing test pulse (Catterall, 00). Therefore, we analyzed the activation kinetics of the Ca^{2+} channels in the presence of adenosine, which could be fitted with the sum of two exponentials. As can be seen in Figure 21D, activation kinetics were noteably slowed under the influence of adenosine. In n = 5 boutons, the activation was best described by a fast time constant of 0.85 ± 0.25 ms (75 %) and a slow time constant of 9.75 ± 3.37 ms (25 %), leading to a weighted time constant τ_w of 2.55 ± 0.35 ms (Figure 21F). This was about 2 times slower than the activation in control solution, with time constants $\tau = 1.17 \pm 0.15$ ms and $\tau_w = 1.39 \pm 0.19$ ms when fitted with a mono- or biexponential function, respectively.

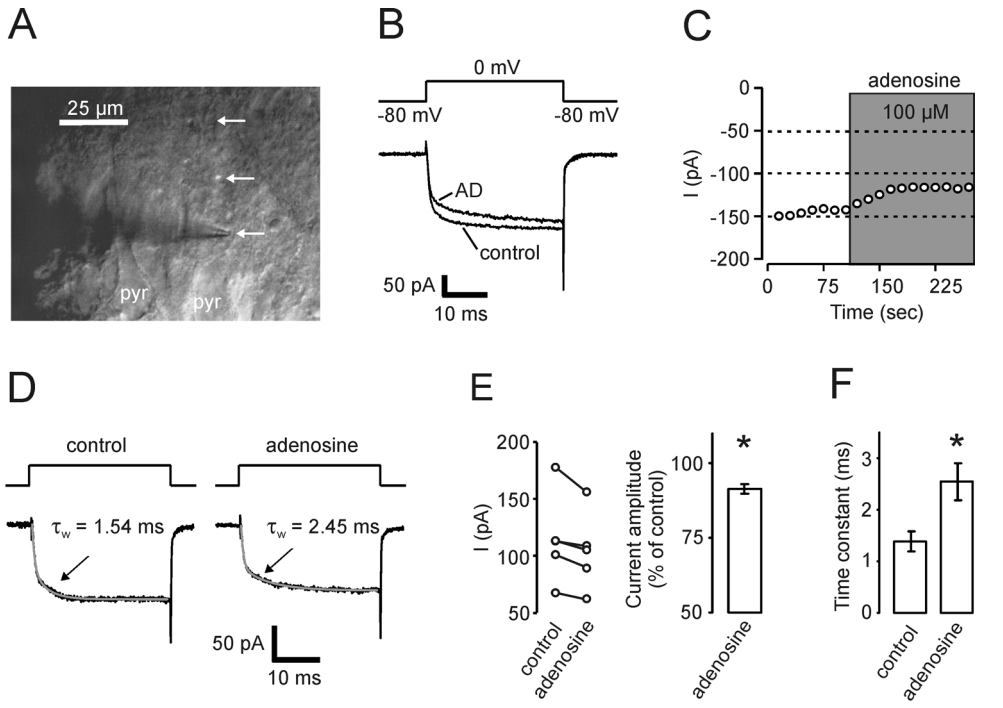

Figure 21: Adenosine inhibits calcium influx into presynaptic mossy fiber boutons. (A) Whole-cell recordings of mossy fiber boutons were performed under visual guidance. Arrows point to mossy fiber boutons, pyr indicates CA3 pyramidal neuron. (B) Application of a 30 ms depolarizing voltage step elicits stable calcium currents in direct voltage-clamp recordings of mossy fiber boutons. Perfusion with 100 µM adenosine leads to a pronounced reduction in amplitude of this current. Traces show averages of 5 to 10 sweeps each. (C) Time course of experiment in A. (D) Adenosine causes a slowing of the activaton time constant of mossy fiber calcium currents. Traces show averages of 7 sweeps each (black lines) and weighted double-exponential fits of the data (grey lines) for control and adenosine condition. (E,F) Summary of n = 5 such experiments. Calcium current amplitude is significantly reduced under application of adenosine, while the activation time constant is significantly increased ($p<0.05$, paired Student's t-test).

These result thus presents evidence for a G protein mediated inhibition of calcium channels by adenosine. Calcium channel kinetics at presynaptic mossy fiber terminals appear to be optimized to produce a transient calcium influx with large amplitude and brief time course in response to action potentials invading bouton (Bischofberger et al., 02). The large calcium influxes are critically important in eliciting transmitter release and the extent of Ca^{2+} current inhibition by adenosine might be more pronounced during short AP-like waveforms in comparison to rectangular activation pulses. Hence, we used a previously recorded action potential waveform as voltage command to elicit more physiological calcium currents (Bischofberger et al., 02). This waveform evoked large and brief Ca^{2+} currents with a peak amplitude of 175.7 ± 37.5 pA and a half duration of 637 ± 116 µs (Figure 22, n = 4 boutons), similar to what was described previously. Application of 100 µM adenosine substantially reduced the Ca^{2+} influx to 79.9 ± 3 % of control values, as estimated by the current integral of 98 ± 9 fC in adenosine versus 123 ± 12 fC in control solution. Calcium currents in mossy fiber boutons as evoked by physiological presynaptic stimuli are hence reduced by adenosine to the same extent as measured with the photo-diode and Nipkow disc systems as described above.

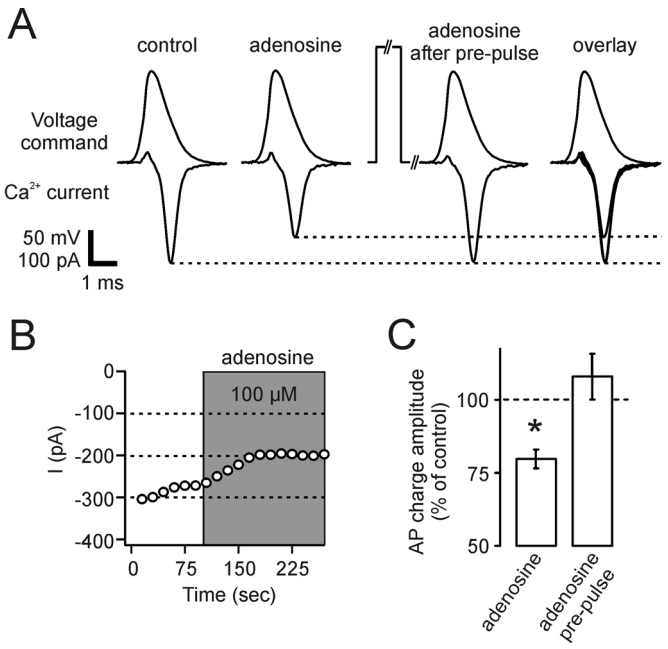

Figure 22: Action potential evoked calcium currents are decreased by adenosine in a membrane-delimited manner. (A) Application of a previously recorded action potential (AP) waveform as voltage-command elicits fast and robust inward calcium currents in direct recordings from mossy fiber boutons, which are significantly inhibited by application of 100 µM adenosine. This decrease in current amplitude is completely recovered with the application of a 50 ms prepulse depolarization to +80 mV shortly before (10 ms) the AP. Traces depict averages of 5 to 10 sweeps each. (B) Time course of experiment in (A) without prepulses. (C) Summary of reduction in AP evoked charge and recovery by prepulse in n=4 boutons.

As Ca^{2+} channel modulation by Gβγ is voltage-dependent, positive voltage pulses transiently relieve any G protein mediated inhibition (Herlitze et al., 96). Therefore, we depolarized the boutons for 50 ms to +80 mV 10 ms prior to the regular AP test pulse to impose such a transient relief. Under control conditions, the pre-pulse robustly led to an increase of the calcium influx in response to the AP pulse to 117.9 ± 3.4 % of values without the pre-pulse. During inhibition of the Ca^{2+} currents by adenosine, application of the pre-pulse consistently led to a recovery of the calcium influx to 108.1 ± 7.5 % of control values (Figure 22 A and C). The same tendency could be observed for calcium currents evoked by rectangular voltage pulses as in Figure 21. Moreover, the activation time constant τ was accelerated to 0.98 ± 0.17 ms after the pre-pulse (83.5 ± 7.8 % of control values without pre-pulse and adenosine).

In this paragraph we could demonstrate that adenosine directly modulates presynaptic calcium channel gating in mossy fiber boutons by a membrane-delimited pathway. This conclusion is based on the findings that adenosine (1) reduces presynaptic calcium influx, (2) slows the rate of activation of calcium channels and (3) these effects can both be reversed by a brief depolarization prior to the test pulses.

3.10 Reduction of Calcium Influx Sufficiently Explains the Effects of Adenosine

Generally, transmitter release is dependent on the presynaptic calcium influx in a highly non-linear fashion (Dodge, Jr. und Rahamimoff, 67; Mintz et al., 95). As shown in the last paragraph, adenosine reduces presynaptic calcium influx to a smaller absolute extent as it reduces postsynaptic response amplitudes at the mossy fiber synapse. Thus, it needs to be clarified whether the described reduction of calcium influx into presynaptic terminals can fully explain the depression of EPSP/Cs by adenosine, or other mechanisms downstream of calcium influx have to be considered.

To probe this question, we needed to know the exact dependence of transmitter release on presynaptic calcium influx. This non-linear relationship differs significantly between different types of synapses (Dittman und Regehr, 96; Kamiya und Ozawa, 98) and can usually best be described by a power function of the form

$$(1) \qquad fEPSP = k \cdot (calcium\,influx)^n$$

We determined the power function of transmitter release for the mossy fiber synapse by modulating the external calcium concentration and thereby changing calcium entry into mossy fiber presynaptic terminals upon stimulation. Corresponding pairs of evoked fEPSPs and presynaptic calcium influx were measured with concentrations of 2.5, 2, 1.5, 1 and 0.5 mM extracellular calcium (Figure 23A). Using data gained under these conditions, we obtained the best power function fit with an exponent of n = 3.7.

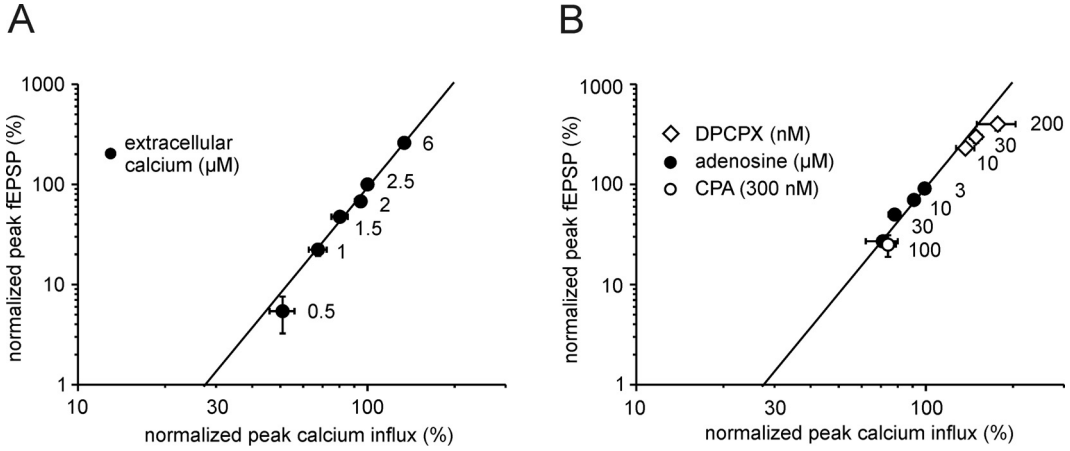

Figure 23: Modulation of presynaptic calcium channels can explain adenosine-mediated modulation of transmission. (A) Relationship between calcium influx and fEPSP for a manipulation exclusively affecting presynaptic calcium influx. Changing the extracellular calcium concentration from 2.5 to 2, 1.5, 1, 0.5 and 6 mM leads to differential alterations in fEPSP and calcium transient amplitudes (n = 5 to 6 experiments each). Values are normalized to the standard extracellular recording solution containing 2.5 mM calcium and 1.3 mM magnesium. The continuous line represents the fit of the data by a power function with an exponent of 3.5. (B) The data of the effects of adenosine (3, 10, 30 and 100 µM), CPA (300 nM) and DPCPX (3, 30 and 200 nM) on calcium influx and fEPSP are compared to the power function fit from the graph in (A).

Importantly, data points gained from comparable experiments using adenosine and the A_1 receptor agonist CPA in various concentrations corresponded well with this power function fit (Figure 23B). Moreover, fitting the power function to data from

measurements with different concentrations of adenosine resulted in a power value of n = 3.5, very similar to what we found as the basal relationship between calcium influx and transmitter release. This finding supports the notion that the inhibition of mossy fiber synaptic transmission by adenosine can be fully explained by a modulation of presynaptic calcium channels.

3.11 Role of Different Calcium Channel Subtypes in Adenosine-Mediated Inhibition of Transmission

As noted above, transmitter release at the mossy fiber synapse is mediated by P-/Q-type and N-type voltage-dependent calcium channels. To investigate whether adenosine selectively modulates a single VDCC subtype (compare (Yawo und Chuhma, 93; Umemiya und Berger, 94) or affects multiple VDCCs (compare (Dittman und Regehr, 96), we performed the following sets of experiments:

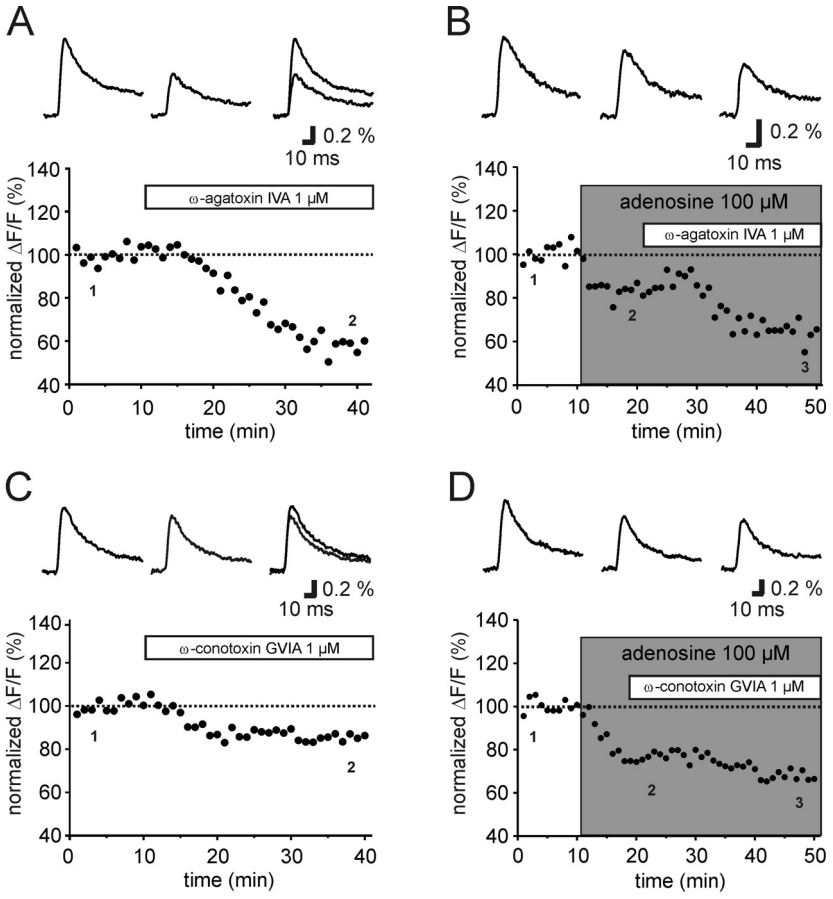

Figure 24: Adenosine inhibits N- and P/Q-type voltage-dependent calcium channels - Absolute contributions. (A) Application of the P/Q-type Ca2+ channel antagonist ω-Agatoxin IVA reduces stimulus-evoked calcium influx by 42 % in the examplary experiment shown. (B) Under preapplication of adenosine, already inhibiting calcium transients, ω-Agatoxin IVA still decreases calcium influx by 20 %. (C) Application of the N-type Ca2+ channel antagonist ω-Conotoxin GVIA leads to a reduction in calcium influx by 15 % in this representative experiment. (D) Under preapplication of adenosine, ω-Conotoxin GVIA still induces a further reduction of calcium influx by 9 %. Upper traces depict averages of 5 sweeps each at timepoints indicated by numbers in the timeplots below, respectively.

First, we measured the specific contributions of P-/Q-type and N-type calcium channels to the total presynaptic calcium influx by applying subtype specific channel blockers. Then, we determined the amount of calcium influx still mediated by the different calcium channels when adenosine already blocks part of them. With these occlusion experiments we were able to determine the relative degree of adenosine-mediated inhibition of the different calcium channel subtypes. Application of the specific P/Q-type channel blocker ω-Agatoxin IVA (1 µM) reduced presynaptic calcium transients by 47 ± 2 % on average (Figure 24A, n = 5). When calcium influx was already partially inhibited by adenosine, addition of ω-Agatoxin IVA led to a smaller relative inhibition of the calcium influx by only 25 ± 3 % (Figure 24B, n = 7, $p < 0.05$). Similarly, application of the N-type specific channel blocker ω-Conotoxin GVIA (1 µM) reduced calcium influx by 20 ± 4 % on average (Figure 24C, n = 7). In the presence of adenosine, ω-Conotoxin GVIA led to smaller relative inhibition of the calcium influx by now only 7 ± 3 % (Figure 24D, n = 7, $p < 0.05$). As can be seen in a summary of all the occlusion experiments in Figure 24 E, adenosine appears to modulate both types of presynaptic calcium channels mediating transmitter release at the mossy fiber synapse.

Based on these results we calculated the relative fractions of each calcium channel subtype that are blocked by adenosine: Adenosine significantly reduced calcium transients through P/Q type channels by 46 % and through N-type channels by 57 % (Figure 25, $p < 0.05$). Thus, adenosine modulates both P/Q- and N-type voltage-dependent calcium channels to inhibit calcium influx into the mossy fiber presynaptic terminals, although to a slightly different extent.

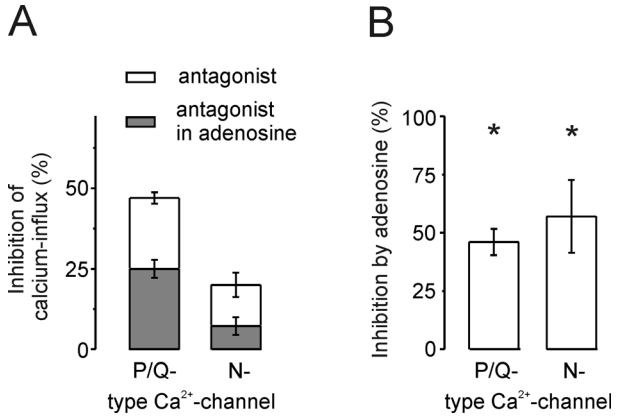

Figure 25: Adenosine inhibits N- and P/Q-type voltage-dependent calcium channels - Relative contributions. (A) The bar diagram depicts the reduction of calcium influx into mossy fiber terminals by the respective calcium channels antagonists in control solution (open bars) and the reduced inhibition of calcium influx in the presence of adenosine (grey bars). (B) Calcium influx through N- and P/Q-type calcium channels is significantly reduced by adenosine. Significances ($p < 0.05$, paired t-test) are indicated by stars (*).

3.12 Concluding Discussion

In this chapter, we have identified and described the transduction pathway by which adenosine reduces synaptic transmission at hippocampal mossy fiber synapses. We could provide evidence that adenosine decreases synaptic responses via presynaptic A_1 receptors involving a direct inhibition of two types of voltage-dependent Ca^{2+} channels (see also Figure 26).

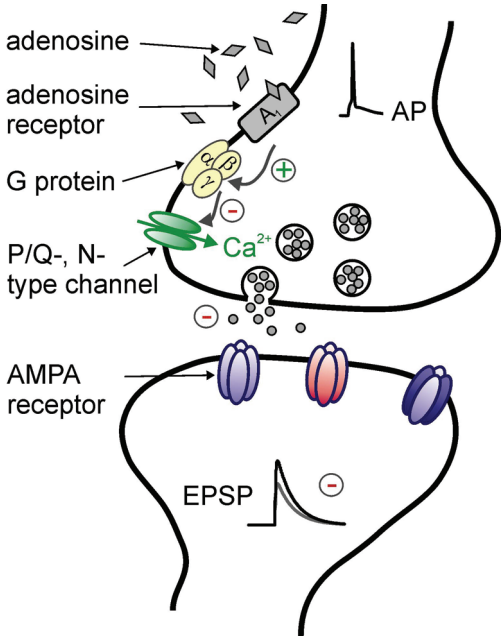

Figure 26: Schematic overview of modulation of mossy fiber synaptic transmission by adenosine. Presynaptically localized adenosine receptors of the A_1 subtype activate the inhibitory $G_{i/o}$ protein. Its βγ-subunit directly modulates Ca^{2+} channel activity in a membrane-delimited manner. AP evoked calcium influx is thus decreased and transmitter release consequently diminished. Postsynaptically, the resulting EPSC is markedly reduced.

The A_1-receptor subtype couples to both G_i- and G_o-proteins in different systems, enabling a number of transduction mechanisms for imposing inhibition of synaptic transmission. These include inhibition of adenylyl cyclase, activation of GIRKs, inhibition of Ca^{2+} channels and activation of phospholipase C (for review see (Dunwiddie und Masino, 01). In principle, adenosine could therefore act at a pre- or a postsynaptic locus of the mossy fiber synapse, or even – by combination of several mechanisms – at both sites.

Our experiments present several lines of positive evidence for a presynaptic locus of action: (1) Short-term plasticity of the synaptic responses was changed after the application of adenosine, in that the fEPSP ratio of the 5th to the 1st response amplitude was significantly increased (Zucker und Regehr, 02). (2) In whole-cell voltage-clamp measurements, application of adenosine significantly increased the rate of transmission failures upon synaptic stimulation, indicating lowered presynaptic release. (3) We found a linear dependence of changes in the coefficient of variation and mean response amplitude of synaptic events (Faber und Korn, 91). And (4), direct patch-clamp recordings from mossy fiber boutons as well as optical measurements showed a reduction of presynaptic calcium currents and calcium influx upon adenosine application. We therefore infer that adenosine mediates inhibition of transmission at the mossy fiber synapse by acting on presynaptic adenosine receptors.

A_1 receptors were shown to be negatively coupled to the adenylyl cyclase-cAMP-PKA signalling cascade in several systems (Ebersolt et al., 83; van Calker et al., 78). In immature hippocampal CA1 neurons, adenosine modulates transmitter release via the PKA pathway, as PKA antagonists block adenosine-mediated reduction of mIPSCs (Jeong et al., 03). At the hippocampal mossy fiber synapse, basal transmitter release and synaptic plasticity crucially depend on activity of the cAMP-PKA cascade (Huang et al.,

94; Tzounopoulos et al., 98). Moreover, the adenylyl cyclase activator forskolin reduces the suppression of mossy fiber synaptic transmission by the group II metabotropic glutamate receptor agonist DCGIV (Kamiya und Yamamoto, 97). Interestingly, this effect is target-specific, as mGluR-mediated depression of transmission of mossy fiber synapses onto CA3 interneurons does not involve cAMP-dependent pathways (Maccaferri et al., 98). In this study, however, we could not detect a direct link between adenosine action and the presynaptic cAMP-PKA transduction pathway. Interference with this signalling pathway by preapplication of forskolin and both the PKA agonist SP-5,6-cBIMPS and antagonist RP-8-CPT-cAMPS did not significantly occlude the efficacy of the A_1 receptor agonist CPA. Thus, adenosine-mediated inhibition of transmission has to be coupled to another transduction mechanism at the mossy fiber synapse.

An efficient way for neuromodulators to influence synaptic transmission is the reduction of presynaptic calcium influx, which has been demonstrated for different modulators in various preparations (Wu und Saggau, 97). Indeed, our electrophysiological as well as the microfluorometric recording experiments provide evidence that adenosine reduces calcium influx into mossy fiber boutons. Both single photodiode measurements and recordings from identified boutons with a Nipkow-spinning-disc confocal system roughly show a 20 % reduction of calcium influx by saturating concentrations of adenosine. In addition, calcium currents induced by action potential like waveforms into mossy fiber terminals were also attenuated by 20 %, confirming the correlation of fluorometric and electrophysiological recordings.

The release sites at the mossy fiber synapse are driven by overlapping domains of multiple calcium channels. This is indicated by the fact that P/Q- and N-type calcium channel blockers add linearly with respect to presynaptic calcium influx but add nonlinearly regarding the effect on synaptic transmission (Castillo et al., 94; Dietrich et al., 03; Breustedt et al., 03). Furthermore the average number of calcium channels that open during action potentials was estimated to be ~20 per release site (Bischofberger et al., 02). Finally, synaptic transmission at the mossy fiber CA3 synapse is sensitive to the slow calcium buffer EGTA (Salin et al., 96b; Blatow et al., 03), indicating a relatively large distance between calcium channels and calcium sensor in the range of several hundred nanometers consistent with overlapping calcium microdomains (Meinrenken et al., 02). Thus, a reduction of calcium flux per channel or a reduction in the number of open calcium channels would show a nonlinear relationship between calcium influx and EPSP (Mintz et al., 95).

The effects of different concentrations of adenosine and of CPA on fEPSP and presynaptic calcium influx amplitudes could be readily approximated by a power function and fit well with our measured calcium dependence of transmitter release for the mossy fiber synapse (with $n = 3.7$). Furthermore, a power function fit based on the agonist experiments yielded a comparable power value n of 3.5. A direct modulation of the release machinery as an additional mechanism for adenosine-mediated inhibition of the synaptic response would have resulted in a considerably higher exponent (Wu und Saggau, 97). Taken together, we conclude that inhibition of presynaptic voltage-dependent calcium channels is sufficient to explain the reduction of synaptic transmission by adenosine.

Both N- and P/Q-type voltage-dependent calcium channels contribute to presynaptic calcium influx and subsequent transmitter release at the mossy fiber synapse (Castillo et al., 94; Kamiya und Ozawa, 99). In contrast, calcium influx through L- or R-type calcium channels is not involved in transmitter release (Castillo et al., 94; Kamiya

und Ozawa, 98; Dietrich et al., 03; Breustedt et al., 03); but see (Gasparini et al., 01). In good agreement with previous studies we found N- and P/Q-type calcium channels to contribute ~ 20 and 47 % of calcium influx, respectively (Miyazaki et al., 05). A selective preference for inhibition of N-type VDCCs by adenosine has been reported at hippocampal Schaffer-collateral synapses (Wu und Saggau, 97), rat brain stem interneurons (Umemiya und Berger, 94), and chick ciliary ganglion neurons (Yawo und Chuhma, 93). On the other hand, an inhibition of multiple VDCC subtypes by neuromodulators has been described at the cerebellar parallel fiber synapse for endocannabinoids, GABA and adenosine (Dittman und Regehr, 96; Brown et al., 04). Using specific toxins for the different channel subtypes we found that adenosine inhibits presynaptic calcium influx through N- and P/Q-type calcium channels to a similar extent (by 57 and 46 %, respectively), arguing for the use of multiple calcium channel subtypes to influence transmitter release at the hippocampal mossy fiber synapse.

Direct G protein βγ-subunit mediated modulation of calcium channels has been almost exclusively described in expression systems and neuronal somata (Bean, 89; Herlitze et al., 96). This is due to the fact that presynaptic terminals are largely inaccessible to direct electrophysiological recordings. A major advancement was made with recordings from the giant presynaptic terminal of the Calyx of Held (Forsythe, 94), where a role for βγ-subunits in GABAB receptor mediated modulation could be established (Takahashi et al., 98; Kajikawa et al., 01). More recently, a technique was developed to obtain patch clamp recordings from identified hippocampal mossy fiber boutons in slice preparations. With this method the functions of intrinsic conductances in transmission and plasticity at this central synapse could be described (Bischofberger et al., 06; Geiger et al., 02). Using direct bouton recordings, we observed two key features of G protein mediated inhibition of calcium currents by adenosine: (1) The slowing of the activation rate of the current and (2) the relief from block by strong depolarization (Bean, 89; Patil et al., 96; Herlitze et al., 96). These results strongly indicate that the activation of adenosine receptors leads to inhibition of calcium channels via a membrane-delimited pathway.

In summary, our results provide evidence that adenosine reduces synaptic transmission at the hippocampal mossy fiber synapse entirely through a presynaptic mechanism involving inhibition of voltage-dependent Ca^{2+} channels by a membrane-delimited pathway. On first sight, this conclusion is in apparent opposition to two earlier reports, which concluded that adenosine acts downstream of calcium influx by monitoring spontaneous synaptic activity (Scholz und Miller, 92; Scanziani et al., 92). Interestingly, a recent study reports that stimulus evoked and spontaneous transmitter release recruit synaptic vesicles from different pools (Sara et al., 05). Whether this selective recruitment from distinct vesicle pools for spontaneous and evoked release holds also true for the mossy fiber synapse and whether adenosine differentially affects these vesicle pools remains to be determined in future studies. In any case, the neuromodulatory action of adenosine contributes to the persistently low release probability at the mossy fiber synapse, enabling for a large range of synaptic facilitation as found under short-term plasticity paradigms, and therefore is of crucial functional importance to the synapse.

4 Interdependence of STP and LTP at the Hippocampal Mossy Fiber Synapse

In the last chapter, we elucidated the intracellular signalling cascade underlying the action of the neuromodulator adenosine at the hippocampal mossy fiber synapse. In addition to such persistent neuromodulatory changes of their efficacy, synapses are dynamic in that they continuously experience short- and long-lasting activity-dependent changes in the size of their postsynaptic response amplitude, or strength. Long-term plasticity (LTP) hereby describes persistent alterations in synaptic strength, whereas short-term plasticity (STP) reflects the instantaneous and reversible modulation of synaptic strength. As discussed already in Chapter 2, the mossy fiber synapse onto CA3 pyramidal cells is known to exhibit both a presynaptic, NMDA-receptor independent form of LTP and a remarkably pronounced form of STP. A detailed description of their functional interdependence is, however, lacking.

In this Chapter, using electrophysiological and modelling techniques, we are going to identify and describe the impact of long-term potentiation on short-term transmission dynamics at the mossy fiber synapse. We will start with an overview of the functional implications of short-term plasticity, compare recent findings on the interdependence of long-term and short-term plasticity in various other synaptic systems, and then present our own findings at the mossy fiber synapse [4].

4.1 Dynamics of Synapses

Synapses exhibit activity-dependent plasticity of their efficacy on timescales ranging from milliseconds to days (for review see (Zucker und Regehr, 02); compare Chapter 1). Consequently, they are not mere relay stations that transmit the incoming information to the next layer of the computational network, but they rather actively govern and modulate the flow of information in neuronal circuits. Based on the timescales of changes in synaptic efficacy, synaptic plasticity is subdivided into (1) short-term plasticity (ms to min) and (2) long-term plasticity (hours to days, or even life-long).

Short-term plasticity describes the instantaneous and reversible increase (facilitation) or decrease (depression) of synaptic response amplitudes under repetitive activation. Functionally, this modulation of synaptic response can generate filtering properties, that might be used in information processing (Galarreta und Hestrin, 98; Fortune und Rose, 01; Abbott und Regehr, 04). Short-term depression usually constitutes low-pass filtering characteristics, favoring onset detection and inducing attenuation to ongoing high-frequency activity. In contrast, short-term facilitation is more prone to produce high-pass filtering characteristics, enabling high reliability of transmission

[4] The results presented in this Chapter are in parts based on the manuscript "Differential Modulation of Short-Term Synaptic Dynamics by Long-Term Potentiation at Mouse Hippocampal Mossy Fibre Synapses" by A. Gundlfinger*, C. Leidbold*, K. Gebert,, M. Moisel, D. Schmitz and R. Kempter (2007). *J Physiol.* Dec 15, 585: 853-65.

during burst like activity epochs (Lisman, 97; Kepecs und Lisman, 03; Klyachko und Stevens, 06a). Experimentally, this history-dependent modulation of transmission can be quantified by measuring synaptic responses to pairs or short trains of constant-frequency stimuli, with inter-stimulus intervals of 50 to 500 ms (see Chapter 1). An additional tool to quantify transmission dynamics of synapses are phenomenological models, that have been applied at various synaptic systems (Sen et al., 96; Varela et al., 97; Tsodyks und Markram, 97; Hanson und Jaeger, 02). Using such models that are based on experimentally obtained transmission parameters one can also predict synaptic responses to arbitrary patterns of stimulation.

Long-term plasticity involves a persistent change in synaptic strength, with long-term depression being a reduction and long-term potentiation an increase in strength. These longer-lasting modulations can be based on a range of pre- and postsynaptic mechanisms. Irrespective of the expression mechanism, however, the function of long-term potentiation was classically regarded as a change in the gain of signals between neurons, as specific synaptic pathways are strengthened. In general, studies on the induction and expression mechanisms of long-term potentiation have been explicitely designed to minimize effects of short-term plasticity on synaptic transmission under investigation, in that synaptic strength is tested by single presynaptic pulses with long inter-stimulus intervals in between. These paradigms are convenient, but hardly physiological. The same holds true for the assessment of short-term plasticity by simple paired-pulse stimuli, merely varying the inter-stimulus intervals between pulses. More recent studies have focussed on using physiologically motivated input distributions, representing irregular in vivo activity of neurons under various behavioral conditions (Dobrunz und Stevens, 99; Dekay et al., 06; Frerking und Ohliger-Frerking, 06). Based on these findings, it has become clear that short- and long-term plasticity processes should not be looked at separately as they critically influence each other, as discussed in the next subsection.

4.2 Interaction of Short- and Long-Term Plasticity

Using a combined experimental and modelling approach, Markram and Tsodyks (Tsodyks und Markram, 97; Tsodyks et al., 96) were one of the first to elegantly highlight the importance of investigating the interactions of short- and long-term plasticity. They could demonstrate that the induction of LTP by temporally pairing action potentials in synaptically connected pairs of layer 5 pyramidal cells in somatosensory cortex resulted in the potentiation of synaptic efficacy as tested with single stimuli. However, when using more complex stimulus trains (in this case bursts of 7 stimuli at 23 Hz), there was no net increase in synaptic strength, as responses to stimuli later in the train were decreased in amplitude. In this case, long-term potentiation thus led to a redistribution rather than a mere gain in synaptic strength due to presynaptic changes in response characteristics. Under *in vivo* conditions, neurons tend to discharge irregular, therefore individual response amplitudes will be altered in a complex manner after the induction of LTP. Broadly speaking, redistribution of synaptic strength might serve as a mechanism to alter the specific dynamics of synaptic transmission and hence alter the content and not the gain of signals between connected neurons.

This new and exciting concept led to investigations of whether redistribution of synaptic strength is a general phenomenon or the interactions of short- and long-term plasticity are distinct in different synaptic systems. In this context, Selig et al. (1999) could demonstrate that both at hippocampal associational-commissural (AC) CA3-CA3

synapses and Schaffer collateral CA3-CA1 synapses, long-term potentiation resulted in a uniform increase of synaptic response amplitudes. Hence, at these types of hippocampal synapses, LTP preserves the fidelity of postsynaptic responses to presynaptic burst stimuli, arguing against redistribution being a general synaptic phenomenon. These differences in results are most likely due to differences in the mechanism of LTP expression at cortical and hippocampal synapses: Whereas synapses between pyramidal cells in the somatosensory cortex undergo a presynaptic change in transmitter release probability after the induction of LTP, both AC and Schaffer collateral synapses exhibit a postsynaptically expressed form of LTP involving a modulation of AMPA-receptor distribution in the postsynaptic membrane. Additionally, somatosensory synapses show a pronounced short-term depression of responses, whereas AC and Schaffer collateral synapses show facilitation. The exact interaction of short- and long-term plasticity is thus synapse-specific and depends on both the STP and LTP characteristics of the synapse under investigation.

As outlined in Chapter 2, the hippocampal mossy fiber synapse at the interface between the dentate gyrus and CA3 region of the hippocampus is a model synapse for an NMDA-receptor independent form of LTP, which is exclusively presynaptically expressed. In addition to LTP, the mossy fiber synapse also shows unique short-term plasticity. Here, a low basal release probability allows for remarkably strong facilitation with decay time constants in the range of up to ten seconds, leading to large paired-pulse facilitation in addition to frequency facilitation (Salin et al., 96b; Lawrence und McBain, 03; Nicoll und Schmitz, 05). To date, the amount and quality of interaction of STP and LTP at the mossy fiber synapse has, however, only partially been determined. Salin et al. (1996b) could show that long-term potentiation reduces the dynamic range of frequency facilitation, in that the relative facilitation at low stimulation frequencies (1/80 to 1/20 Hz) was unchanged, while facilitation at higher stimulation frequencies (1/10 to 1/3 Hz) was significantly decreased. However, Salin et al. have employed constant-frequency test paradigms for the two temporal domains of facilitation at the mossy fiber synapse, which does not reflect the physiological range of transmitter release dynamics and leads to an overlap of the two processes in higher-frequency stimulation domains. Also, paired-pulse facilitation is modulated by LTP, but PPF is typically only determined for one specific inter-stimulus interval, and the reduction in PPF due to LTP can therefore only be used as a qualitative argument for a presynaptic expression locus (Lei und McBain, 04). Thus, using arbitrarily chosen constant-frequency stimuli could neither fully unravel the interactions of mossy fiber long- and short-term plasticity nor detect possible differential modulations of the distinct forms of short-term plasticity.

4.3 Open Questions at the Mossy Fiber Synapse

Why are we interested in studying the interdependence of STP and LTP at the mossy fiber synapse at all? What can we learn about the functional consequences of this interaction? In order to answer these questions we will first look into the main ideas on computational properties and functions of the MF synapse. Classically, owing to the relatively high efficacy of individual synapses and their large facilitatory capacity, the hippocampal mossy fiber synapse was regarded as a detonator or teacher synapse (Urban et al., 01). Activation of a single synapse is able to produce strong depolarization in the postsynaptic CA3 pyramidal cell, even leading to action potential initiation under certain conditions. Therefore, the mossy fiber synapse had been looked at as the primary source of afferent input to CA3 pyramidal cells. More recently, more attention has been given to

the fact that CA3 pyramdidal cells also receive numerous excitatory synaptic input from the perforant path and recurrent AC fibers (see Chapter 2). Still, in terms of the computational properties, this large synaptic efficacy guarantees relatively reliable information transmission between dentate gyrus granule cells and the CA3 region. Additionally taking into account the large and frequency-dependent short-term facilitation, the mossy fiber synapse also provides a substrate for coding of the recent input history. The higher the input frequency, the larger the postsynaptic response amplitude. The synapse hereby acts as a conditional detonator (Lawrence und McBain, 03), in that high input frequencies guarantee spike transmission (Henze et al., 02) from dentate gyrus granule cells over CA3 pyramidal cells to the CA1 region. In contrast to largely depressing synapses, which can act as onset detectors, the hippocampal mossy fiber synapse seems to be tuned to reliably transmit periods of higher frequency input, as for example found in burst events (Lisman, 97). The exact relationship of input statistics and postsynaptic response, i.e. what kind of presynaptic stimulus leads to which postsynaptic EPSC/P amplitude, however, is crucially dependent on the short-term plasticity behavior of the synapse. How large is the facilitation expected to be given certain input frequencies or inter-stimulus intervals, respectively? Is the synapse tuned to specific input distributions? And is this tuning changed after longer lasting changes in synaptic efficacy as found under LTP expression?

In what follows, we will elucidate these questions by investigating the interdependence of short- and long-term synaptic plasticity at the mossy fiber synapse. We will start with a detailed description of STP by electrophysiological experiments. These are the basis for a computational model of the short-term transmission dynamics, which we will use to dissect the underlying short-term plasticity processes, responsible for the characteristics of mossy fiber STP. Then, we will investigate the consequences of mossy fiber long-term potentiation on STP, again using both electrophysiological and computational tools. Finally, we will conclude with a hypothesis about the functional relevance of mossy fiber long-term potentiation.

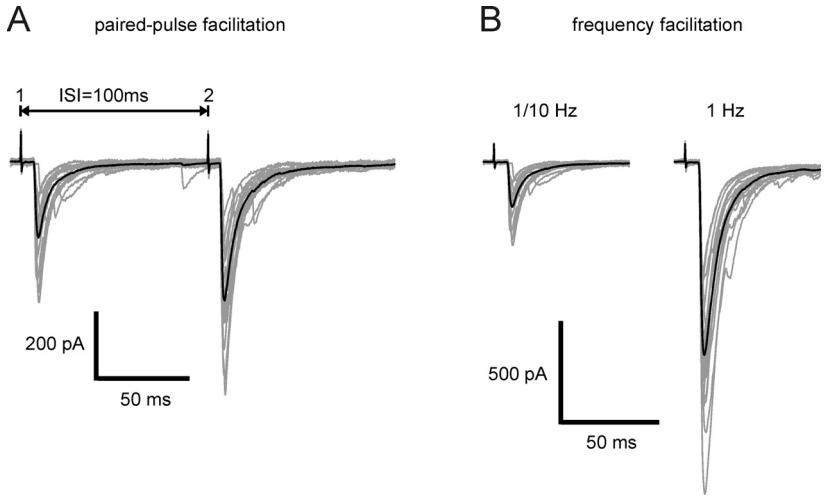

Figure 27: Short-term plasticity as determined by paired-pulse and frequency facilitation paradigms. (A) Applying paired-pulse stimulation with an interstimulus interval (ISI) of 100 ms leads to marked facilitation of mossy fiber synaptic responses in a CA3 pyramidal cell whole-cell recording. Traces depict overlay of 20 trials (grey) and their mean response (black). (B) Applying a frequency facilitation paradigm in the same cell leads to large facilitation of response amplitude. Traces again depict overlay of 20 trials (grey) and mean response (black).

4.4 *Modulation of Synaptic Efficacy by Irregular Stimulus Trains*

In order to assess the short-term transmission dynamics of the hippocampal mossy fiber synapse, we recorded stimulus-evoked excitatory postsynaptic currents (EPSCs) from CA3 pyramidal neurons in whole-cell voltage-clamp mode. Low-intensity extracellular stimulation of presynaptic mossy fibers at constant frequency generally resulted in postsynaptic responses of variable amplitude (compare Figure 7) and the occurrence of failures of transmission of on average 14.2 ± 6.1 % (n = 5 cells). This value is similar to results by Mori-Kawakami et al. (2003), who reported between 14 and 16 % failures depending on age of the animals. In this study, minimal stimulation techniques had been used, so that we have indication of stimulating only a very small number of presynaptic mossy fibers. Having established robust mossy fiber stimulation in single-cell recordings, we could then have determined the short-term response dynamics of the synapse by applying numerous paired-pulse stimuli with varying inter-stimulus intervals in addition to testing the frequency facilitation parameters at different stimulus frequencies (Figure 27). As discussed above, this approach had been used previously at other synapses, but due to the wide temporal range of plasticity at mossy fiber synapses it (1) is largely time-consuming and (2) does not fully reflect the synapse's true dynamics, as not all of the important frequencies and ISIs can be studied in the limited experimental time.

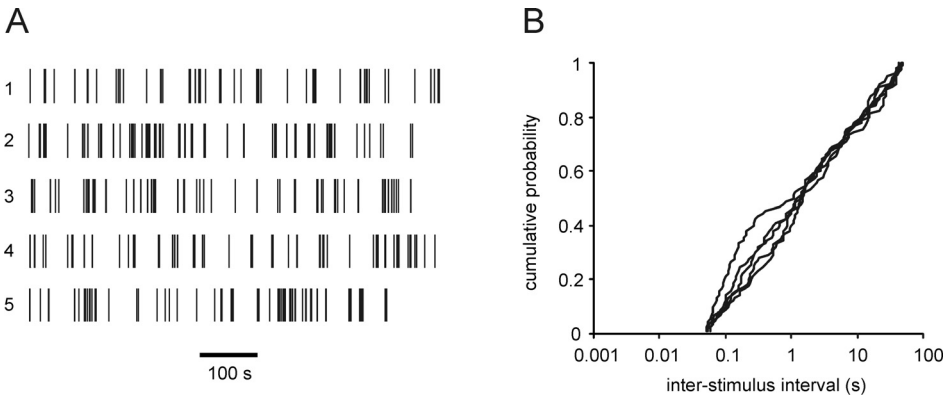

Figure 28: Characteristics of irregular stimulus trains. (A) Five examples of used irregular stimulus trains are depicted. Trains were drawn from a distribution with the probability of a presynaptic spike occuring following a 1/ISI relationship. (B) The 1/ISI distribution is also characterized by the cumulative probability of presynaptic spike occurrence being linearly correlated with the logarithmic ISI.

For unravelling the interdependence of mossy fiber short- and long-term plasticity, however, we needed to accurately quantify STP on all relevant timescales. In order to elucidate short-term plasticity in this more physiological setting, we thus stimulated presynaptic mossy fibers using irregular stimulus trains, that were motivated by in vivo spike train statistics of dentate gyrus granule cells (Mizumori et al., 89; Jung und McNaughton, 93). The chosen stimulus trains followed a 1/ISI distribution and covered a large range of instantaneous input frequencies, with inter-stimulus intervals from 50 ms to 50 s and a resulting median of ~1.5 s (Figure 28). Typically, they consisted of 90-100 stimulation pulses in about 10 minutes.

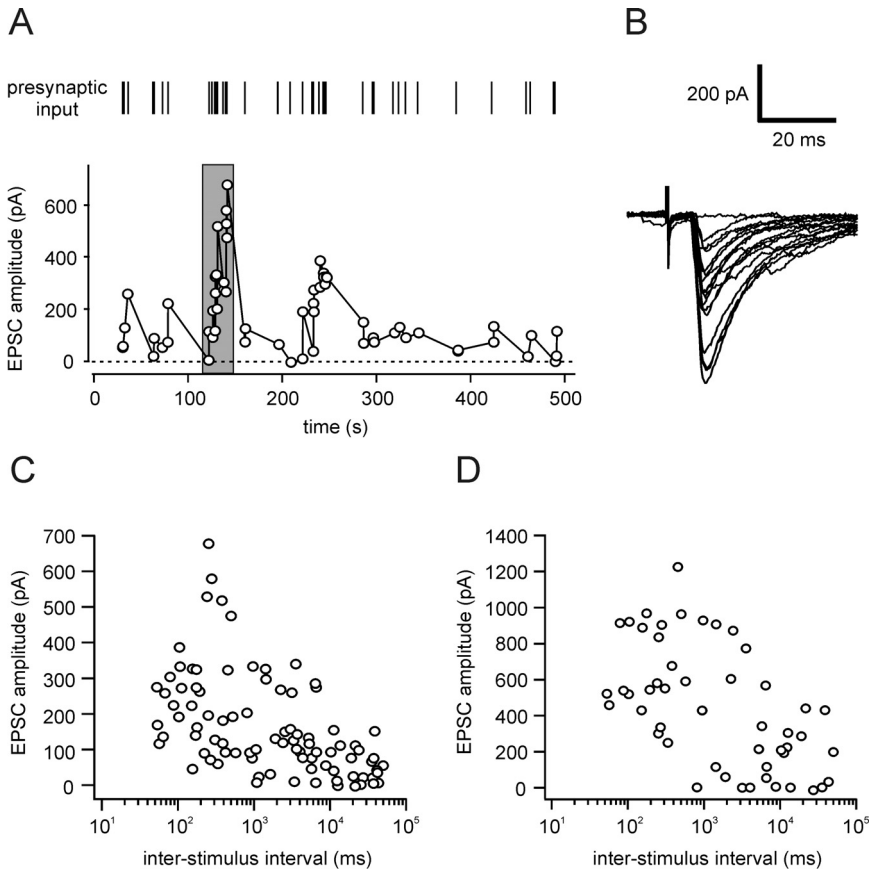

Figure 29: Modulation of synaptic efficacy by irregular stimulus trains. (A) In a whole-cell recordings of a CA3 pyramidal cell, presynaptic mossy fibers were extracellularly stimulated with an irregular stimulus train. Irregular stimulation led to highly dynamic postsynaptic response amplitudes. EPSCs exhibited failures of transmission, pointing at minimal stimulation strength. (B) Overlay of examplary traces from time window marked by grey box in A. (C) Response amplitudes were negatively correlated with the length of the preceding ISI, although a large jitter was detectable. (D) Correlation of responses and ISIs in another exemplary recording, using a different stimulus train.

Application of such irregular stimulus trains led to a strong modulation of postsynaptic response amplitudes in CA3 pyramidal cells (Figure 29A and B). EPSCs following shorter inter-stimulus intervals (ISIs) were typically larger than responses following long ISIs (Figure 29C and D). This pronounced modulation of synaptic response amplitudes with varying presynaptic input reflects the short-term plasticity parameters of mossy fiber synapses. It becomes already clear, however, that the postsynaptic response amplitude is not exclusively determined by the last inter-stimulus interval, owing to the long time constants of facilitation as discussed in Chapter 2. Also, responses in different cells were quantitatively different.

To be able to compare STP across experiments and conditions, we then determined the synaptic 'gain' of response amplitudes as defined recently (Klyachko und Stevens, 06b; Klyachko und Stevens, 06a). Hereby, the gain is the ratio of each individual response amplitude during the stimulus train to the mean 'basal response amplitude' obtained by constant stimulation at 0.05 Hz. Gains of the cell shown in Figure 4-3A ranged from 0 (indicating failures) to 8.9, with a mean ± std value of 2.1 ± 1.9 (Figure 30A). The summary of n = 5 measured cells clearly illustrates the large dynamic

range of EPSC amplitudes at the mossy fiber synapse with gains from 0 to 13.5 and a mean value of 2.7 ± 2.5 (Figure 30B). These values are strikingly larger than at Schaffer collateral (SC) synapses with gains between 0.8 and 3 (Klyachko und Stevens, 06a). Similarly, the coefficient of variation (CV) of response amplitudes as an additional measure for variability was relatively high with a mean value of 0.88 ± 0.04 compared to 0.18 ± 0.07 at SC synapses (Dobrunz und Stevens, 99).

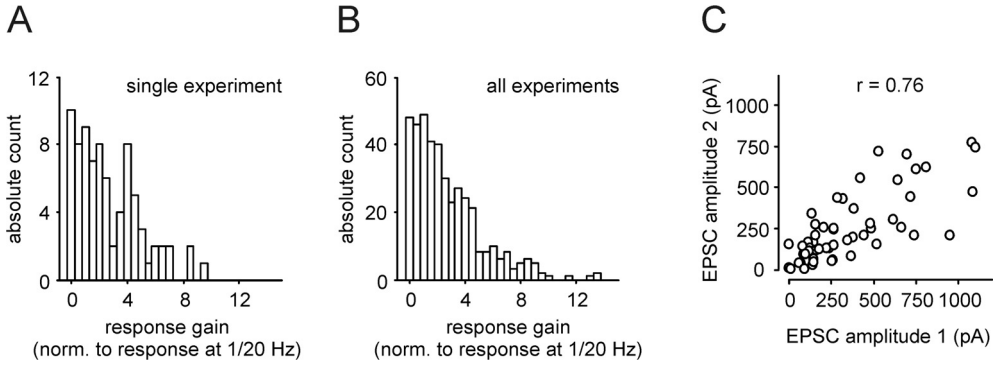

Figure 30: Range of synaptic gains and reproducibility in whole-cell recordings. (A) In the whole-cell recording of 4-3, gains of synaptic responses during stimulus train (i.e. instantaneous amplitude / mean basal response amplitude to 0.05 Hz stimulation) ranged from 0 to ~10. (B) Synaptic gains in n = 5 cells show a similar distribution, ranging from 0 to ~13. (C) Two consecutive repetitions of the same stimulus train in a single whole-cell recording reveal large response variability. This variability in EPSC amplitudes is mainly due to variance in mossy fiber synaptic transmission.

In order to differentiate between the two different sources of response variability, namely the modulation of response amplitudes due to (1) short-term plasticity and (2) the stochastic transmitter release of mossy fiber synapses, we repetitively applied the same stimulus train in one single-cell recording. The correlation between EPSC amplitudes to the first and second presentation of the stimulus demonstrates comparable dynamics of responses within one experiment, but also a considerable amount of jitter (Figure 30C, same cell as in Figure 29A). Thus, the large variability in response amplitudes reflects both the short-term transmission dynamics in response to a varying presynaptic stimulus frequency (i.e. the implicit information the responses shall transmit) and the intrinsic synapse-specific stochastic transmitter release.

In field excitatory postsynaptic potential (fEPSP) recordings, we measured short-term dynamics comparable to whole-cell recordings, given mossy fiber stimulation with the same irregular stimulus train (Figure 31A and B, same stimulus train as in Figure 29). Again, synaptic response amplitudes depended on the length of the inter-stimulus interval, with short ISIs triggering larger fEPSPs and long ISIs inducing relatively small fEPSPs. Still, even using field potential recordings, which average over a large number of synapses and postsynaptic cells, the size of the postsynaptic response cannot deterministically be predicted from the length of the last preceding ISI (see Figure 31C and D). To compare the dynamic range of fEPSP responses between experiments and also to EPSC recordings, we calculated synaptic gains for all fEPSP recordings (n = 13, using 5 distinct stimulus trains). Gains here ranged between 0.2 and 13.4 with a mean value of 2.9 ± 2.0, very similar to results in the whole-cell experiments (Figure 32A and B). Thus, mossy fiber synaptic STP is equally reflected in field potential responses. Importantly, repetitive application of the same stimulus train in one experiment evoked almost identical fEPSP amplitudes (Figure 32C).

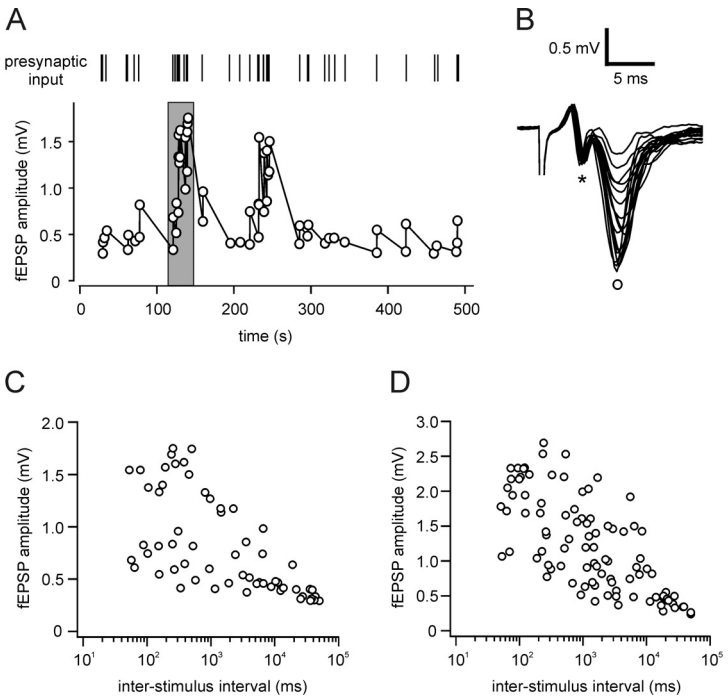

Figure 31: Modulation of synaptic efficacy by irregular stimulus trains. (A) In field potential recordings, mossy fiber synaptic response amplitudes were largely modulated by application of an irregular stimulus train, very comparable to whole-cell recordings. (B) Overlay of examplary response traces from time window marked by grey box in A. Star indicates peak of presynaptic fiber volley, open circle points to peak of postsynaptic fEPSP. (C) fEPSP amplitudes were negatively correlated with the length of the preceding ISI, still a large jitter was detectable. (D) Correlation of responses and ISIs in another exemplary recording, using a different stimulus train.

Thus, in fEPSP recordings we can circumvene the variability in response amplitudes due to the stochastic transmitter release at mossy fiber synapses and exclusively focus on features of short-term plasticity. Additionally, the response amplitudes and gains of EPSCs and fEPSPs were significantly correlated given the same stimulus train (Figure 32D and E). Since field potential recordings also allow for long-lasting stable recording and stimulation conditions, we continued using fEPSPs to assess the dynamics of mossy fiber synaptic short-term plasticity.

4.5 Computational Model of Short-Term Synaptic Plasticity

In order to quantitatively describe transmission dynamics, mathematical models have been established for several other synaptic systems as described above. Here, we have developed a computational model of mossy fiber synaptic short-term plasticity based on the experimental data gained from fEPSP measurements using irregular stimulus trains.

For determining the most suitable and yet minimal description of STP, we fitted the experimental data to a number of different model types. All of these were based on processes that after presynaptic stimulation facilitate transmission by a certain amplitude and exponentially decay to zero with a certain time constant.

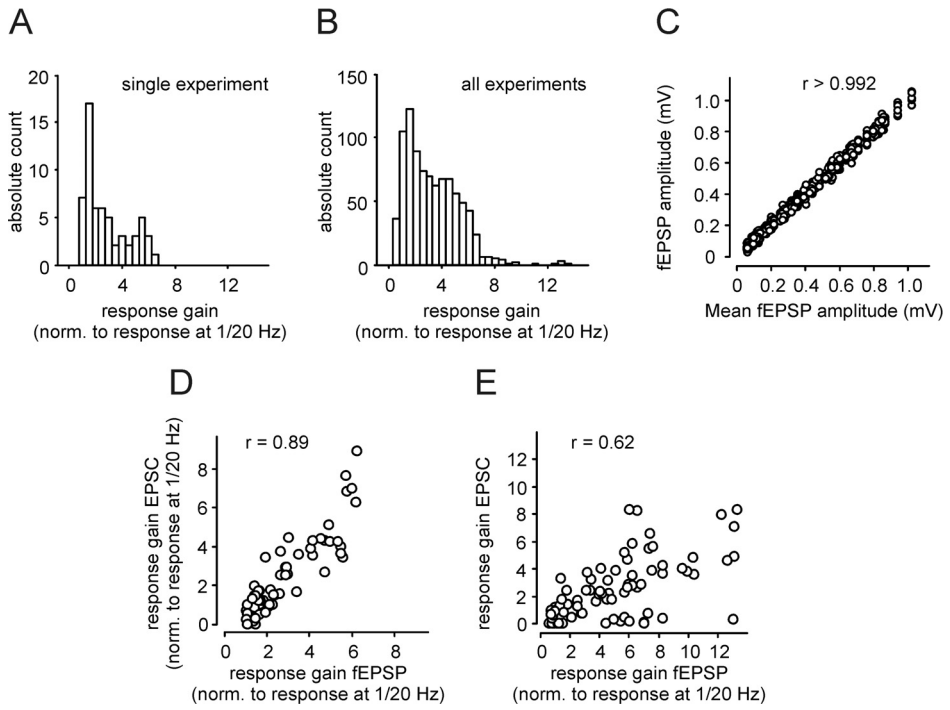

Figure 32: Range of synaptic gains and reproducibility in fEPSP recordings, and correlation of EPSC and fEPSP experiments. (A) In the fEPSP recording of Figure 4-5, gains of responses during stimulus train ranged from 0 to ~7. (B) Synaptic gains in n = 13 fEPSP recordings show similar distribution, ranging from 0 to ~13. (C) 7 consecutive presentations of the same stimulus train in a single fEPSP recording led to highly reproducible response amplitudes. (D,E) Two exemplary correlations of response amplitudes of EPSC and fEPSP recordings to the same stimulus train, respectively.

Fitting experimental data to models with only one facilitatory process or two facilitatory processes (a slower one 's' and a faster one 'f ') interacting with different additive or multiplicative cooperativities resulted in significantly different values for the goodness of fit, as determined by the χ^2-test (Figure 33A). In general, additive models exhibited smaller χ^2-values with a weak dependence on the exponents of the two processes. In particular, a model of the form 's^4+f' yielded the lowest χ^2-value of on average 5.1 ± 6.9 (n = 12 experiments) and was therefore chosen for all further analyses.

In our chosen model (Figure 33B), an irregular stimulus train is translated into two dynamical variables, x_{slow} and x_{fast}, via first-order kinetics. The variable $x_{slow}(t)$ describes the strength of the slow facilitation at time t. It is increased by 1 at each time t of synaptic activation,

$$x_{slow}(t+0) = x_{slow}(t-0) + 1 \quad (1)$$

and decays exponentially to zero with time constant τ_{slow} afterwards. Similarly, we have

$$x_{fast}(t+0) = x_{fast}(t-0) + 1 \quad (2)$$

and a decay with τ_{fast} . In addition, to account for saturation of facilitatory amplitudes, the strength of the slow facilitation was limited by an upper bound, implemented by a Michaelis Menten saturation function:

$$y_{slow} = G(x_{slow}) = x_{slow}(1+g)/(1+x_{slow}g) \quad (3)$$

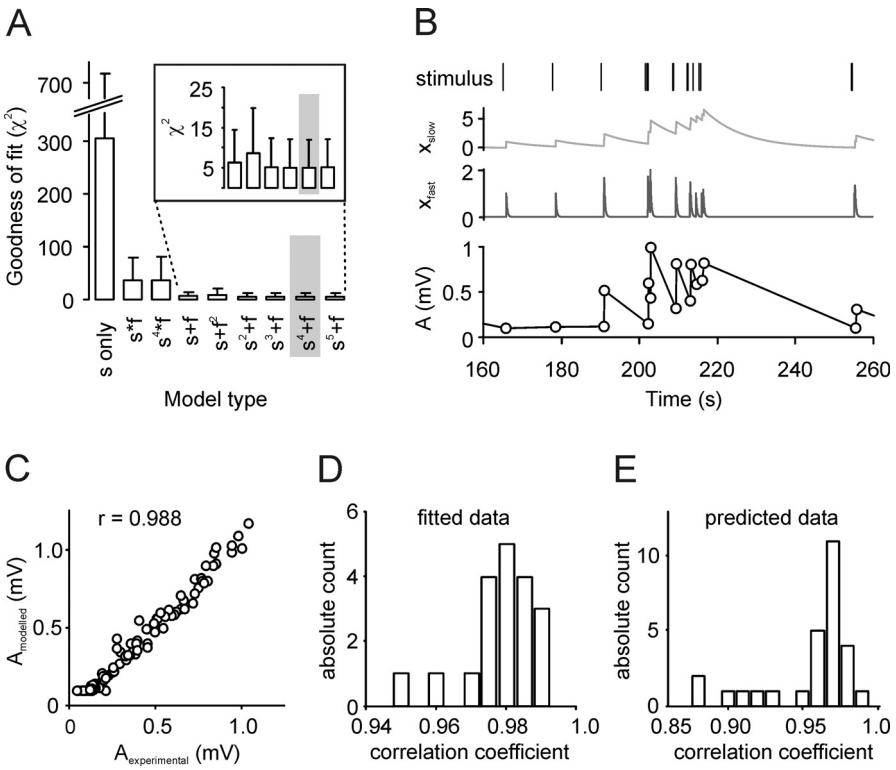

Figure 33: Descriptive model of mossy fiber short-term plasticity. (A) Goodness of fit χ2 was significantly different for various additive and multiplicative interactions of slow and fast facilitatory processes. The combination ‚s4+f' (highlighted in grey) yielded the lowest χ2-values and was therefore chosen for all further analysis. (B) Exemplary scheme of model description of mossy fiber STP evoked by part of irregular stimulus train (top). Response amplitudes A (down) are obtained from an additive combination of slow and fast facilitatory process (middle). (C) Fitted model amplitudes were highly correlated to measured fEPSP amplitudes, as shown for one example with corresponding experimental and model data. (D) Correlations between experimental and model amplitudes were generally high, as seen in n = 19 fits under control condition. (E) Predictions for response amplitudes with parameters obtained from a fit of the model to a different data set show similarly good correlations (n = 28 predictions)

We calculated the response amplitude A from the baseline amplitude A_0 and the additive combination of two facilitation terms, where powers of y_{slow} and x_{fast} are scaled by the amplitudes a_{slow} and a_{fast}, respectively:

$$A = A_0\left[1 + a_{slow}(y_{slow})^4 + a_{fast}(x_{fast})^1\right] \quad (4)$$

Using this model we were able to reliably reconstruct response amplitudes within the irregular stimulus trains.

In general, correlations between experimentally measured fEPSPs and fitted amplitudes were larger than 0.95 with a median value of 0.98 (n = 19), demonstrating the good characterization of mossy fiber short-term dynamics (Figure 33C and D). Additionally, given the parameters obtained through fitting of one stimulus train, we were able to reliably predict amplitudes obtained with a different stimulus train in the same slice (Figure 33E). Here, correlation coefficients between experimentally measured and predicted model amplitudes were larger than 0.88 with a median value of 0.97 (n = 28 predictions), highlighting the generalization capability of the model.

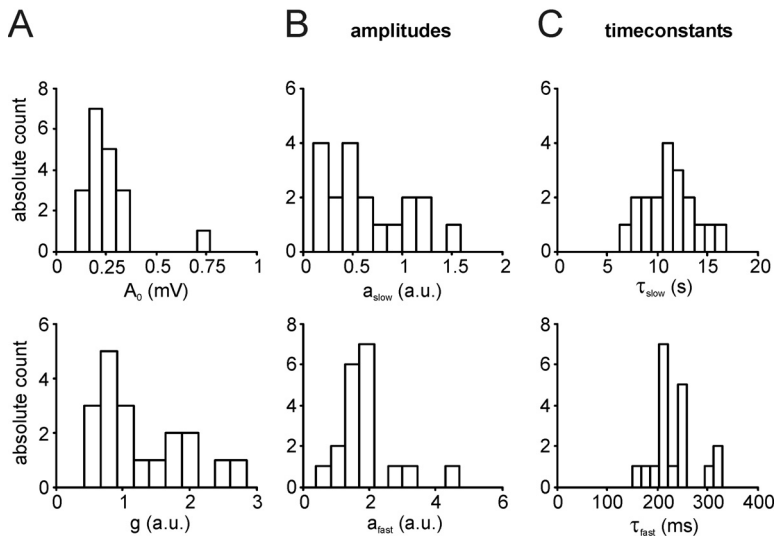

Figure 34: Parameters of mossy fiber short-term plasticity. (A-C) Histograms depict the distributions of model parameters , g, a_{slow}, a_{fast}, τ_{slow} and τ_{fast} under control conditions for n = 19 datasets.

In more detail, our computational model describes mossy fiber short-term plasticity by two exponentially decaying facilitatory processes x_{slow} and x_{fast} with a total of 6 parameters (Figure 34): A_0 reflecting the basal response amplitude, a_{slow} and a_{fast} for the specific amplitudes of facilitation, τ_{slow} and τ_{fast} as the time constants of facilitation, and g for a saturation of the slow process. Using the model, we could determine two relevant timescales of mossy fiber short-term plasticity as described by the two facilitatory processes. The slower process x_{slow} exponentially decays with a time constant of $\tau_{slow} = 11.2 \pm 0.6$ s and the faster process x_{fast} decays with $\tau_{fast} = 232 \pm 11$ ms (Figure 34C). These results are in line with the experimentally well-described STP phenomena of frequency facilitation and paired-pulse facilitation at the mossy fiber synapse. The model also shows that the amplitudes of the slow process need to saturate as quantified by the saturation parameter g, whereas an additional saturation of the fast process did not improve the model fits, so we discarded this parameter for simplicity. In contrast to other studies (Tsodyks und Markram, 97; Varela et al., 97), synaptic depression was generally not observed to be a critical degree of freedom for mossy fiber short-term plasticity given our stimulus trains. Summarizing, our computational model allows us to qualitatively and quantitatively capture and predict essential features of short-term plasticity at the mossy fiber synapse with a robustly high correlation to experimental data. Importantly, the qualitative results presented in all of the following did not depend on the specific additive cooperativity of the chosen model.

4.6 Interactions of STP and LTP at the Mossy Fiber Synapse

The hippocampal mossy fiber synapse not only exhibits pronounced short-term dynamics but is also a model synapse for NMDA-receptor independent, presynaptic form of LTP. To unravel the impact of long-term synaptic changes on short-term plasticity, we repetitively applied identical irregular stimulus trains before and after the induction of LTP by tetanic stimulation (Figure 35A and B).

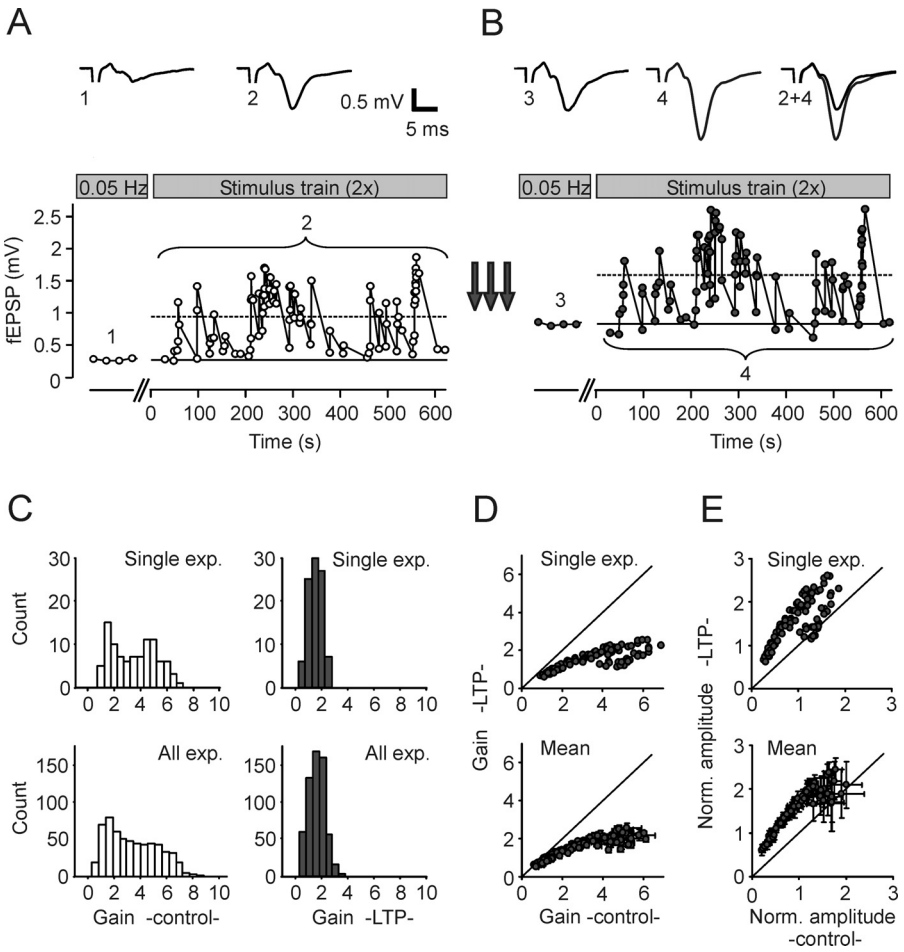

Figure 35: Short-term plasticity before and after the induction of LTP. (A,B) After initial constant stimulation at 0.05 Hz for establishing a basal response amplitude (solid lines), an irregular stimulus train was applied at least twice. Induction of LTP (arrows) led to increased responses in both basal response amplitude and mean response during complete stimulus train (dashed lines). Insets show averages of 10 sweeps each for 0.05 Hz stimulation before (1) and after LTP induction (3), and averages of all responses during the stimulus train (2 and 4). (C) Distribution of gains in a single example (upper panels) and pooled data from n = 8 experiments using 3 different stimulus trains (lower panels) differ remarkably between control (left) and LTP condition (right). (D) Gains of response amplitudes are decreased and the dynamic range of responses significantly reduced after the induction of LTP, both in a single experiment and the summary of several analog experiments. (E) The amount of short-term facilitation after LTP-induction is related to the corresponding response amplitude before LTP. Amplitudes are normalized to mean during stimulus train in control condition.

Following LTP, both the mean fEPSP amplitudes averaged over all responses in a stimulus train and the basal response to constant frequency stimulation were clearly enhanced. Still, synaptic response amplitudes clearly showed remarkable short-term plasticity, the amount of which, however, was changed after LTP. After the induction of LTP, the dynamic range of synaptic responses was strongly reduced. In the same experiment, the distributions of the measured synaptic gains significantly differed between the control and LTP condition, with a lower mean gain and a more narrow distribution (Figure 35C, upper panels). This tendency was a general phenomenon and independent of the specific realization of the used stimulus train for a given distribution

of ISIs, in that LTP decreased the mean gain and narrowed the deviation within the distribution from 2.65 ± 1.68 in control condition to 1.50 ± 0.66 following LTP (Figure 35C, lower panels; n = 8 experiments using 3 distinct stimulus trains). The alteration in the distributions of synaptic gains only gives information about the broad changes in short-term plasticity, but leaves the question of how each individual response amplitude is modulated after the induction of LTP.

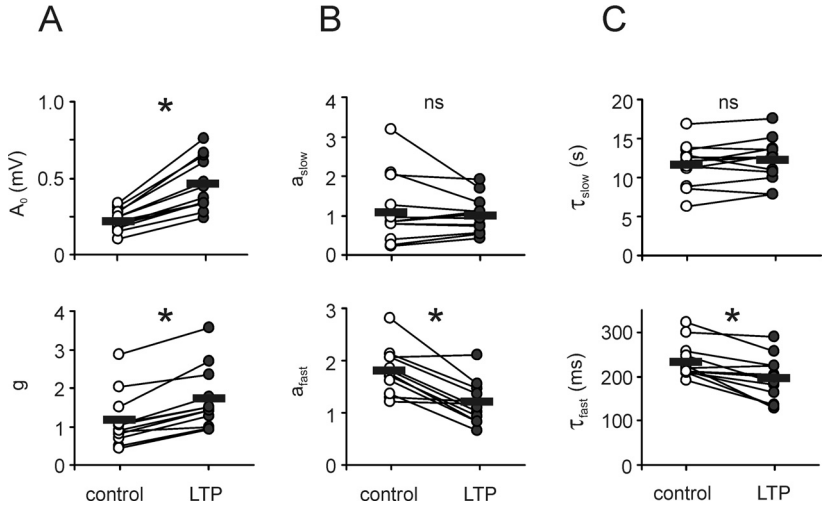

Figure 36: Modulation of model parameters after LTP. (A-C) Scatter plots depict changes in model parameters of mossy fiber STP after the induction of LTP. Data points are individual fits to experimental data before (open markers) and after LTP (filled markers). Asterisks point to significant changes in mean parameter values (paired Student's t-test. *: $p < 0.001$, ns: $p > 0.14$).

As can be seen in Figure 35D, we found that the amount of change of a specific synaptic gain depended on its value before the induction of LTP. Initially small synaptic gains were only slightly reduced, whereas initially large synaptic gains showed a drastic reduction (means ± std, n = 7 experiments using the same stimulus train). This specificity can also be seen when directly comparing response amplitudes before and after the induction of LTP (Figure 35E). Initially small fEPSP amplitudes were uniformly enhanced after LTP, whereas initially large amplitudes were less potentiated or even slightly depressed. In summary, analysis of the experimental data indicates that the induction of mossy fiber LTP leads to amplitude-dependent changes in the size of fEPSPs, but does not reveal which dynamical properties of the synapse are modified. In the following, we will therefore utilize our computational model of transmission dynamics to disentangle the impact of LTP on different components of STP.

4.7 Differential Modulation of STP by LTP

For the correct interpretation of the experimental results, it was crucial that our model of mossy fiber transmission dynamics fitted data equally well before and after the induction of LTP. Reassuringly, the goodness of fit as indicated by the mean χ^2-value was only slightly increased from 5.1 ± 6.9 under control to 6.0 ± 7.8 (n = 12) following LTP and the correlation coefficients between measured and predicted response amplitudes were in the same range as in control experiments (> 0.95, median of 0.97; compare Figure 33).

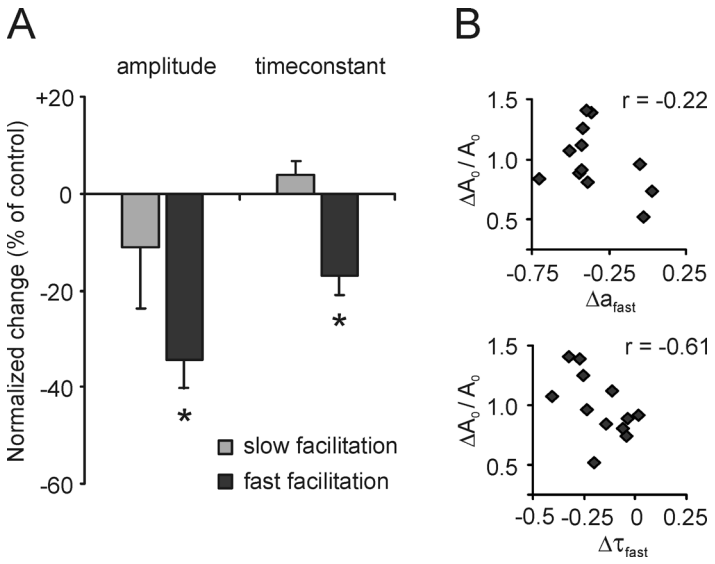

Figure 37: Relative differential impact of LTP on STP. (A) Both amplitude and time constant of the fast facilitatory process were significantly decreased after LTP in contrast to no significant changes in the corresponding parameters of the slow process. Changes are normalized to mean parameter values before LTP. Bars show mean ± sem; n = 12 experiments. Relative changes of parameters in relation to mean parameter values under the different conditions were calculated. (B) The decrease of the fast time constant τ_{fast} after LTP is significantly correlated to the relative change in A_0, while the amplitude of the fast process a_{fast} is not.

Hence, our model of short-term dynamics allowed us to quantify the impact of LTP on STP. Induction of LTP modulated the synaptic parameters as given by the model as follows (Figure 36): The basal response amplitude A_0 was increased by 100 ± 8 % (mean ± sem, n = 12 for all of Figure 36), but the relative amount of overall facilitation was reduced. This finding is in agreement with the description of LTP-induced modulation of STP at the mossy fiber synapse in Salin et al. (1996b). Extending this result, however, we find the two facilitatory processes to be attenuated differentially in their amplitudes (Figure 36A and B). The facilitation amplitude a_{slow} of the slow process was not changed significantly and therefore suppression in amplitude of the slow facilitation is only due to an increase in the saturation parameter g by 59 ± 9 % ($p < 0.001$, paired t-test). In contrast, the fast facilitatory process is suppressed by a direct decrease of its amplitude a_{fast} by -34 ± 6 % ($p < 0.001$). Hereby, the change in a_{fast} was not significantly correlated to the change in A_0.

In addition to a quantification of facilitation amplitudes, our model also enabled us to unravel alterations of time constants of short-term dynamics. Again, we find that LTP differentially modulated the timecourses of the two facilitatory processes (Figure 4-10C). While there was no significant change in the time constant τslow of the slow facilitation, the time constant τfast of the fast process was reduced by 17 ± 4 % ($p < 0.001$). This tendency was also true in all additive models tested following the form of 's^k+f' with k = 1,…,5 ($p < 0.008$). The change in τ_{fast} was negatively correlated to the relative change in A_0 (Figure 4-11B, right panel). The results concerning the respective changes in model parameters are summarized in Figure 37, where the percental changes of the model parameters are depicted. Importantly, we could reproduce the reduction of both amplitude and time constant of the fast facilitation with concurrent stable parameters of the slow facilitation in experiments performed under nearly physiological recording temperatures

(~34°C). Here, the induction of LTP decreased a_{fast} by 37 ± 14 % and τ_{fast} by 11 ± 3 % (n = 5 experiments, $p < 0.05$).

Summarizing, our computational model of short-term transmission dynamics shows that mossy fiber long-term potentiation results in a relative decrease of the influence of the fast facilitatory process in short-term plasticity. This reduced impact is manifested in that the facilitatory amplitude and time constant of the fast process are reduced. The change of the time constant τ_{fast} consequently narrows the range of inter-stimulus intervals of the presynaptic input distribution that are able to elicit the fast synaptic facilitation. The selective weakening of the fast process will thus result in altered postsynaptic response distributions.

4.8 Concluding Discussion

The results presented in this Chapter offer new insights into the consequences of the presynaptic, NMDA-receptor independent form of long-term plasticity at the hippocampal mossy fiber synapse. We could demonstrate that LTP changes the kinetics of mossy fiber synaptic short-term dynamics, which is characterized by two facilitatory processes: a faster one with a time constant of a few hundred milliseconds and a slower one with a time constant of about ten seconds. Moreover, we found that mossy fiber LTP selectively decreases the relative impact of the faster facilitatory processes by changing its amplitude and time constant. This differential modulation of synaptic dynamics is different from other established models of LTP (Markram und Tsodyks, 96; Tsodyks und Markram, 97; Selig et al., 99). The observed selective reduction of relative facilitation is, however, consistent with previous experimental findings at the mossy fiber synapse by Salin et al. (1996b), who reported an overall reduction of frequency facilitation. From our model we can now conclude that this reduction is due to a non-linear saturation effect rather than a direct decrease of the relative facilitatory amplitude of the slow process.

In vivo activity of neurons is irregular, whereas studies on synaptic plasticity typically use constant-frequency stimulation to activate synapses. Such regular stimulus trains cannot fully unravel the dynamic interplay between short- and long-term plasticity and effects on synaptic parameters other than response amplitudes. In order to quantify STP at the hippocampal mossy fiber synapse in a biologically reasonable setting we have employed complex stimulus trains. These should ideally resemble spike trains of dentate gyrus granule cells in vivo. However, little is known about the spiking statistics of hippocampal granule cells due to challenges in spike sorting within this area (Buzsaki und Czeh, 92). The available spike data (Mizumori et al., 89; Jung und McNaughton, 93) suggests that the firing statistics does not follow a Poisson distribution, but rather a power law. Applying *1/ISI* input statistics in vitro we found that synaptic responses of CA3 pyramidal cells are strongly modulated, varying 10-fold or more. This feature is in striking contrast to the neighboring associational-commissural synapses as well as to Schaffer-collateral synapses in area CA1, in which only little modulation occurs (Salin et al., 96b; Dobrunz und Stevens, 99). Even though the variability of response amplitudes within a train is very high (CV = 0.88, large range of gains), the modulation of synaptic strength in response to varying ISIs is precise and deterministic, as repetitive application of the same stimulus train revealed highly reliable responses in the field potential recordings of the synaptic responses.

On the level of a single synapse, however, mossy fiber EPSCs show a considerable variability in amplitude, including failures of transmission, even when stimulated with a

constant input frequency. This is due to stochastic transmitter release at the morphologically complex mossy fiber boutons, with up to 40 release sites (Jonas et al., 93; Acsady et al., 98; Henze et al., 00; Mori-Kawakami et al., 03; Hallermann et al., 03). In order to establish a predictive computational model for quantifying STP, one, however, needs reliable responses reflecting the preceding ISIs. There are two possibilities to acquire such a reliable mean response amplitude: First, one could average postsynaptic responses over a large number of repetitions (several tens of repetitions, see Appendix section B) of stimulus trains. This, however, would require several hours of constant recording from the same cell and stable single fiber stimulation. Even in a highly conservative calculation with ten applications of a stimulus train before and after induction of LTP, respectively, and twelve minutes per stimulus train, plus induction and stabilization of LTP, one experiment would amount to almost 5 hours. This, to our reasoning, is impossible to any satisfactory standards in whole-cell recordings. Therefore, we used the second possibility: field potential recordings, which simultaneously average over a large number of synaptic inputs and postsynaptic cells. As demonstrated in Figure 4-6, these data exhibit a significant correlation with the single synaptic response distributions, and are highly reproducible over time. Thus, to characterize LTP-induced changes in the dynamics of STP, we believe that field potential recordings of mossy fiber responses are a well-suited approach.

The high reproducibility of field potential recordings allowed us to construct a quantitative model of synaptic dynamics at the hippocampal mossy fiber synapse. Using this model, we were able to characterize synaptic facilitation on all relevant time scales much faster, more accurately and more conveniently than with conventional constant-frequency stimulation paradigms. Data were best described by two facilitation processes acting on clearly distinct time scales. The faster process, which exponentially decays with a time constant of a few hundred milliseconds, might be due to the accumulation of residual Ca^{2+} in the presynaptic element and its effect on subsequent events. The slower process operates on a time scale larger than ten seconds which cannot be explained by residual Ca^{2+} (Regehr et al., 94). This time course rather implies an intermediate biochemical pathway that might in part rely on presynaptic Calcium/calmodulin-dependent protein kinase II (CaMKII) (Salin et al., 96b). Our model, which additively combines two facilitatory processes on different time scales, is different from quantitative studies of synaptic short-term dynamics at the neuromuscular junction (Sen et al., 96), the visual cortex (Abbott et al., 97; Varela et al., 97) and the globus pallidus (Hanson und Jaeger, 02). There STP was found to multiplicatively combine facilitatory and depressing terms that operate on similar time scales. In our model, introduction of a depression term did not lead to improvement of the goodness of fit, so that we discarded depressing components. It has, however, to be noted that this exclusion might be due to the chosen range of presynaptic inter-stimulus intervals in our input distribution. Persistent instantaneous stimulus frequencies above 20 Hz (i.e. ISIs of <50 ms) could lead to a depression in synaptic response amplitudes later in the train due to a depletion of releasable vesicles after an initial saturating facilitation. Thus, given our input statistics we can conclude that mossy fiber synaptic short-term plasticity is dominated by two facilitating processes acting on different timescales.

Our STP model fits postsynaptic response amplitudes of mossy fiber synapses well before and after LTP, which allowed us to investigate the interplay of both forms of synaptic plasticity. We induced mossy fiber LTP by repetitive tetanic stimulation of the fiber tract at 25 Hz, which is a commonly used stimulation paradigm. Following LTP expression, we found synaptic short-term dynamics to be changed such that the fast

facilitatory process is selectively weakened. The observed decrease of the fast time constant reduces the range of interstimulus intervals that can trigger the fast facilitatory process, which suggests that one of the functional roles of mossy fiber LTP is to adapt the synapse to specific input features. The selective decrease of the fast facilitatory process after long-term potentiation can already be further confirmed by paired-pulse experiments with inter-stimulus intervals in the critical temporal range for the fast short-term plasticity. Under control conditions, paired-pulse facilitation is largest at short ISIs of 50 ms, with a PPR of ~3 (Figure 38A, n = 6). This paired-pulse facilitation decays with increasing ISIs and stabilizes at a value of ~1.5 for ISIs of 400 to 500 ms. After the induction of LTP, the paired-pulse ratio is significantly reduced at short inter-stimulus intervals, while remaining almost constant for ISIs of 400 to 500 ms. Hence, particularly the postsynaptic responses triggered after short interstimulus intervals will undergo a relative decrease in amplitude after long-term potentiation.

The interdependence of long- and short-term plasticity had been investigated before at other synaptic systems exhibiting NMDA-receptor dependent LTP. At neocortical synapses, LTP is accompanied by a redistribution of response amplitudes, with some responses being enhanced and others attenuated (Markram und Tsodyks, 96; Tsodyks und Markram, 97). At hippocampal Schaffer collateral and associational-commissural synapses, LTP has been found to uniformly enhance synaptic efficacy (Selig et al., 99). Here, we could demonstrate a complex interaction of short- and long-term plasticity at the hippocampal mossy fiber synapse, which constitutes of an almost uniform increase in synaptic strength in the low-frequency stimulus regime, and a redistribution of response amplitudes in the higher frequency range of the input distribution. Nevertheless, long-term potentiation at the mossy fiber synapse will strengthen the overall reliability of spike transmission, as the mean postsynaptic responses both during low-frequency constant stimulation and averaged over the irregular stimulus trains were significantly increased.

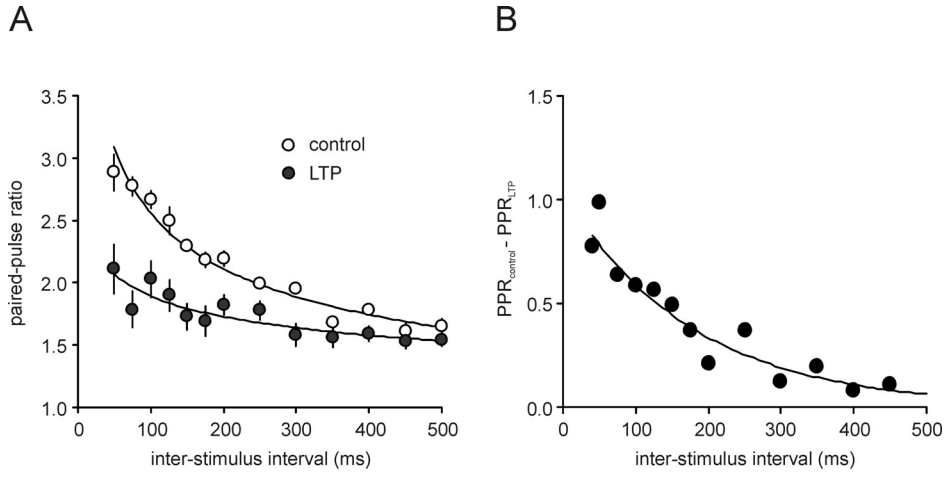

Figure 38: Influence of LTP on paired-pulse facilitation. (A) After the induction of LTP, the paired-pulse ratio of mossy fiber fEPSP responses is significantly reduced. This reduction is most prominent at short inter-stimulus intervals between 50 and 200 ms. Data show mean ± sem for n = 6 experiments. Grey lines are best monoexponential fit to data. (B) The absolute difference between the paired-pulse ratios before and after LTP more clearly depicts the preferential change in the low ISI regime.

4.9 Outlook

Two general fields remain to be investigated in more detail in future studies: (1) Do the input distributions chosen in this study reflect in vivo spike patterns of dentate gyrus granule cells well enough? And (2), can long-term potentiation of mossy fiber synaptic response amplitudes be induced by behaviorally triggered activity of granule cells?

Regarding the first question, it is to date not clear what the "typical" granule cell firing activity is composed of under *in vivo* conditions. Studies using tetrode extracellular recordings of unit activity in the dentate gyrus region face the challenge of sorting different activity, first to separate units and second to distinct cell types. This presents serious complications, as granule cells appear not to be readily detectable and distinguishable from e.g. hilar interneurons by their action potential waveform, the most commonly used basis for cluster separation in spike sorting. The published data on mean spike frequencies, ranges and inter-spike interval distributions of dentate gyrus granule cell firing vary significantly between studies and behavioral conditions, from a mean firing rate of 0.2 Hz during locomotor activity (Jung und McNaughton, 93), over up to behaviorally coupled 10 Hz in Wiebe & Staubli (1999), to a mean rate of 1.7 Hz during freely behaving locomotion while the animal was out of a place field and 26 Hz inside a place field for short periods of time (Henze et al., 02). In our study, we have chosen irregular stimulus trains as a presynaptic input to CA3 pyramidal cells, with the probability of a stimulus inversely proportional to the length of the inter-stimulus interval. The stimulus trains showed ISIs ranging from 50 ms to 50 s and a resulting median of ~1.5 s. To our understanding, these input distribution represent *in vivo* firing activity of dentate gyrus granule cells reasonably well and most importantly cover the wide scope of ISIs needed to evoke the large range of short-term plasticity found at the mossy fiber synapse. With the help of more advanced experimental techniques, such as *in vivo* patch clamp recordings (Lee et al., 06) of dentate gyrus granule cells in freely moving animals, this question will hopefully be clarified in the near future.

The second question has been posed for all synaptic systems since the initial discovery of long-term potentiation at perforant path synapses onto dentate gyrus granule cells in the hippocampal formation (Bliss und Lomo, 73). Would such high-frequency presynaptic stimulation as used in the tetanic stimulation paradigms for artificially inducing LTP be found during behaviorally related neuronal activity? For mossy fiber synaptic plasticity, it will in this context again be important to focus on identifying the firing activity of granule cells. As stated above, in extracellular unit recordings, irregular dentate granule cell activity was measured with mean frequencies of over 20 Hz for short periods of time while the animal was passing a place field (Henze et al., 02). Interestingly, stimulation of the mossy fiber tract by repetitive application of such an in vivo high-frequency stimulus train led to a marked increase in fEPSP amplitudes in a first set of *in vitro* experiments (Figure 39). After 5 repetitions of the roughly 1.5 s long stimulus train, the basal synaptic response was increased to 236 ± 24 % (n = 3) of control values 20 minutes after the last stimulus. Hence, naturally occuring spike patterns are able to induce long-lasting changes in synaptic transmission. This finding additionally highlights that stimulus paradigms leading to large short-term plasticity can in the end also lead to long-lasting changes in synaptic efficacy. Future studies will have to determine whether the mossy fiber synapse is therefore constantly modulated in their strength by behaviorally-related firing activity.

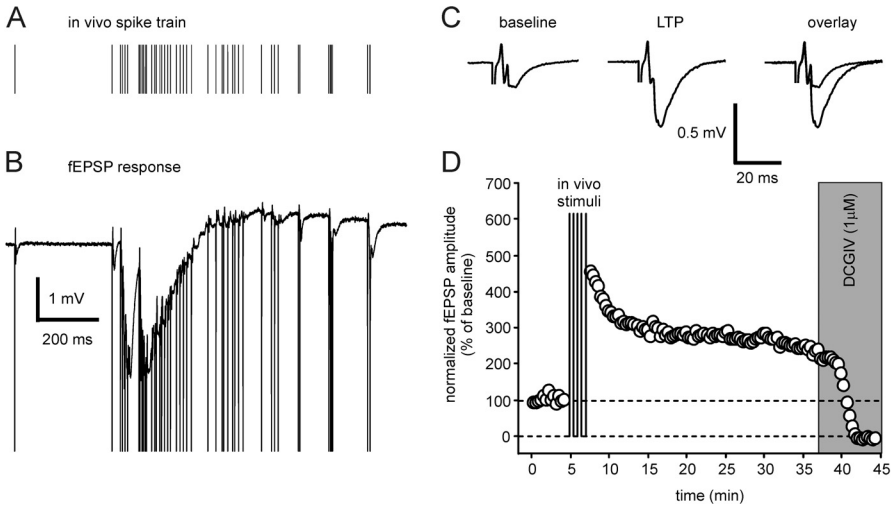

Figure 39: In vivo activity of granule cells induces mossy fiber LTP. (A) High frequency hippocampal granule cell activity recorded in a behaving mouse, while the animal was passing through a place field. Spike train was taken from Henze et al. (2002), Figure 5. (B) Under application of the in vivo spike train, mossy fiber fEPSP responses recorded in vitro undergo massive depolarization and short-term plasticity of their response amplitudes. (C,D) In the same experiment, repetitive application of the spike train (5x, with 30 second pauses in between) led to a significant increase in basal response amplitude tested with single stimulating pulses at 0.05 Hz, as seen in exemplary traces (C) and the timecourse of the experiment (D). Mossy fiber origin was verified by complete blockage of responses under application of DCGIV at the end of the experiment.

Finally, presynaptic, NMDAR-independent forms of LTP are not only expressed at hippocampal mossy fiber synapses, but were also found at cerebellar parallel fiber (Salin et al., 96a) and corticothalamic terminals (Castro-Alamancos und Calcagnotto, 99). It is, therefore, of further interest to investigate whether similar effects of LTP on short-term synaptic dynamics are expressed in these systems as well. Moreover, in addition to long-lasting increases in synaptic strength, hippocampal mossy fiber synapses also express long-term depression (Kobayashi et al., 96). Here, LTD is again NMDAR-independent and relies on presynaptic metabotropic glutamate receptors (Yokoi et al., 96; Tzounopoulos et al., 98). In this context, future studies will have to define whether the observed multidimensional changes in short-term dynamics are bidirectional.

5 Temporal Coding Mediated by Short-Term Synaptic Facilitation

As we have seen in the last Chapter, synapses change their transmission efficacy in response to repetitive activation. Up to now, hypotheses on the functional role of short-term plasticity, and short-term depression in particular, focus on aspects of filtering of presynaptic input. Little, however, is know on the behavioral role of synaptic facilitation. Especially for synaptic facilitation on the time scale of seconds as found at the hippocampal mossy fiber synapse functional ideas are few, although this time scale is the most relevant one for behavior.

In this Chapter, as a final concluding outlook, we will propose a mechanism on how such synaptic facilitation can be used to generate a temporal spike code. From experimental and modelling investigations we derive the hypothesis that synaptic facilitation in combination with subthreshold membrane potential oscillations transfers temporal information of the input activity to the phase (and therefore timing) of postsynaptic action potentials. In doing so, the synapse might act as a temporal compression device mapping input correlations on a behavioral time scale to spike correlations in the range of few 10 milliseconds [5].

5.1 Neuronal Coding of Information

A neuron's dynamics, that is the sequence of action potential firing in time, is determined by its driving stimulus. In sensory systems, this stimulus may be the relevant trigger in the external environment, while in more central nervous pathways it is given by the presynaptic input onto the neuron. Neuronal dynamics can represent information about their driving stimuli in two broad ways: (1) A 'rate code' typically refers to a neuronal mechanism, where the average firing rate of individual or ensembles of neurons over a specified time encodes the relevant information about the stimulus. (2) A 'temporal code' refers to a mechanism where the precise timing of action potentials in reference to the input stimulus contains the information to be encoded. This phenomenon is of high importance in scenarios where precise correlations of firing between neurons are required. A clear separation of these two phenomena is, however, not always possible and sometimes even misleading, as they are descriptions of the same content only on different temporal resolutions (Dayan und Abbott, 01), and the two types of neural encoding may be even used in parallel (Mehta et al., 02).

A well-described example of a combination between a rate and a temporal code is the phenomenon of hippocampal 'phase precession' in vivo. Phase precession is based on

[5] The results presented in this Chapter are in parts based on the manuscripts "Temporal Compression Mediated by Short-Term Synaptic Plasticity" by C. Leibold*, A. Gundlfinger*, R. Schmidt, K. Thurley, D. Schmitz and R. Kempter (2008), *Proc Natl Acad Sci USA*. Mar 18, 105(11):4417-22; and "Phase Precession through Synaptic Facilitation" by K. Thurley, C. Leibold, A.Gundlfinger, D. Schmitz and R. Kempter (2008), *Neural Comput*. May 20 (5):1285-324.

two phenomena linked to spatial behavior of rodents: (1) The firing activity of hippocampal neurons (dentate gyrus granule cells, CA1 and CA3 pyramidal cells) varies with the location of the behaving mice and rats. In this context, neurons are referred to as 'place cells' if they specifically enhance their spiking actity as soon as the animal enters a specific location, the 'place field', in their environment (O'Keefe und Dostrovsky, 71; O'Keefe, 79; Miller und Best, 80). The firing rate is hereby maximal at the center of the place field. The location of the animal, can thus be deduced from the firing rate of the place cells and a precise map of the environment can be established by the combination of firing activities in several place cells. (2) When rats or mice exhibit spatial navigation or exploratory behavior, the ensemble firing activity of hippocampal neurons shows oscillations in the theta range (6-12 Hz). This theta oscillation is classically thought to be caused by the coordinated, summed activity of inhibitory and excitatory input on the somata and dendrites of principal cells, respectively (Buzsaki, 02).

The phenomenon of phase precession now comprises the following: During the animal's traversal of a place field, the timing of individual spikes of a place cell in relation to the membrane potential theta oscillation progressively shifts to earlier phases in the oscillatory cycle (O'Keefe und Recce, 93; Skaggs et al., 96). The relative temporal precession of action potentials occurs over the time scale of seconds, when the animal traverses the place field, and shifts the timing of action potentials for several tens of milliseconds. Hence, besides a rate code as introduced above, in vivo neuronal activity of hippocampal neurons also shows a type of temporal coding of location. It is important to note, however, that phase precession is not redundant to the firing rate coding, in that it is unidirectional (i.e. only a precession and no recession of spike timing is found) during traversal of the place field, whereas mere firing rates can be ambiguous, as they decrease again after the animal's traversal of the center of the place field. In summary, as exemplary discussed for hippocampal phase precession, coding of information in neuronal activity can be achieved using different complementary strategies, which act on various time scales.

5.2 Time Scales of Plasticity, Learning and Behavior

Neuronal dynamics carrying information about external stimuli occur on time scales ranging from a few to several hundreds of milliseconds. These time scales are imposed on the network by intrinsic cellular properties, such as membrane time constant or resonance characteristics, the kinetics of synaptic transmission, and short-term plasticity properties of the synapses involved. Correlated firing in synaptically connected neurons in time scales of tens of milliseconds seems to be optimized to induce changes in synaptic strength as seen in spike-timing dependent plasticity (Gerstner et al., 96; Markram et al., 97; Bi und Poo, 98; Dan und Poo, 04). In this context, it is presumed that such long-lasting forms of synaptic plasticity present a means to learn the detection and discrimination of cellular activity patterns in networks.

In contrast to these relatively fast cellular phenomena in the range of tens to hundreds of of milliseconds, behavioral tasks, such as spatial navigation or short-term memory of events, occur in the temporal range of seconds to minutes. Here, the in vivo phenomenon of phase precession presents an appealing mechanism to bridge the behavioral time scales in the range of seconds to a neural representation in the range of 10s to 100s of milliseconds (Mehta et al., 02; Harris et al., 02). However, although numerous experimental studies could reproduce the initial description of phase precession of CA1 units in various other hippocampal regions, and manifold computational models

have been developed, the cellular mechanism underlying phase precession remains unclear.

Short-term plasticity of synaptic transmission typically modulates cellular network dynamics in the range of hundreds of milliseconds. This time scale appears well-suited to combine the fast cellular phenomena of precise firing and the slower behavioral phenomena in vivo, and might be used as a short-term memory buffer.

In the last two Chapters of this thesis, we have investigated the foundations and characteristics of short-term plasticity at the hippocampal mossy fiber synapse in particular. We could elucidate that mossy fiber synaptic transmission is dynamically regulated on a broad time scale. Furthermore, the amount of mossy fiber synaptic facilitation is dependent on the presynaptic temporal input distribution, in that shorter inter-stimulus intervals usually trigger larger facilitation. Hence, the amplitude of the postsynaptic response gives information about the recent input history of the synapse in the range of tens of seconds. Until here, however, we have measured the postsynaptic response only in terms of excitatory postsynaptic potentials or currents (EPSP/Cs), that is (from the postsynaptic neuron's perspective) one step short of action potential initiation. It therefore remains to be clarified whether and to what extent the temporal information of the presynaptic input can be transferred to the next relay station in the neuronal network in the sequence of CA3 pyramidal cell action potential firing.

In this context, a strong input current to a neuron generally elicits a faster depolarization of the postsynaptic membrane potential than a weak input current. Near the threshold of action potential generation, strong inputs thus give rise to shorter action potential latencies than weak inputs. In this manner, the amplitudes of EPSCs should be represented or encoded in the precise timing of the action potentials. To investigate such temporal encoding at the hippocampal mossy fiber onto CA3 pyramidal cell synapse, we are going to adress the following questions in the upcoming paragraphs:

(1) How is the information of postsynaptic facilitatory responses transmitted and conserved in the resulting action potential sequences of a CA3 pyramidal cell?

(2) How could this information transmission be enhanced?

(3) And finally, what might be the functional use for the CA3 region and the hippocampal network in general?

5.3 Range of Temporal Coding through Facilitation

For answering these questions, we first aimed at determining the temporal range of action potential occurrence that is induced by synaptic facilitation in the mossy fiber CA3 pyramidal cell system. To this end, we measured the AP sequences of a CA3 pyramidal cell in response to simulated facilitating EPSCs under current-clamp conditions. These facilitating EPSCs are hereby to represent the postsynaptic response amplitude distributions triggered by physiological presynaptic input to the mossy fiber synapse.

The kinetics and amplitudes of the simulated EPSCs were based on synaptic currents obtained during voltage-clamp measurements in CA3 pyramidal cells under extracellular stimulation of the mossy fiber tract. Here, the measurements revealed a 10-90 % rise time of 1.9 ± 0.3 ms and a 63 % decay time of 10.6 ± 1.4 ms (mean ± std, $n = 8$, see also Figure 40).

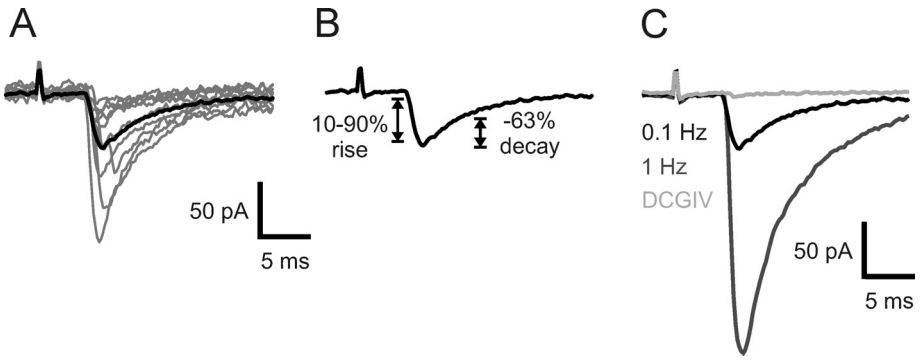

Figure 40: Kinetics of mossy fiber synaptic EPSCs onto CA3 pyramidal cell. (A) Exemplary recording of mossy fiber synaptic EPSCs by extraxellular stimulation of the mossy fiber tract. Gray lines depict individual trials, black line represents mean response. (B) From the mean response in (A) we calculated the 10-90 % rise time and 63 % decay time to characterize the EPSC kinetics. (C) Mossy fiber origin of the EPSCs was verified by induction of frequency facilitation (switch from 0.1 Hz to 1 Hz stimulation frequency), which led to a significant increase in response amplitude, and the blockage of response by application of DCGIV.

In all of the following, the simulated EPSCs are described by

$$I_{syn}(t) = A\left[\exp(-t/\tau_1) - \exp(-t/\tau_2)\right]\Theta(t) \quad (1)$$

with τ_1 = 1.5 ms and τ_2 = 10 ms, which resulted in a 10-90 % rise time of 1.8 ms, and the function $\Theta(t)$ denoting the Heaviside step function. The amplitude A of the artifical EPSC takes different values depending on the state of dynamical synaptic transmission and was kept at minimal and maximal current values to match mossy fiber synaptic facilitation (see Chapter 2).

Stimulus trains composed of periodic repetition of these artificial EPSCs were applied to the measured cells somatically via the amplifier in order to mimic facilitating mossy fiber synaptic input. Figure 41A depicts the overlay of action potential responses of a CA3 pyramidal cell upon repetitive application of such a train of simulated EPSCs. As can be seen in the voltage-response of the cell, postsynaptic action potentials were evoked when the simulated EPSC reached a specific amplitude (in this case ~340 pA). The exact timepoint of AP occurrence hereby depends on the degree of facilitation, with further increasing amplitudes leading to earlier APs. Several repetitions of the stimulus train evoked a reliable pattern of postsynaptic APs, with a typical time difference between late and earlier APs of ~7 ms (Figure 41B). For n = 5 cells, the average time difference between EPSC onset and AP ranged from 31 ± 6 ms (mean ± sem) for low EPSC amplitudes to 7 ± 2 ms for high EPSC amplitudes (Figure 41C). Hence, action potentials are evoked at specific timepoints representing the amplitude of the triggering EPSC.

5.4 Increase of Coding Range through Membrane Potential Oscillations

In the above described experiments, the frequency of the periodic and facilitating synaptic input was set to 9 Hz, as this is a typical value observed during epochs of hippocampal theta oscillations. The theta rhythm is also reflected through oscillations in the membrane potential of neurons in vitro (Alonso und Llinas, 89) and in anaesthetized (Kamondi et al., 98; Bland et al., 05) and behaving animals (Lee et al., 06).

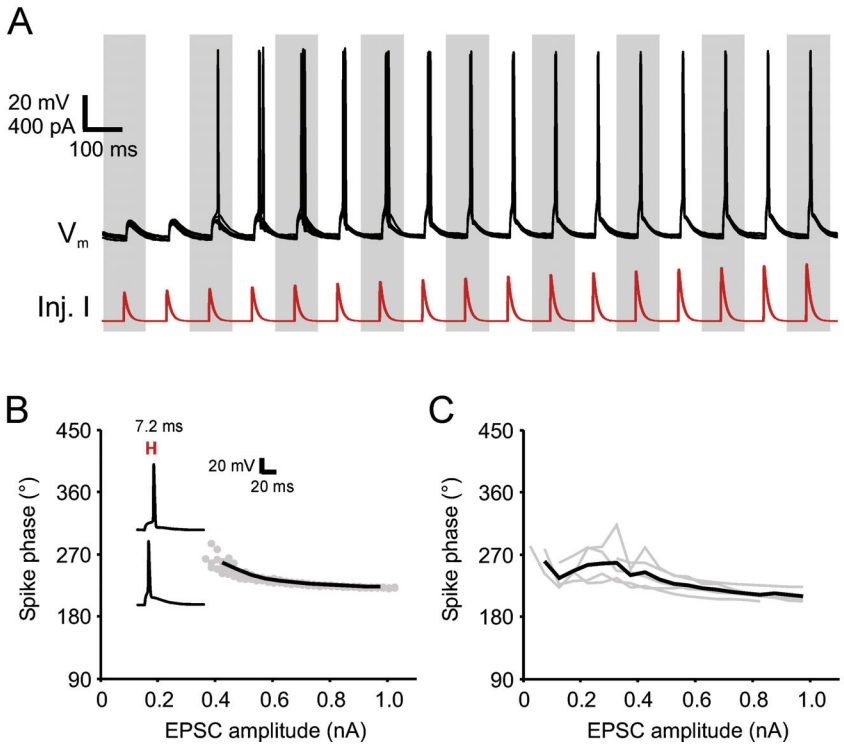

Figure 41: Temporal coding range due to synaptic facilitation. (A) 9 Hz periodic application of simulated facilitating EPSCs (Inj. I) to a hippocampal CA3 pyramidal cell evoked a reliable pattern of action potential (AP) firing. Upper traces (Vm) depict an overlay of voltage responses for 7 repetitions of the stimulus. The cell was held at 58 mV, the amplitude of the injected EPSC was initially set to 300 pA and increased by 20 pA per cycle. White and grey pattern indicates 9 Hz phase cycles (i.e. 111.11 ms per cycle). (B) Phase of firing during cycle (grey dots) is plotted as a function of EPSC amplitude for the experiment in (A). Black line refers to the mean firing phase averaged over amplitude intervals of 0.1 nA. Inset depicts single APs evoked by small (cycle 3) and large (cycle 10) EPSCs. (C) Mean firing phases from n = 5 cells (grey lines) in response to the same stimulus yielded a comparable temporal coding range. Black line depicts the population mean.

To study the effect of such subthreshold oscillations on the temporal coding range generated by facilitating inputs, we next measured action potential responses to the injection of an oscillatory current in addition to the facilitating EPSCs. The subthreshold membrane potential oscillations were induced by somatic current input via the amplifier of the form

$$I_{osc}(t) = I_1 \cos(2\pi f_\theta t) \tag{2}$$

Here, the theta frequency was chosen as $f_\theta = 9$ Hz and the oscillatory current amplitude I_1 was adjusted from 40 to 120 pA such that the amplitude of the membrane potential oscillations was about 5 mV (compare (Kamondi et al., 98). The onset phase of the facilitating input in this example was set to 180° with respect to the subthreshold oscillations (see Appendix for further details about phase shifts between current input and membrane potential output in the cells). Figure 42A depicts the overlay of AP responses to a facilitating stimulus train and a 9 Hz oscillatory current injection to the soma of a CA3 pyramidal cell. Again, action potentials were evoked by the facilitating input at a specific threshold amplitude of EPSCs.

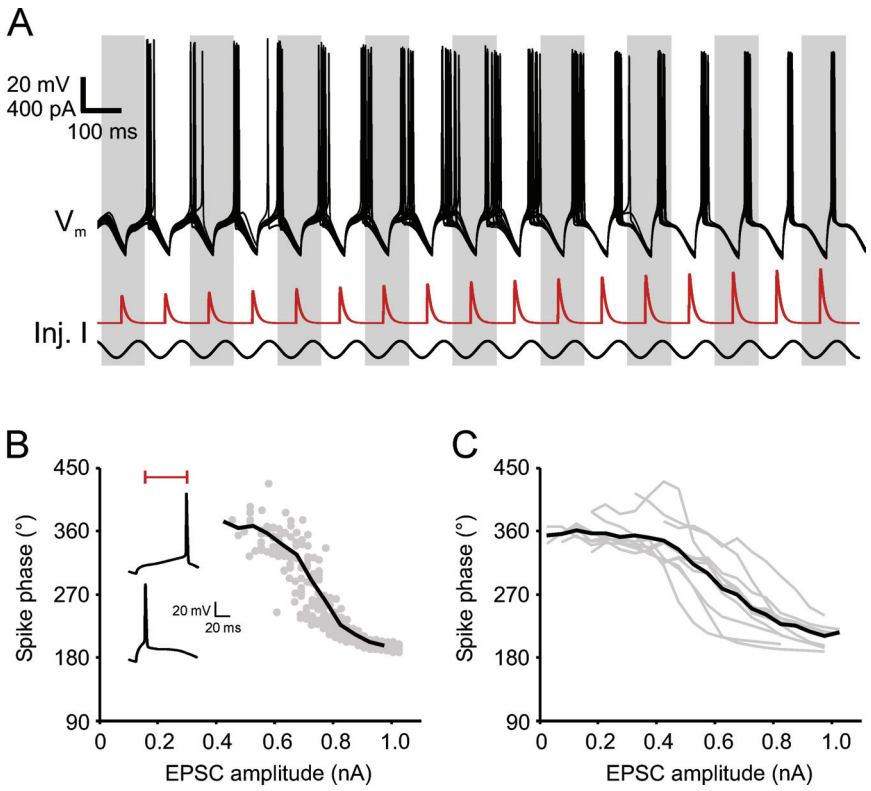

Figure 42: Temporal coding range due to synaptic facilitation and subthreshold oscillations. (A) In the same cell as in Figure 41, an additional application of an oscillating input current led to a noticable precession of AP phases with increasing EPSC amplitudes. Voltage traces show overly of 16 repetitions of the stimulus. The EPSC phase was set to 180° with respect to the subthreshold oscillations. (B) Oscillations extend the temporal coding range to about half a theta cycle. (C) The mean spike phases for n = 10 cells (grey lines) yielded a temporal coding range of 51 ± 2 ms, corresponding to a phase range of 166 ± 6°. Black line depicts the population mean.

It can already be noted in the exemplary experiment, however, that the temporal offset between EPSC input and AP output is markedly larger for small EPSC amplitudes compared to the experiments without subthreshold oscillations. With increasing EPSC amplitudes, the APs are gradually evoked earlier, resulting in a temporal coding range of in this case ~60 ms or ~190° (Figure 42B). In n = 10 cells, the combination of subthreshold membrane potential oscillations and facilitating EPSC input increased the temporal coding range to 51 ± 2 ms. This range corresponds to about half a theta period and is about twice as large as without subthreshold oscillations. Membrane potential oscillations thus can significantly extend the possible range for temporal coding.

5.5 Models of Temporal Coding through Synaptic Facilitation

The increase of the temporal coding range via subthreshold oscillations can be explained by a qualitative schematic model (see also (Thurley et al., 07). If one considers the effect of subthreshold oscillations as a periodic modulation of the neuronal firing threshold, firing phases can be determined from the intersections between an oscillating spike threshold and the facilitating EPSPs (Figure 43).

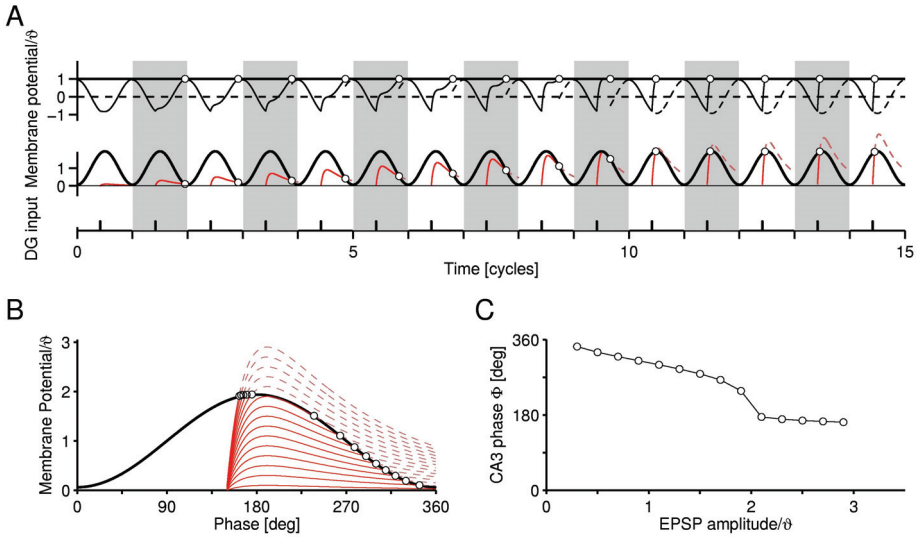

Figure 43: Schematic model of temporal encoding by synaptic facilitation and membrane potential oscillations. (A) Middle: EPSPs (red lines) occur at input phase ψ = 180° with respect to the firing threshold oscillation (black line). The time series of postsynaptic APs (white circles) is obtained by the points of intersection of the threshold and EPSPs. Top: The superposition of subthreshold oscillations and EPSPs mimics the voltage traces of the whole-cell recordings of Figure 41. Dashed lines represent contributions of oscillations and EPSPs that occur after AP generation. (B) The middle panel from A is collapsed into a single cycle in order to illustrate a coding range from 180° to almost 360°. (C) The postsynaptic firing phase is a decreasing function of the EPSP amplitude and, hence, the number of the input pulse.

As a result, for low input amplitudes, APs only occur at the troughs of the firing threshold at around 360°, which corresponds to the peaks of the sinusoidal membrane potential oscillations. When the EPSP amplitude increases, the point of intersection between EPSP and oscillating firing threshold preceeds towards earlier phases. At first, for low amplitudes, this phase precession is virtually linear. For AP phases close to the maximum of the threshold, phase precession is curved and can even exhibit discontinuities (Thurley et al., 07).

To also quantitatively assess the transmission of information, we applied stimuli combining oscillatory currents and facilitating EPSCs to the conductance-based two-compartment model of a CA3 pyramidal cell by Pinsky & Rinzel (Pinsky und Rinzel, 94); see also Appendix). Given our input parameters, the two-compartment model similarly accounts for the experimental phenomenology. Specifically, it provides a range for temporal coding of about half a theta cycle with increasing EPSC amplitudes leading to an earlier occurrence of postsynaptic action potentials. Using these two models we can thus (1) qualitatively describe the generation of the temporal precession of AP occurrence and (2) quantitatively simulate the amount of precession through synaptic facilitation and subthreshold oscillations.

5.6 Influence of Input Phase ψ on Temporal Coding

Until here, we have illustrated the generation of a temporal code for fixed input phases ψ, amplitude and frequency of the subthreshold oscillations to reflect properties observed during hippocampal theta oscillations (Kamondi et al., 98; Bland et al., 05; Lee

et al., 06). From the qualitative model presented in paragraph 5.5, one can already deduce that the input phase ψ, that is the relation of EPSC input to the oscillatory modulation of the membrane potential, limits the amount of precession to be generated by the AP sequences.

In Figure 44A, we now depict the experimentally obtained firing phases of a CA3 pyramidal cell as a function of the EPSC amplitude for three different input phases ψ. A late input phase $\psi = 180°$ resulted in only little curvature of the firing phase Φ as a function of the amplitude, with the phase of APs gradually precessing with increasing input amplitudes. The resulting phase range covers an interval of about 160°. For an early input phase of $\psi = 120°$, the AP phases are strongly curved with a pronounced discontinuity, yet the obtained coding range amounted to about 230°. Qualitatively, temporal coding was either in a straight, almost linear regime with a low coding range, or in a curved regime with a large coding range. We thus conclude that the amount of information provided by the firing phase about the preceding amplitude of an EPSC critically depends on the mean input phase. It remains, however, to be determined whether a large coding range on the one hand or straightness of the transfer function on the other hand is more beneficial to the transmission of information.

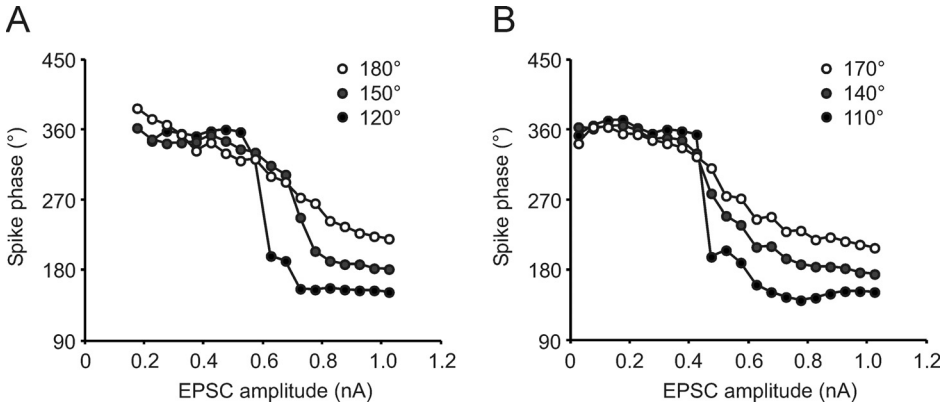

Figure 44: Temporal coding depends on the input phase ψ. (A) Exemplary recording of a CA3 pyramidal cell shows that the firing phase Φ (averaged over 15 trials, bins of 0.05 nA) as a function of the EPSC amplitude A is only slightly curved for a late input phase and strongly curved for an early input phase. (B) This tendency was seen in all experiments for three different mean input phases (110°: n = 3, 140°: n = 8, 170°: n = 9; see Appendix for determination of mean input phase over several cells).

5.7 Transmission of EPSC Amplitude Information

In order to gain insight into the criteria beneficial for the transmission of EPSC amplitude information we have performed the following modelling and experimental studies. Using the Pinsky-Rinzel model, we have determined the output AP phases for 180 different input phases ψ and 141 different amplitudes A of the EPSCs. The obtained transfer function is depicted using a color code for the phase offset between injected EPSC and the resulting postsynaptic AP (Figure 45 A). From the modelling results it is evident that there is a window of opportunity between ~100° and ~300° of the input phase ψ that ensures a sufficiently large coding range, that is a broad range of phase offsets with increasing EPSC amplitudes.

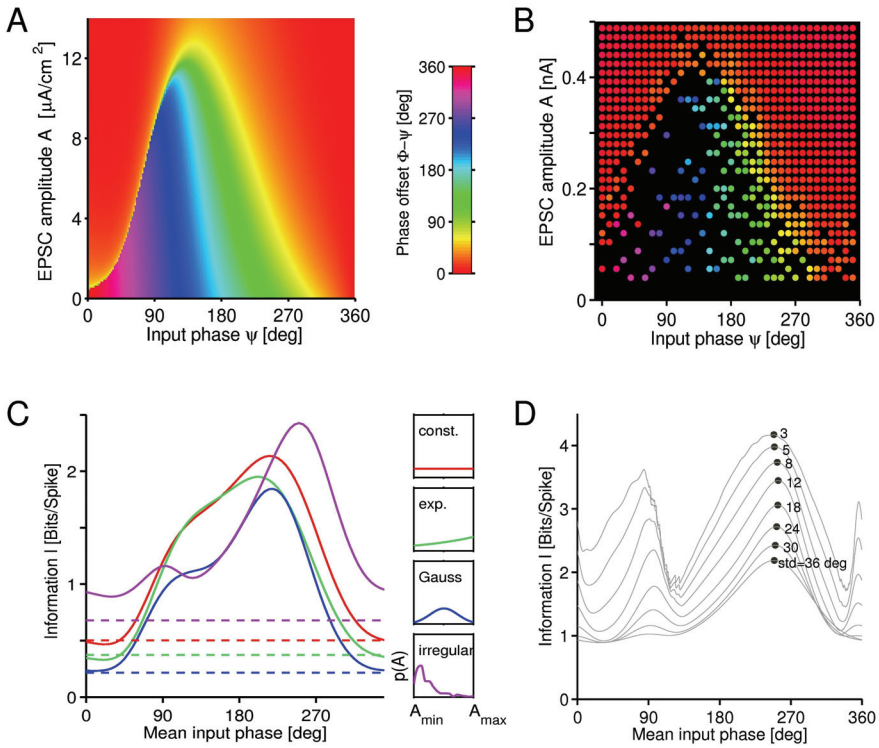

Abbildung 45: Information transmission via a temporal code. (A) The phase offset Φ-ψ between the phase Φ of postsynaptic firing and phase ψ of presynaptic input is depicted in a color code. Data were obtained from model simulations with a 0.1 µA/cm^2 resolution of the EPSC amplitudes and a 2° resolution of input phases. (B) Phase offsets of APs (colored dots) were obtained from an exemplary experiment with a 10° resolution of input phases. Data resemble the simulations in (A). (C) From the model simulations, the mutual information I between AP phase Φ and the synaptic amplitude A reveals optimal mean phases between 180° and 270° depending on the amplitude statistics p(A) (see text for details). Dashed lines mark the amount of transmitted information without additional membrane potential oscillations. (D) The maximal information transmission (black dots) obtained with the irregular amplitude distribution from (C) decreases by about 49 % for a 12-fold increase of the standard deviation of p(ψ) (std, see labels).

Similarly we have experimentally determined the output AP phases for facilitating EPSC amplitudes and 36 different input phases ψ in CA3 pyramidal cells. As depicted in Figure 45B, the comparison between model and experimentally obtained transfer functions indicates a good qualitative agreement, especially for input phases $\psi > 120°$. In order to now obtain the input phase ψ optimally suited for transmitting amplitude information to AP phases, we calculated the mutual information I between synaptic amplitude A and firing phase Φ using the transfer function $\Phi\psi(A)$ obtained by the model and several distinct distributions $p(A)$ of synaptic amplitudes. These distributions $p(A)$ were set as (1) constant, (2) exponential, (3) Gaussian and (4) irregular (i.e. obtained from irregular stimulation of the mossy fiber tract as in Chapter 4) , when describing the probability of synaptic amplitudes from A_{min} to A_{max}.

In general, we find that independently of the distribution $p(A)$ of synaptic amplitudes, the information as a function of mean input phase is similar for all distributions (Figure 45C): Maximal information transmission requires late mean input phases ψ that give rise to straight transfer functions $\Phi\psi(A)$ without strongly curved parts.

Therefore, strongly curved parts in $\Phi\psi(A)$ are disadvantageous for information transmission, given generic unimodal amplitude distributions.

When comparing the mutual information for the four amplitude distributions $p(A)$ of qualitatively different shapes, however, we found the highest information transmission for the distribution obtained from irregular stimulations of the mossy fiber tract, motivated by *in vivo* spike train statistics. Interestingly, only the mossy fiber evoked amplitude distribution exhibits a distinct peak at small amplitude values, at which the transfer function $\Phi\psi(A)$ has its highest sensitivity. Moreover, not only there is an optimal mean input phase with respect to a subthreshold oscillation cycle, but also the maximum amount of information that can be conveyed is enhanced as compared to simulations without subthreshold oscillations for all considered amplitude distributions (compare dashed lines in Figure 45C). Finally, to check how information transmission depends on the width of the distribution $p(\psi)$ of input phases, we calculated the information maximum as a function of the standard deviation (std) of $p(\psi)$ (Figure 45D). The maximal information increases from 2.2 bits per spike at std = 36° to 4.2 bits per spike at std = 3° for the mossy fiber evoked amplitude distribution and a maximum synaptic amplitude A_{max} = 14 μA/cm^2. The optimal mean input phase ψ only varies between 249° at std = 3° and 254° at std = 12°. Our results thus reveal the optimal mean input phase to be rather insensitive to the width of $p(\psi)$.

5.8 Concluding Discussion

In this Chapter, we could elucidate how the information encoded in mossy fiber synaptic response amplitudes onto CA3 pyramidal cells through short-term plasticity can be transferred into a temporal code in the postsynaptic action potentials. Using in vitro electrophysiological experiments and a computational model, we could reveal that subthreshold membrane potential oscillations considerably increase the range for temporal encoding, with a window of opportunity of input phases ψ between 100° and 300°. These can be best used with an input distribution of synaptic amplitudes that resembles irregular, in vivo like activity found at the hippocampal mossy fiber synapse.

The feasibility and applicability of the presented mechanism is crucially dependent on a number of parameters, which will be adressed in the following. Whether these constraints can be plausibly matched under physiological circumstances, remains to be investigated in respective in vivo and in vitro experiments in the future. Finally, potential functional uses of the mechanism will be discussed and critically compared to the literature.

5.8.1 Input Phase of EPSCs

A crucial parameter for this manner of temporal coding is the input phase ψ of the facilitating synaptic currents in relation to the membrane potential oscillation. For late input phases $\psi \geq 180°$, the firing phase of the postsynaptic neuron is a straight, only slightly curved function of the synaptic amplitude A, whereas for early input phases $\psi \leq 120°$ this transfer function is strongly curved and exhibits discontinuities. Late input phases, however, provide a smaller possible range of temporal coding than early input phases, as the action potential phases are confined to the interval between the input phase and the peak of the subthreshold oscillation at 360°. In this context we found that information about the amplitude of synaptic input is best transferred into the phase of pyramidal cell action potentials if the mean input phase is ~250°. The transmission of

information is particularly high if we use EPSC amplitude statistics evoked by irregular, in vivo like activity patterns, as introduced in Chapter 4 of this thesis. Short-term facilitation of synaptic EPSCs in combination with subthreshold membrane potential oscillations therefore synergize to generate a temporal spike code. The mean firing and thus input phase of granule cell activity in vivo is, however, still under debate, with reports of firing phases for example locked to the theta cycle between 30° to 120° (Ylinen et al., 1995) or firing phases loosely clustered around 270° (Skaggs et al., 96).

5.8.2 Relation of Theta Oscillation and EPSP Kinetics

The presented mechanism of generation of a temporal code is based on the intersection of a modulatory firing threshold of the CA3 pyramidal neuron by membrane potential oscillations and the depolarizing EPSP. In addition to the input phase ψ, the temporal relation of the EPSP decay and the theta oscillation should be crucial for the amount and quality of temporal coding. This temporal relation can be modulated in two ways, namely by (1) changing the frequency of the subthreshold membrane potential oscillation and (2) a change in the kinetics of the EPSP. Although similar in their effect, physiologically these two mechanisms have distinct causes:

In vivo, the frequency of theta oscillations can vary in a behaviorally-related manner, with a typical range between 6 and 12 Hz. This change is gradual and fast (Robert Schmidt, personal communication) and can even occur between individual trials of the same task. In the context of our mechanism, lower oscillatory frequencies result in longer oscillation cycles. Thus, there should be less opportunity for the EPSP to intersect with the oscillating firing threshold during its decaying phase. Higher oscillatory frequencies on the other hand, result in shorter oscillation cycles, leading to a larger overlap of EPSP and membrane potential oscillation given the same EPSP kinetics. In a set of preliminary experiments (n = 5, data not shown), we have investigated the influence of the theta oscillatory frequency on the temporal coding. Indeed, application of a 6 Hz oscillatory subthreshold membrane potential oscillation led to either a linear precession of AP phases with a limited range of temporal coding, or a discontinuously curved preceding function with a larger temporal range. This finding is similar to the precession found at early input phases ψ as described in paragraph 5.6. Theta frequencies of 9 or 12 Hz on the other hand, enabled a more gradual precession of action potential phases with increasing EPSP amplitudes. Thus, higher oscillatory frequencies favor the generation of the temporal code as presented in this Chapter. These results, however, have to be confirmed more thoroughly in further experiments to draw solid conclusions.

In the context of EPSP kinetics, it was reported previously that in CA1 pyramidal cells synaptically generated currents are dependent on the membrane potential of the postsynaptic cell (Fricker und Miles, 00). Axmacher et al. (Axmacher und Miles, 04) could more specifically show that in particular the EPSP decay time was significantly slowed at membrane potentials near the firing threshold, with timeconstants increased from ~30 ms to up to 300 ms, due to a maintained component of Na^+ currents. If this also holds true for CA3 pyramidal cells, our proposed mechanism of temporal coding should be highly voltage-dependent. We therefore studied the influence of the somatic holding potential on the kinetics of the EPSPs induced by the artificial current injections (Figure 46). As can be seen in the exemplary recordings of three cells, the dependence of EPSP kinetics on the membrane potential in CA3 pyramidal cells is not as prominent as in CA1 pyramidal neurons. In all measured cells, only a slight increase in EPSP amplitude with more depolarizing membrane potentials was detectable. Most importantly, depolarizing the cells to values near the action potential threshold did lead only to small

increases in the EPSP decay time constant, which was even reversed with a further depolarizing step (see Figure 46C and D). Hence, we conclude that the membrane potential of the CA3 pyramidal cell does not play a crucial role in the generation of the temporal code, apart from the general necessity of the cell being near the firing threshold.

In the intact synaptic network, mossy fiber EPSP kinetics may be varied by a number of additional factors: Activation of synaptic kainate receptors activity-dependently generates a slow excitatory synaptic current, which will increase the decay timeconstant and greatly augment the excitatory drive of CA3 pyramidal cells (Castillo et al., 97). Furthermore, mossy fibers not only project onto CA3 pyramidal cells, but also onto local interneurons, which can impose a strong feedforward inhibitory drive onto the synaptic network (compare Chapter 2). This feedforward inhibition may lead to a decrease in the EPSP decay timeconstant and increased precision in AP timing (Pouille und Scanziani, 01). As short-term plasticity of mossy fiber synapses onto CA3 pyramidal cells and interneurons is target-specific in quality and amount (strong facilitation onto pyramidal cells, facilitation or depression onto interneurons), EPSP kinetics in CA3 pyramidal cells will be modulated differently depending on the recent temporal input. The interplay between mossy fiber-driven inhibition and excitation and net result in CA3 pyramidal cells has recently only been investigated in slice cultures (Mori et al., 04) and therefore will have to be determined further.

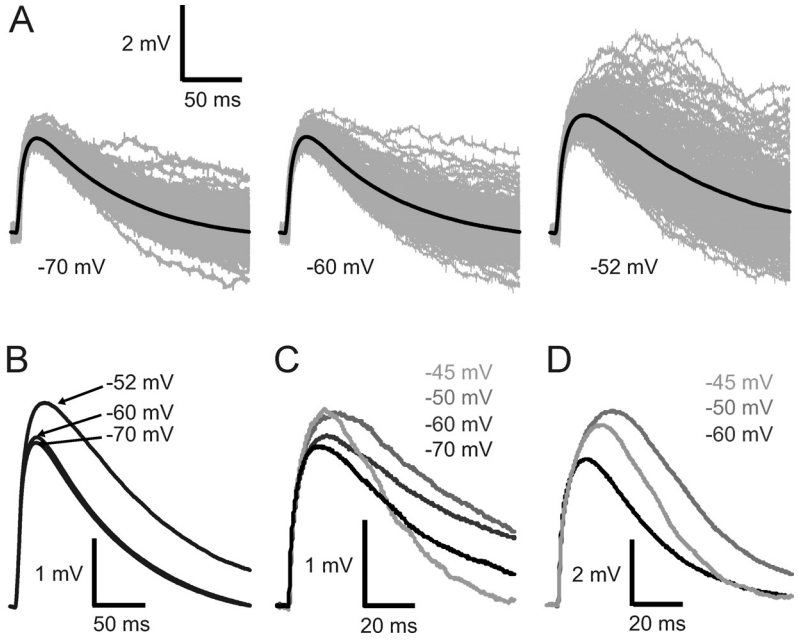

Figure 46: Influence of membrane potential on EPSP kinetics. (A) Exemplary recording of EPSPs of a CA3 pyramidal cell in response to application of the artificial input currents at different membrane potentials. Grey lines depict overlay of 40 trials each, black lines are mean EPSPs. Note the increase in both amplitude and variability in response with increasing depolarization. (B) Overlay of mean EPSPs from A. (C,D) Two different examples where further depolarization leads to faster EPSP kinetics.

5.8.3 Phase Precession and Synaptic Facilitation

The temporal code generated by facilitating synaptic inputs in combination with subthreshold oscillations presented here is similar to the *in vivo* firing pattern of hippocampal principal neurons referred to as phase precession. Herefore, the mossy fiber

synaptic EPSC amplitude had to be associated with the place of the animal on a linear track. If the animal crosses a place field, the firing activity of dentate gyrus granule cells is gradually increased, leading to marked facilitation of mossy fiber synaptic response amplitudes, the prerequisite for our described mechanism. When compared to in vivo findings, our model can account for the qualitative and quantitative parameters of phase precession: Phase precession has been reported to evolve more or less linear with time spent in the place field, which we could reproduce with late input phases and according EPSC amplitude parameters. Moreover, phase precession typically covers a phase range of up to 300°, which we can account for by our transfer function in combination with a broad distribution of input phases. Synaptic facilitation of mossy fiber responses in combination with subthreshold membrane potential oscillations might thus present a cellular model for hippocampal phase precession.

Other suggested mechanisms of hippocampal phase precession make use of a slow dendritic depolarization in contrast to our fast synaptic depolarization. This slow increase of dendritic depolarization is hereby assumed to represent the animal's movement towards the center of a place field, whereas the following slow repolarization would represent the movement away from the place field center. Cellular adaptation (Magee, 01; Harris et al., 02) or assymmetry of the place fields (Mehta et al., 00) could then explain why the cells fire only at rising depolarization (with precessing phase) but not during repolarization. While still appealing, these mechanisms require mean modulatory currents that are substantially larger than the facilitatory EPSCs and oscillations in our model.

Phase precession has not only been found in area CA3 of the hippocampal formation, but also in area CA1, the dentate gyrus and recently also the entorhinal cortex. Although in this Chapter, we have formulated and discussed the generation of a temporal code for dynamical transmission at the mossy fiber to CA3 pyramidal cell synapse, the underlying mechanism may principally apply to all synapses exhibiting pronounced short-term facilitation with matching time scales in the subthreshold membrane potential oscillations. Furthermore, also short-term depression of inhibitory synaptic inputs would result in a net increase of postsynaptic current amplitudes and might therefore account for the same phenomenon.

5.8.4 Temporal Compression of Time Scales

Finally, the proposed mechanism of the generation of a temporal spike code might provide a cellular correlate for bridging the slow behavioral time scales in the order of seconds with the fast time scales of a few milliseconds needed for the induction of plasticity by correlated firing in several neurons (Figure 47). Let us assume that a single CA3 cell's activity reflects the passing of the animals through one place field. If the animal now enters several place fields sequentially, several CA3 pyramidal cells will exhibit a precession of action potential firing in relation to the theta oscillation, one after another in time, depending on the sequence of place field activation. This behavioral order in the range of seconds would thus be conserved in the precise timing of action potentials of several neurons in relation to the theta oscillation. Repetitive activation of the same action potential chronology could therefore be used by the network to learn behaviorally relevant sequences by spike-timing dependent plasticity (Skaggs et al., 96; Melamed et al., 04). We here propose that synaptic facilitation in combination with subthreshold membrane potential oscillations might be the underlying cellular mechanism to achieve such temporal compression.

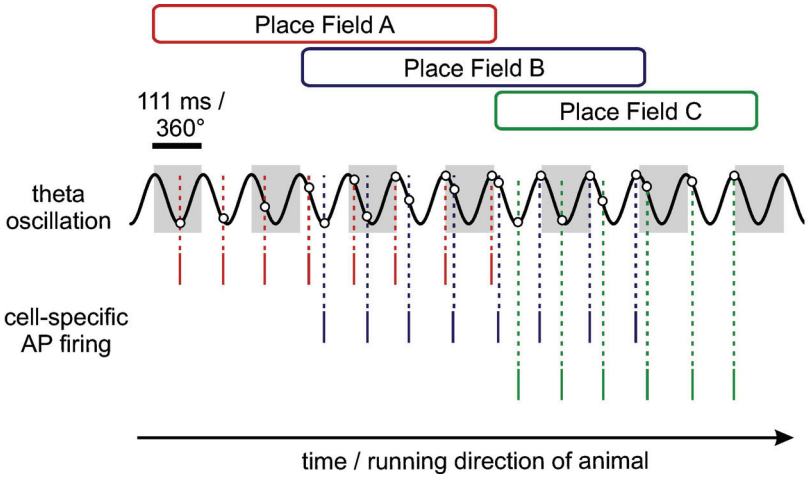

Figure 47: Temporal compression of timescales. Schematic description of the compression of behavioral timescales of seconds to timescales relevant for synaptic plasticity of tens of milliseconds. As the animal traverses place fields A to C, several place cells will sequentially become activated. As the action potentials of place cells A to C precess in relation to the theta oscillation, the sequence of events is preserved in the exact timing of APs. Time differences between firing of different cells are on the order of tens of milliseconds, relevant for spike-timing dependent plasticity.

5.9 Outlook

Summarizing, in this Chapter we have introduced in a proof of principle that the combination of a facilitating input current with subthreshold membrane potential oscillations can be utilized by the postsynaptic neuron to generate a temporal code. The facilitating amplitudes of the synaptic input are hereby represented by the timing of the postsynaptic action potential firing. We have, however, utilized artificial synaptic currents that resembled those of mossy fiber synaptic inputs onto CA3 pyramidal cells. In order to test the biological feasibility of the proposed model, it remains to be determined whether the innate synaptic system would be capable of providing the necessary parameters, such as robustness of facilitation, constant EPSP kinetics and lack of synaptic attenuation. To this end, further *in vitro* experiments using synaptic stimulation of preferably single mossy fibers onto CA3 pyramidal cells will be needed in the future. Furthermore, our proposed model for the generation of a temporal code yields several predictions, which may be tested in in vivo experiments: Selective lesions to the dentate gyrus region should significantly impair phase precession in the CA3 and CA1 area. Also, behaviorally-related modulation of theta oscillation frequency should vary the amount of detectable phase precession. This might even be investigated in already existing data when analyzing single trial phase precession and correlating phase precession with the instantaneous length of a theta cycle. Thus, further investigations will hopefully broaden and strengthen our understanding of the validity of the proposed mechanism.

6 Concluding Remarks

Chemical synapses are key elements for the communication between nerve cells. This communication can be regulated on various time scales and through different mechanisms affecting synaptic transmission. Amongst these are slow and long-lasting adjustments by endogenous neuromodulators, instantaneous and reversible activity-dependent regulation by short-term plasticity and persistent activity-dependent changes by long-term plasticity. Within this thesis, we have investigated several aspects of modulation of synaptic transmission and its function relevance at the example of the hippocampal mossy fiber synapse. As this synapse crucially differs from many other synapses in the central nervous system, Chapters 1 and 2 were dedicated to introducing the conceptual background of chemical synaptic transmission in general and the anatomy and physiology of the hippocampal mossy fiber synapse in particular.

In Chapter 3, we have begun our own investigations at the molecular level of neuromodulation of mossy fiber synaptic transmission. Modulation of synaptic transmission by presynaptic ionotropic and metabotropic receptors is generally an important means to control and adjust synaptic strength. Even though synaptic transmission and plasticity at the hippocampal mossy fiber synapse has been shown to be tightly controlled by presynaptic receptors, little is known about the downstream signalling mechanisms and targets of the different receptor systems. Here, we could identify the cellular signalling cascade by which the purinergic neuromodulator adenosine regulates mossy fiber synaptic transmission. By means of electrophysiological and optical recordings techniques we found that adenosine activates presynaptic A_1 receptors and thereby reduces calcium influx into mossy fiber terminals. Calcium currents are directly modulated via a membrane-delimited pathway and the reduction of presynaptic calcium influx can entirely explain the adenosine-mediated inhibition of synaptic transmission. Specifically, we could demonstrate that adenosine modulates both P/Q- and N-type presynaptic voltage-dependent calcium channels and thereby controls transmitter release at the mossy fiber synapse onto CA3 pyramidal cells. Neuromodulation of synaptic transmission will also crucially affect the short-term plasticity characteristics of mossy fiber synapses, as transmitter release probability inversely regulates the magnitude of short-term facilitation.

In Chapter 4, we then descriptively explored the short-term plasticity features of mossy fiber synaptic transmission using electrophysiological and computational means. The focus of investigation shifts to the relation between presynaptic input and postsynaptic excitatory potentials. Many synapses are dynamic on various timescales, with instantaneous changes in postsynaptic response amplitudes ranging from tens of milliseconds to tens of seconds. Here, we have developed a mathematical model of transmission dynamics at the hippocampal mossy fiber synapse to quantify these distinct forms of plasticity. We found that synaptic short-term plasticity is best described by two facilitatory processes acting on timescales of a few hundred milliseconds and about ten seconds. These different types of facilitation are differentially influenced by long-term potentiation such that the impact of the fast process is weakened compared to that of the slow process. This attenuation is reflected by a selective decrease of not only the amplitude but also the time constant of the fast facilitation. We henceforth argue that

mossy fiber long-term potentiation, involving a modulation of parameters determining both amplitude and timecourse of short-term plasticity, might serve as a mechanism to adapt the synapse to its temporal input.

In Chapter 5, we finally investigate how short-term plasticity of postsynaptic excitatory potentials influences the action potential output sequences of postsynaptic neurons. In general, short-term synaptic plasticity translates a temporal pattern of presynaptic input to a distinct series of postsynaptic response amplitudes. Here, we have now introduced a mechanism on how the temporal information contained in this response distribution may be preserved in the resulting action potential sequence of the postsynaptic neuron. As a model system we have again explored the mossy fiber onto CA3 pyramidal cell synapse using electrophysiological and modelling techniques. We could quantify the temporal range of action potential firing generated by short-term plasticity and discuss how this range is increased by the addition of subthreshold membrane potential oscillations in the theta range. The proposed mechanism of translating temporal input information into output spike sequencing is similar to the *in vivo* phenomenon of phase precession of action potentials and may be used to compress behavioral onto synaptic plasticity timescales relevant for learning and memory. We thus hypothesize that short-term plasticity in combination with subthreshold membrane potential oscillations may serve an important role in information transmission in the CA3 hippocampal network.

Taken together, the hippocampal mossy fiber synapse exhibits most intriguing short- and long-term plasticity of transmission. Throughout this thesis, the focus of investigating the underlying mechanism, extent and implications of such plasticity evolved: We have covered aspects spanning from the presynaptic subcellular regulation of transmitter release at mossy fiber terminals, over the description of short-term plasticity of mossy fiber postsynaptic responses, to the functional role of short-term dynamics on the action potential output of CA3 pyramidal cells. With these results, we could make a small contribution to further the understanding of the functioning and relevance of this complex and special synaptic system.

7 Appendices: Materials, Methods and Mathematical Descriptions

7.1 Adenosine at the Mossy Fiber Synapse

7.1.1 Preparation of Hippocampal Slices

For field potential, somatic whole-cell and calcium imaging experiments hippocampal slices were prepared from C57/Bl6 mice (age: postnatal days P 16-42) as previously described (Schmitz et al., 03). All experiments were performed according to the animal welfare guidelines of the Charité, Universitätsmedizin Berlin. In brief, the animals were anesthetized with diethylether, decapitated and the brains removed. Tissue blocks containing the subicular area and hippocampus were mounted on a Vibratome (Campden Instruments MA752 or DSK DTK-1000) in a chamber filled with ice-cold artificial cerebrospinal fluid (ACSF), containing (in mM): 50 NaCl (87 for whole-cell recordings), 150 sucrose (75 for whole-cell recordings), 25 $NaHCO_3$, 2.5 KCl, 1 NaH_2PO_4, 0.5 $CaCl_2$, 7 $MgSO_4$, 10 glucose; pH 7.4. Slices were cut at 300-400 µm thickness and heated to 35°C for 30 minutes. The slices were then cooled to room temperature and transferred to ACSF containing (in mM): 124 NaCl, 26 $NaHCO_3$, 10 glucose, 3 KCl, 2.5 $CaCl_2$, 1.3 $MgSO_4$, 1.25 NaH_2PO_4. All ACSF was equilibrated with 95 % O_2 and 5 % CO_2. The slices were stored in a submerged chamber for 1-7 hours before being transferred to the recording chamber, where they were perfused with ACSF at a rate of 3-4 ml/min.

For direct recordings from mossy fiber boutons, hippocampal slices were prepared as described previously (Bischofberger et al., 06). In brief, transverse 300 µm thick slices were cut from the hippocampus of 21- to 24-day-old Wistar rats with a custom-built vibratome (Geiger et al., 02). For the dissection and storage of slices, a saline with (in mM) 64 NaCl, 25 $NaHCO_3$, 10 glucose, 120 sucrose, 2.5 KCl, 1.25 NaH_2PO_4, 0.5 $CaCl_2$, and 7 $MgCl_2$ was used.

7.1.2 Field potential and postsynaptic whole-cell recordings

Whole-cell voltage-clamp and field excitatory postsynaptic potential (fEPSP) recordings were performed with an Axopatch 700A (Axon Instruments, Foster City, CA, USA). Data were digitized (National Instruments BNC-2090) at 5-10 kHz and recorded and analyzed with custom-made software in IGOR Pro (WaveMetrics Inc., OR, USA). Patch electrodes (with electrode resistances ranging from 3 to 6 MΩ) were filled with (in mM): 117.5 gluconate, 2.5 CsCl, 10 TEA, 8 NaCl, 10 HEPES, 0.2 EGTA, 4 MgATP, 0.3 Na_3GTP and 5 QX-314, pH adjusted to 7.3 with CsOH. Series resistances were 14 ± 4 MΩ, were continuously checked during the recordings and not allowed to vary more than 25 % during the course of the experiment. No series resistance compensation was used. Field potential recordings were performed with low resistance patch pipettes filled with external solution placed in stratum lucidum. All recordings were performed at room temperature.

7.1.3 Stimulation of mossy fibers

Mossy fibers were extracellularly stimulated with patch pipettes filled with external solution placed in the granule cell layer or in the hilus region (see Figure 2-2A). The mossy fiber origin of recorded signals was routinely verified by the following procedures and experiments were discarded if they did not match the criteria: Both in field potential and whole-cell recordings, synaptic response amplitudes were largely increased when the 'frequency facilitation' paradigm was applied, i.e. a switch in stimulation frequency from 0.05 (0.1 in whole-cell recordings) to 1 Hz (Figure 2-2B and C). fEPSPs were only accepted if responses showed more than 400 % synaptic facilitation. In addition, application of the group II metabotropic glutamate receptor agonist DCGIV (0.5-1 µM) at the end of the experiment had to block synaptic transmission. In field potential recordings, synaptic responses were generally completely blocked (see also Chapter 2). In a few cases, a repetitive fiber volley was detectable, which was still present with subsequent application of NBQX and could then be subtracted from every trace. In whole-cell recordings an increase of synaptic failures from 11 ± 3 % under control conditions to 86 ± 7 % after application of DCGIV was obtained, also reflected by an inhibition of synaptic transmission by 94 ± 3 % (n = 6).

7.1.4 Presynaptic patch-clamp recordings

Mossy fiber boutons in stratum lucidum of the hippocampal CA3 region were visually identified by their size and location (3-4 µm apparent diameter) using infrared differential interference contrast videomicroscopy. Furthermore, identification was confirmed by the small capacitance (~1 pF) and the high input resistance (>1 GΩ,. Patch pipettes were pulled from borosilicate glass tubing (2.0 mm outer diameter, 0.7 mm wall thickness; Hilgenberg, Malsfeld, Germany). Whole-cell voltage-clamp recordings were performed with an Axopatch 200A amplifier (Axon Instruments, Foster City, CA, USA). Current signals were filtered at 5 kHz, with a 4-pole low-pass Bessel filter and sampled at a frequency of 20 kHz using a CED 1401plus interface (Cambridge Electronic Design, Cambridge, UK) connected to a personal computer. Pulses were generated using custom-made software running under IGOR Pro, which allowed us to apply a previously recorded action potential (AP) as voltage-clamp command. The presynaptic AP waveform was taken from Figure 5A in Bischofberger et al. (2002). For whole-cell voltage-clamp recordings, we used 5 to 8 MΩ pipettes filled with a solution containing (in mM): 135 CsCl, 10 EGTA, 4 $MgCl_2$, 4 Na_2ATP, 0.3 NaGTP, 10 Na_2-phosphocreatine, and 10 HEPES (the pH was adjusted to 7.3 with CsOH). The bath solution contained (in mM): 105 NaCl, 25 $NaHCO_3$, 25 glucose, 2.5 KCl, 1.25 NaH_2PO_4, 2 $CaCl_2$, 1 $MgCl_2$, 2 µM tetrodotoxin (TTX), 20 tetraethylammonium chloride, and 5-4-aminopyridine to block voltage-gated Na^+ and K^+ channels, respectively. Leak and capacitive currents were subtracted using two P/ 4 sequences within each protocol. Current traces shown in the figures represent the averages of 5-10 sweeps. The series resistance (typically between 20 and 50 MΩ) was compensated by 80-90 % with a lag of 20 30 µsec. In some recordings, unclamped tail currents with very slow time course were apparent (these currents may have been generated in neighboring boutons). These recordings were discarded. All Ca^{2+} current recordings were done at room temperature (~22°C).

7.1.5 Fluorescence measurements

Mossy fibers were locally labelled with a pressure stream of the low-affinity calcium indicator Magnesium Green AM (100 µM, Kd = 6 µM; Molecular Probes, Eugene, OR) for photodiode measurements or with 200 µM of the calcium indicator

Oregon Green BAPTA 1-AM (Kd = 170 nM, Molecular Probes, Eugene, OR) dissolved in 20 % Pluronic/DMSO for confocal imaging experiments. The final DMSO concentration in the injection ringer was 5 %. Recordings were started 2-3 h after labelling. Epifluorescence was measured with a single photodiode from a spot more than 200 µm away from the loading site with an Olympus LumPlan FI 60x 0.9NA water immersion objective. The signals from the photodiode were low pass filtered with 1 kHz, digitized at 5 kHz and captured with IGOR Pro software. The change in fluorescence intensity (ΔF) relative to the baseline intensity of fluorescence (F) was calculated as ΔF/F.

For time-lapse confocal recordings, a Yokogawa CSU-22 spinning disc confocal system (BFI Optilas, Puchheim, Germany) was deployed with an Olympus BX-51WI upright microscope and a RedShirt NeuroCCD-SMQ camera (Life Imaging Services, Reinach, Switzerland). Excitation was provided at 488 nM by a Coherent Sapphire 488-50 Laser (Coherent, Utrecht, Netherlands). With the Olympus LumPlan FI 60x 0.9NA water immersion objective, the lateral pixel size was 0.4 µm. With the same objective, the pinhole size of the Yokogawa CSU-22 spinning disc confocal corresponded to 1.18 Airy units at 520 nm emission wavelength. Full frames were recorded at 125 Hz. Only boutons in the periphery of the stained structures were chosen to circumvent any crosstalk between adjacent pinholes in thick fluorescent specimen. Boutons were discarded if there was an increase in the exponential decay time constant of the calcium transient >20 % over the time of the recording. For morphological representation of the stained mossy fiber boutons, we switched to a Hamamatsu ORCA ER CCD camera. At 20x and 60x the lateral pixel size was 0.32 µm and 0.11 µm, respectively. A frame size of 1344 x 1024 pixels was collected at 1 Hz. Images of single boutons were digitally deconvoluted using the Huygens essential software (SVI imaging, Hilversum, Netherlands).

7.1.6 Analysis and Statistics

In presynaptic bouton recordings, Ca^{2+} currents were evoked by 30 ms voltage-steps to 0 mV from a holding potential of -80 mV and current amplitude was measured as the mean current value during the last 20 ms of the voltage pulse. The activation time course of the Ca^{2+} current *I(t)* was fitted with either a monoexponential function

$$I(t) = I_0(1 - \exp[-(t-\delta)/\tau]) \quad (1)$$

for $t \geq \delta$, or with the sum of two exponentials

$$I(t) = I_0(1 - \exp[-(t-\delta)/\tau]) \quad (2)$$

for $t \geq \delta$, with delayed onset accounting for the delay in Ca^{2+} channel activation. According to previous results, the delay δ was constrained to $\delta \approx 200\text{-}300$ µs. To account for the additional small delay introduced by the lag of series resistance compensation (20-30 µs) and by electronic filtering (5 kHz), the current trace was shifted in time by 100 µsec. With this shift, the end of the rectangular current pulse corresponded to the time when the tail current rose to ~50 % of its peak amplitude. The fitted peak-current amplitudes (I_0, I_1, and I_2) were either given as absolute values or as relative amplitude contributions $A_1 = I_1 / (I_1+I_2)$ and $A_2 = I_2 / (I_1+I_2)$. Accordingly, the amplitude-weighted sum of the activation time constants τ was calculated as $\tau_w = A_1 \bullet \tau_1 + A_2 \bullet \tau_2$. Time-course fitting was performed using IGOR Pro and coefficient values were adjusted by nonlinear least-square fitting based on a built-in Levenberg-Marquardt algorithm.

In field potential and optical recordings, dose-response curves were fitted with a logistic equation of the form:

$$y = A_f + (100 - A_f)/(1 + ([adeno\sin e]/EC_{50})^n) \quad (3)$$

with A_f being the maximum effect of the drug in percent and y being the normalized fEPSP or ΔF/F (Microcal Origin, Northampton, MA, USA). Throughout the text, average values are expressed as mean ± standard error of the mean. Statistical significance was tested with a Student´s t-test, except for the experiments with forskolin, the PKA agonist and antagonist (Figure 3-5), where an ANOVA test was used to compare the three different test groups against the control group with CPA alone, followed by Dunnett´s multiple comparison test (Prism software package, Graph Pad; El Camino Real, CA, USA).

7.1.7 Drugs and Chemical Compounds

Adenosine, CGS (4-[2-[[6-Amino-9-(N-ethyl-β-D-ribofuranuronamidosyl)-9H-purin-2-yl]amino]ethyl]benzenepropanoicacid-hydrochloride), CPA (N6-cyclopentyl-adenosine), D-AP5, DCG-IV, DPCPX (8-Cyclopentyl-1,3-dipropylxanthine), forskolin, IB-MECA (1-[2-Chloro-6-[[(idophenyl)methyl]amino]-9H-purin-9-yl]-1-deoxy-N-methyl-β-D-ribofuranuronamid and NBQX were obtained from Tocris International (via Biotrend, Cologne, Germany). Cadmium and nickel were from Sigma-Aldrich (Munich, Germany), the toxins ω-Agatoxin IVA and ω-Conotoxin GVIA were from Peptides International (Louisville Kentucky, USA). Cytochrome c (0.1 mg/ml) and bovine serum albumine (0.1 %) were added to solutions containing toxins. Sp-5,6-DCl-cBIMPS (5,6-Dichloro-1-β-D-ribofuranosylbenzimidazole-3',5'-cyclic monophosphorothioate) and RP-8-CPT-cAMPS (8-(4- Chlorophenylthio) adenosine- 3', 5'- cyclic monophosphorothioate, Rp-isomer) were purchased from BIOLOG Life Science Institute (Bremen, Germany). After each experiment involving the usage of DPCPX the complete perfusion system was exchanged in order to prevent accumulation of the drug in the tubing and the recording chamber cleaned with ethanol.

7.2 Interdependence of STP and LTP

7.2.1 Slice Preparation

Hippocampal slices were prepared from 3-6 week old B6/C57 mice. For further details, see Appendix A.

7.2.2 Whole-cell and field potential recordings

Whole-cell recording electrodes were filled with intracellular solution containing in mM: 120 Cs-gluconate, 5 CsCl, 10 TEA-Cl, 8 NaCl, 10 HEPES, 5 EGTA, 4 MgATP, 0.3 Na_3GTP and 5 QX-314; pH adjusted to 7.3 with CsOH. In whole-cell recordings, inhibitory responses were blocked with gabazine (1 μM). Field potential recordings were performed with low-resistance patch pipettes filled with external solution placed in stratum lucidum. Most of the recordings were done at room temperature. However, the most critical experiments were repeated at physiological temperature. Field EPSP and EPSC amplitudes were stored and analyzed online and offline using Igor Pro (WaveMetrics Inc., Lake Oswego, OR, USA) and analyzed offline using Matlab (The MathWorks Inc., Natick, MA, USA).

7.2.3 Mossy Fiber Stimulation

Mossy fibers were stimulated and mossy fiber synaptic responses recorded as detailed in Appendix 7.1.

7.2.4 Irregular Stimulus Trains

We used irregular stimulus trains resembling the natural spike statistics from dentate gyrus granule cells (Mizumori et al., 89; Jung und McNaughton, 93) to physiologically modulate transmission at the mossy fiber synapse. Stimulus trains followed a 1/ISI-distribution, where the probability of an inter-stimulus interval (ISI) was proportional to 1/ISI with minimal and maximal ISIs of 50 ms and 50 s, respectively, and a resulting median ISI of about 1.5 s. We applied the same stimulus trains in whole-cell and field potential recordings and used 5 different stimulus trains in total (i.e. different drawings from the same distribution) consisting of 90-100 pulses in about 10 minutes each.

7.2.5 Experimental paradigm LTP

Field potential experiments involving the induction of LTP were conducted as follows: After establishing mossy fiber synaptic stimulation, irregular stimulus trains were applied at least twice. LTP was then induced by three repetitions of tetanic stimulation at 25 Hz for 5 s with 30 s pauses inbetween trains. After a stabilizing period of about 15 minutes following the induction protocol, the irregular stimulus trains were applied again.

7.2.6 Quantification of Variability in fEPSPs

Within one field potential experiment, fEPSP amplitudes in response to a given stimulus train were highly reproducible for repetitive use of the same stimulus train (see Figure 4-6C; $r > 0.99$). The variability σ of the fEPSP amplitudes is estimated under the assumption of additive noise. We therefore applied the same random stimulus train at least twice before as well as after the induction of LTP to obtain two sets of fEPSP amplitudes $A_n^{(1)}$ and $A_n^{(2)}$, with $n = 1,...,N$ and N being the number of stimulation pulses. To detect non-stationarities in the data, we calculated the slope α of the regression line of $A_n^{(2)}$ as function of $A_n^{(1)}$. The variability of the fEPSP amplitudes is then estimated as

$$\sigma^2 = \frac{1}{1+\alpha^2}\left[\alpha^2 \operatorname{var}\left(A^{(1)}\right) + \operatorname{var}\left(A^{(2)}\right) - 2r\alpha\sqrt{\operatorname{var}(A^{(1)})\operatorname{var}(A^{(2)})}\right] \quad (1)$$

The slope correction α accounts for weak non-stationarities. We checked that α and α-1 never exceeded a value of 1.2. In this case and for a high value of r, σ^2 is about half of the so-called square error $\sigma 2\{2|1\}$ of a linear regression of $A_n^{(2)}$ on $A_n^{(1)}$.

7.2.7 Modelling

To quantify STP at the hippocampal mossy fiber synapse, we developed a phenomenological model that can fit physiologically obtained response amplitudes. Our model is motivated by previous approaches (Sen et al., 96; Varela et al., 97; Hanson und Jaeger, 02) that describe dynamical synaptic transmission at other synapses. Parameters of our model are the baseline amplitude A_0, the amplitude a_{slow} and time constant τ_{slow} of the slow facilitation, the amplitude a_{fast} and time constant τ_{fast} of the fast facilitation, and the factor g that describes the saturation of the slow facilitation (see Chapter 4-5 for

details). We omitted a saturation of the fast facilitation, as it did not improve the goodness of fit.

The model was chosen such that a_{slow} and a_{fast} denote the relative amplitudes of the slow and fast process, respectively. This is convenient since experimental data generally provide normalized synaptic response amplitudes. For example, in our model the paired-pulse ratio amounts to

(2) $$1 + a_{slow} + a_{fast}$$

in the limit of ISIs being much smaller than τ_{fast} . The relative frequency facilitation for stimulation frequencies $f << 1 / \tau_{fast}$ can be computed as

(3) $$1 + a_{slow}\left[X_{slow}(f)(1+g)/(1+gX_{slow}(f))\right]^k$$

with

(4) $$X_{slow}(f) = 1/\{\exp[1/(f\tau_{slow})] - 1\}$$

as an abbreviation for the equilibrium value of the slow dynamical variable at stimulus frequency f. We tested various models with different exponents (k = 1,2,3,4,5 and m = 0,1,2) as well as a multiplicative combination of the two facilitation terms. For a specific model, the parameters A_0 , a_{slow} , τ_{slow} , g , a_{fast} , and τ_{fast} were determined by multidimensional minimization of the mean squared error between observed amplitudes and model predictions. We therefor used a line search algorithm (COBYLA: implementation of Powell's method from http://www.jeannot.org/~js/code/index.en.html). The procedure was implemented using the C programming language. For a set of N experimentally obtained fEPSP amplitudes $A_n^{(exp)}$, n=1,...,N, and the noise variance σ^2 from equation (1), the quality of a model prediction A_n is quantified by the goodness of fit

(5) $$\chi^2 = \sum_{n=1}^{N} (A_n - A_n^{(\exp)})^2 / [\sigma^2 (N - M)]$$

where M is the number of parameters.

7.2.8 Estimation of the Number of Synapses Contributing to Field Potential Recordings

In whole-cell recordings of CA3 pyramidal cells, mossy fiber synaptic response amplitudes are highly variable due to stochastic release of transmitter (see Chapter 2). Under the assumption that this release is stochastically independent within a population of recorded synapses, one can derive an estimate of the number S of synapses contributing to a field potential recording through comparing the relative variabilities CV^2 of whole-cell (wc) and field potential recordings (field) as $CV^2_{wc} = S \bullet CV^2_{field}$ with

(6) $$CV^2 = \mathrm{var}\,iance / mean^2$$

Analyzing exemplary 30-40 data points under constant frequency stimulation at 0.1 Hz respectively, we determined mean values of $CV^2_{wc} = 0.3479 \pm 0.0335$ (n = 5 cells) and $CV^2_{field} = 0.0052 \pm 0.0013$ (n = 6 fEPSP recordings) and thus obtain $S = 67$ synapses. In other words, in order to acquire whole-cell data with the same low variability as observed in field potential recordings, one would need about 67 repetitions of whole-cell measurements.

7.3 Temporal Coding via Synaptic Facilitation

7.3.1 Slice Preparations

Hippocampal slices were prepared from 15-26 day old Wistar rats. For preparation details, see Appendix 7.1.

7.3.2 Recordings

Whole-cell recording electrodes were filled with an intracellular solution containing: 135 K-gluconate, 20 KCl, 2 MgATP, 10 HEPES, 0.2 EGTA, 5 phosphocreatine, and was adjusted to pH 7.3. All recordings were done at near physiological temperature (34°C). In part of the experiments, spontaneous network activity was blocked with gabazine (1 µM) and CNQX (25 µM). Measurements were performed using a Multiclamp 700A amplifier (Axon Instruments, Foster City, CA, USA). Data were stored and analyzed using custom-made software in Igor Pro (WaveMetrics Inc., Lake Oswego, OR, USA) and Matlab (The Mathworks Inc., Natick, MA, USA). In the current-clamp experiments depicted in the Chapter 5, CA3 pyramidal cells were held at membrane potentials between -55 and -48 mV by positive current injection (junction potential of ~10 mV not corrected). These values are in the same range as the resting potentials of CA1 pyramidal cells in vivo (Lee et al., 2006).

7.3.3 Definition of Phase of Action Potential Firing

The phase Φ of the postsynaptic action potentials is given relative to the peaks of the membrane potential oscillations. These peaks were determined from an average of five oscillation cycles without additional EPSC injection. Phase zero thus corresponds to the maximum of the intracellular membrane potential oscillation, which in the hippocampus, coincides with the through of the in vivo extracellular local field potential in stratum pyramidale (Buzsaki, 02). From n = 21 applications of stimulation protocols with combined oscillatory and EPSC currents we determined a phase shift of 62 ± 8° (mean ± std) between the injected current oscillation I_{osc} and the measurable membrane potential oscillation due to the membrane time constant of the CA3 pyramidal cell. This phase shift was cell-specific. However, whenever pooled phase data from several cells are depicted, we corrected the firing phase by a constant phase shift of 60°. All data shown was obtained from at least 10 repetitions of a stimulus train and represents results from n = 11 cells.

7.3.4 Two Compartment CA3 Pyramidal Cell Model

Computer simulations made use of a two compartment neuron model of a CA3 pyramidal cell by Pinsky and Rinzel (1994). The model consists of a somatic and a dendritic compartment. The somatic compartment contains standard Hodgkin-Huxley-type inactivating sodium and potassium delayed-rectifier currents. The dendritic compartment contains a calcium current, a potassium-mediated slowly activating afterhyperpolarization (AHP) current and a fast activating potassium-mediated current, which calcium-dependently saturates. The model has been extensively studied and can be considered as one of the standard models for CA3 pyramidal cells. The external currents applied to the model have the same shape as I_{osc} and I_{syn} in the electrophysiological recordings. The amplitude of the oscillatory current was $I_1 = 2$ µA/cm^2, resulting in an amplitude of about 5 mV for the membrane potential oscillation. The firing threshold was

adjusted by an additional application of a constant current of I_0 =-0.3 μA/cm^2 to prevent firing for EPSC amplitudes A = 0. For simulations without subthreshold oscillations, we chose I_1 = 0 and I_0 =-2.3 μA/cm^2, which lead to a maximal delay of 70 ms between EPSC onset and action potential. The model was implemented in C programming language. Integration was performed using a 4th order Runge-Kutta algorithm with adaptive step size (Press WH et al., 92).

7.3.5 Mutual Information

The sensitivity of the AP phase Φ on changes of the EPSC amplitude *A* was quantified by the mutual information

(1)
$$I = \int_{A\min}^{A\max} dA p(A) \int_0^{360^\circ} d\Phi p(\Phi \mid A) \lg_2 \left[\frac{p(\Phi \mid A)}{\int_{A\min}^{A\max} dA' \, p(\Phi \mid A') p(A')} \right]$$

between Φ and *A*. We therefore require a model of the amplitude distribution *p(A)* and the conditional probability p(Φ|A) of having Φ, given *A*. The latter distribution is obtained through

(2)
$$p(\Phi \mid A) = \int_0^{360^\circ} d\Psi p(\Psi) \delta(\Phi - \Phi_\Psi(A))$$

in which the phase transfer function Φψ(*A*) is derived from the two-compartment model. The distribution *p(ψ)* of input phases is assumed to be Gaussian. Unless stated otherwise, the standard deviation of *p(ψ)* was set to the exemplary value of 30°. The minimal and maximal EPSC amplitudes were $A_{min} = 0$ and $A_{max} = 14$ μA/cm^2, respectively.

8 Statement of Contribution

The projects discussed in this thesis have been conducted in a collaborative approach. In the following, I will state the respective contributions to the data presented.

Chapter 2

I have performed all the experiments presented in this Chapter.

Chapter 3

I have conducted all the field potential and whole-cell recordings of CA3 pyramidal cells presented in this Chapter, except the measurements with CGS and IB-MECA in Figure 3-2B, which were contributed by Maria Torvinen. Jörg Breustedt has performed the microfluorometric recordings of calcium transients using the photodiode, and, together with Friedrich Johenning, contributed the optical recordings using the Nipkow-Spinning Disc recordings. Josef Bischofberger has conducted the single-bouton measurements of presynaptic calcium currents.

Chapter 4

I have performed all the electrophysiological experiments presented in this Chapter. The computational modelling was conceived and conducted by Christian Leibold and Richard Kempter, with contributions by Katja Gebert and Marion Moisel.

Chapter 5

I have conducted all the electrophysiological experiments presented in this Chapter. The computational modelling presented was conceived and conducted by Christian Leibold, Kay Thurley and Richard Kempter.

In addition, and referring to all the Chapters above, I have analyzed all my experimental data, developed new analytical tools, designed experiments and contributed to writing the respective manuscripts.

9 Deutsche Zusammenfassung

Synapsen sind spezialisierte neuronale Strukturen im Gehirn, die die Kommunikation zwischen Nervenzellen auf elektrischem oder chemischen Weg ermöglichen. Die Struktur und Wirkungsweise chemischer Synapsen konnte im Laufe des letzten Jahrhunderts mit Hilfe anatomischer, optischer und elektrophysiologischer Studien detailliert beschrieben werden. Anatomisch und physiologisch sind Synapsen jedoch erstaunlich divers, unter anderem abhängig von der untersuchten Hirnregion, der Identität der prä- und postsynaptischen Neurone, den präsynaptisch ausgeschütteten Neurotransmittern und postsynaptischen Rezeptorsystemen.

Die Effizienz oder Stärke synaptischer Übertragung kann durch unterschiedliche Mechanismen beeinflusst werden: Neuromodulation bezeichnet die langsame und persistierende Regulation der synaptischen Transmission durch endogene Neuromodulatoren, welche spezifische intrazelluläre Kaskaden aktivieren und dadurch z.B. die Ausschüttung von Neurotransmitter modulieren. Kurzzeit-Plastizität beschreibt die instantane und reversible, aktivitätsabhängige Modulation synaptischer Transmission, die durch eine Veränderung der Wahrscheinlichkeit der präsynaptischen Transmitter-Freisetzung entweder fazilitierend oder deprimierend wirken kann. Unter Langzeit-Plastizität versteht man die persistierende, ebenfalls aktivitätsabhängige Stärkung oder Schwächung der synaptischen Effizienz. In dieser Dissertation wurden nun verschiedene Aspekte der Neuromodulation, Kurzzeit- und Langzeit-Plastizität am Beispiel der hippokampalen Moosfaser-Synapse erörtert. Im folgenden sollen die wichtigsten Aussagen und Ergebnisse der einzelnen Kapitel der Arbeit zusammengefasst werden.

Die hippokampale Moosfaser-Synapse auf CA3 Pyramidenzellen stellt einen wichtigen Verarbeitungsschritt im exzitatorischen hippokampalen Netzwerk dar. Jedoch unterscheidet sie sich von anderen Synapsen im zentralen Nervensystem sowohl anatomisch als auch funktionell. Kapitel 1 erläutert daher die allgemeinen Konzepte chemischer synaptischer Transmission, während in Kapitel 2 der Dissertation die spezifischen morphologischen und physiologischen Eigenschaften der hippokampalen Moosfaser-Synapse eingeführt werden.

Kapitel 3 der Arbeit ist einem subzellulären Mechanismus der Neuromodulation der Transmission der Moosfaser-Synapse auf CA3 Pyramidenzellen gewidmet. Hier beginnt auch die eigentliche Darstellung unserer neuen Forschungsergebnisse. Die Modulation synaptischer Transmission durch präsynaptische ionotrope und metabotrope Rezeptoren ist generell ein wichtiger Weg um synaptische Stärke zu kontrollieren und anzupassen. Transmission und Plastizität der hippokampalen Moosfaser-Synapse wird eng durch präsynaptische Rezeptoren reguliert, es ist jedoch teilweise nur wenig über die nachfolgenden aktivierten Signalkaskaden der verschiedenen Rezeptorsysteme bekannt. In diesem Kapitel konnten wir nun die zelluläre Signalkaskade identifizieren, durch die der purinerge, inhibierende Neuromodulator Adenosin die Transmission an der hippokampalen Moosfaser-Synapse kontrolliert. Mittels elektrophysiologischer und optischer Ableittechniken konnten wir feststellen, dass Adenosin präsynaptische Rezeptoren des Subtyps A_1 aktiviert und dadurch den Aktionspotential-vermittelten Einstrom von Kalzium in die Moosfaser-Terminale reduziert. Präsynaptische Kalzium-Ströme werden direkt über einen membrangebundenen Mechanismus moduliert und

deren Reduktion kann gänzlich die Adenosin-vermittelte Inhibition der synaptischen Transmission erklären. Im Speziellen konnten wir nachweisen, dass Adenosin präsynaptische Kalzium Kanäle sowohl des P/Q- als auch N-Typs moduliert und dadurch die Transmitter-Ausschüttung kontrolliert. Diese langfristige Neuromodulation der synaptischen Transmission wird zusätzlich auch die Charakteristik der Kurzzeit-Plastizität verändern, da die Wahrscheinlichkeit der Transmitter-Ausschüttung invers mit der Ausprägung der Kurzzeit-Fazilitierung korreliert.

In Kapitel 4 der Dissertation folgt dann eine beschreibende Untersuchung der Eigenschaften der Kurzzeit-Plastizität synaptischer Transmission an der Moosfaser-Synapse anhand elektrophysiologischer und theoretischer Methoden. Der Schwerpunkt der Betrachtung verlagert sich hier auf den Zusammenhang zwischen präsynaptischer zeitlicher Eingangsaktivierung und postsynaptischer exzitatorischer Potentiale. Die meisten Synapsen zeigen instantane Veränderungen in ihren postsynaptischen Antwort-Amplituden in Reaktion auf zeitlich variierenden präsynaptischen Eingang. Diese merkbare Dynamik besitzt Zeitkonstanten zwischen mehreren Hundert Millisekunden und mehreren Sekunden. Hier haben wir nun auf der Basis experimenteller Befunde ein mathematisches Modell entwickelt, das diese Transmissions-Dynamik an der hippokampalen Moosfaser-Synapse umfasst und dadurch die Ausprägungen der Kurzzeit-Plastizität quantifiziert. Wir konnten zeigen, dass synaptische Kurzzeit-Plastizität am besten durch zwei fazilitierende Prozesse beschrieben werden kann, die auf Zeitskalen von wenigen Hundert Millisekunden und ungefähr zehn Sekunden agieren. Diese unterschiedlichen Formen der Fazilitierung werden differentiell durch Langzeit-Plastizität beeinflusst, so dass der Einfluss der schnellen Fazilitierung auf die Gesamt-Fazilitierung vermindert wird in Relation zur langsamen Fazilitierung. Diese Schwächung ist messbar durch eine selektive Abnahme sowohl der Amplitude als auch Zeitkonstante der schnellen Fazilitierung, während die langsame Fazilitierung nach Ausprägung von Langzeit-Potenzierung unverändert bleibt. Eine Schlussfolgerung dieser Ergebnisse ist daher, dass Langzeit-Plastizität an der Moosfaser-Synapse einen Mechanismus darstellt, die Synapse an veränderte zeitliche Eingangsstatistiken anzupassen.

Im Allgemeinen überführt Kurzzeit-Plastizität ein zeitliches Muster präsynaptischen Eingangs in eine bestimmte Verteilung postsynaptischer Antwortamplituden. Kapitel 5 der Arbeit stellt nun abschließend einen Mechanismus vor, wie die zeitliche Information dieser Amplitudenverteilung in der Abfolge von Aktionspotentialen als Ausgangssignal der postsynaptischen Zelle erhalten bleiben kann. Als Modellsystem haben wir wiederum die Moosfaser-Synapse auf CA3 Pyramidenzellen mit Hilfe elektrophysiologischer Methoden und mathematischer Modellierung untersucht. Wir konnten den zeitlichen Bereich nach einem präsynaptischen Stimulus quantifizieren, im dem Aktionspotentiale durch Kurzzeit-Plastizität ausgelöst werden und diskutieren wie dieser Bereich durch zusätzliche unterschwellige Membranpotential-Oszillationen in Theta-Frequenz vergrößert werden kann. Der vorgeschlagene Mechanismus zur Übertragung zeitlicher Eingangsinformation in Ausgangssequenzen von Aktionspotentialen ist vergleichbar mit dem *in vivo* Phänomen ‚Phasenpräzession'. Ausserdem könnte er eingesetzt werden, um verhaltensrelevante Zeitskalen im Sekundenbereich auf Zeitskalen synaptischer Plastizität im Millisekundenbereich relevant für Lernen und Gedächtnisbildung zu komprimieren. Kurzzeit-Plastizität in Kombination mit unterschwelligen Membranpotential-Oszillationen könnte daher eine wichtige Rolle zur Informationstransmission in der CA3 Region des Hippokampus einnehmen.

Zusammenfassend lässt sich festhalten, dass die hippokampale Moosfaser-Synapse eine faszinierende Ausprägung von sowohl Kurzzeit- als auch Langzeit-Plastizität der

synaptischen Transmission zeigt. Im Laufe der vorliegenden Arbeit entwickelt sich der Fokus der Untersuchungen zu den zugrunde liegenden Mechanismen, der Ausprägung und Auswirkungen solcher Plastizität: Wir haben verschiedene Teilaspekte behandelt, ausgehend von der präsynaptischen, subzellulären Regulation von Transmitter-Ausschüttung an Moosfaser-Terminalen, über die Beschreibung von Kurzzeit-Plastizität der postsynaptischen Moosfaser Antwortamplituden, zu einem Ausblick auf die potenziell funktionelle Rolle der Kurzzeit-Dynamik zum Aktionspotential Ausgang aus CA3 Pyramidenzellen. Anhand dieser Ergebnisse konnten wir einen kleinen Beitrag dazu leisten, die Funktionsweise und Relevanz des komplexen und ungewöhnlichen Systems der Moosfaser-Synapse besser zu verstehen.

Lebenslauf

Anja Gundlfinger, geboren am 11.06.1976 in Aachen

1982-1986	Gemeinschafts-Grundschule Laurensberg in Aachen
1986-1995	Anne-Frank Gymnasium in Aachen
1995	Abitur
1995-1998	Biologiestudium an der Rheinisch-Westfälischen Technischen Hochschule Aachen
1998	Vordiplom
1998	2-monatiger Studienaufenthalt an der University of California San Diego, CA, USA
1998-2002	Biologiestudium an der Albert-Ludwigs-Universität Freiburg
1999-2000	Studienjahr an der University of Massachusetts, Amherst, MA, USA
2002	Sommerschule Neuroinformatics an der University of Edinburgh, Scotland, UK
2002	Diplom in Biologie
seit 02 / 2003	Promotion in der Arbeitsgruppe von Prof. Dr. Dietmar Schmitz, Charité, Universitätsmedizin Berlin
2004	Sommerschule Methods in Computational Neuroscience am Marine Biological Laboratory, Woods Hole, MA, USA
seit 02 / 2005	PhD Fellow des Bernstein Center for Computational Neuroscience Berlin
2005	Sommerschule In-vivo Intracellular Recordings Techniques am Inter-University Institute, Eilat, Israel

Veröffentlichungen

Fachartikel

- Gundlfinger A, Kapfhammer JP, Kruse F, Leitges M, Metzger F (2003). Different regulation of Purkinje cell dendritic development in cerebellar slice cultures by protein kinase C alpha and beta. J Neurobiol, Oct;57(1):95-109
- Gundlfinger A, Schmitz D (2005). Inactivity Sets XL Synapses in Motion. Neuron (Preview), 47(5):623-625
- Gundlfinger A, Bischofberger J, Johenning FW, Torvinen M, Schmitz D, Breustedt J (2007). Adenosine modulates transmission at the hippocampal mossy fibre synapse via direct inhibition of presynaptic calcium channels. J Physiol, Jul 1; 582(Pt 1):263-77
- Gundlfinger A*, Leibold C*, Gebert K, Moisel M, Schmitz D, Kempter R (2007). Differential Modulation of Short-Term Synaptic Dynamics by Long-Term Potentiation at Mouse Hippocampal Mossy Fibre Synapses. J Physiol. Dec 15;585(Pt 3):853-65.
- Thurley K, Leibold C, Gundlfinger A, Schmitz D, Kempter R (2007). Phase Precession through Synaptic Facilitation. Neural Comput. Dec 17, Epub ahead of print.
- Leibold C*, Gundlfinger A*, Schmidt R., Thurley K, Schmitz D, Kempter R (2007). Temporal Compression Mediated by Short-Term Synaptic Plasticity. PNAS, In Revision.

Ausgewählte Tagungsbeiträge

- Gundlfinger A., Metzger F., Aertsen A., Egert U. (2002). Protein Kinase C Activity Modulates Neuronal Connectivity in Cerebellar Slice Cultures. Proc of the 3rd Forum of European Neuroscience. Paris, France.
- Gundlfinger A., Metzger F., Aertsen A., Egert U. (2003). Chronic Modulation of PKC-activity Affects Neuronal Connectivity in Cerebellar Slice Cultures. Proc of the 29th Göttingen Neurobiology Conference. Göttingen, Germany.
- Gundlfinger A, Breustedt J, Torvinen M, Schmitz D (2005). The Role of Adenosine at the Hippocampal Mossy Fiber Synapse. Proc of the 30th Göttingen Neurobiology Conference. Göttingen, Germany.
- Gundlfinger A, Leibold C, Kempter R, Schmitz D (2005). Interdependence of Short- and Long-Term Plasticity at the Hippocampal Mossy Fiber Synapse. 35th Annual Meeting of the Society for Neuroscience. Washington DC, USA.
- Gundlfinger A, Leibold C, Kempter R, Schmitz D (2005). Multidimensional Long-Term Potentiation at the Hippocampal Mossy Fiber Synapse. Annual Meeting of the Israeli Neuroscience Society. Eilat, Israel.

- Leibold C, Thurley K, Gundlfinger A, Schmidt R, Schmitz D, Kempter R (2006). One-Shot Learning of Behavioral Sequences Through Hippocampal Phase Precession: A Functional Hypthesis on Short-Term Synaptic Plasticity. Proc of the 3rd COSYNE Conference. Salt Lake City, USA.
- Gundlfinger A, Leibold C, Kempter R, Schmitz D (2007). Multidimensional Long-Term Potentiation at the Hippocampal Mossy Fiber Synapse. Proc of the 31st Göttingen Neurobiology Conference. Göttingen, Germany

Vorträge

- Autumn School of the Institute for Theoretical Biology Berlin on Learning and Memory, October 2004. Short- and Long-Term Plasticity at the Hippocampal Mossy Fiber Synapse.
- 1st Meeting of the Bernstein Centers for Computational Neuroscience, October 2005. Differential Modulation of Synaptic Dynamics by Long-Term Potentiation.
- Bernstein Seminar of the BCCN Freiburg, September 2007. The Hippocampal Mossy Fiber Synapse: Transmission, Modulation and Plasticity.

Eidesstattliche Erklärung

Hiermit erkläre ich, dass ich die vorliegende Dissertation selbständig verfasst und keine anderen als die angegebenen Hilfsmittel benutzt habe.

Berlin, 22. Oktober 2007

Acknowledgements

Completing this thesis has only be possible with the ongoing support, advice and encouragement of many people. First and foremost I want to thank DIETMAR SCHMITZ for giving me the opportunity to work in his research group, which I could witness growing from the very beginning. His scientific enthusiasm in combination with uncomparable experimental advice and knowledge of the literature was a constant source of inspiration.

In addition, I am most grateful to the following people for so many aspects of my work, without them these pages would not be the same:

- ANDREAS HERZ for being my "Doktorvater" and advisor in questions regarding Computational Neuroscience. Also for introducing me to Dietmar in the first place.
- JÖRG BREUSTEDT for our fruitful and smooth collaboration on the adenosine project and for critically reading parts of this thesis.
- JOSEF BISCHOFBERGER for contributing the single mossy fiber bouton recordings and giving me the opportunity to try out this elaborate technique myself.
- RICHARD KEMPTER and CHRISTIAN LEIBOLD for the very intensive collaboration on the projects involving theoretical investigations of mossy fiber synaptic transmission.
- All the members of the Schmitz Lab for the very special and warm working atmosphere, which I was lucky to experience and participate in. BENJAMIN ROST in particular for critically reading this thesis.
- HENRIKE BERKEFELD for reading and commenting on parts of this thesis and being a most valuable friend.
- My FAMILY.

References

Abbott, L. F. und Regehr, W. G. (2004): Synaptic computation, Nature (volume 431), issue 7010, pp. 796-803. URL: PM:15483601

Abbott, L. F.; Varela, J. A.; Sen, K. und Nelson, S. B. (1997): Synaptic depression and cortical gain control, Science (volume 275), issue 5297, pp. 220-224. URL: PM:8985017

Acsady, L.; Kamondi, A.; Sik, A.; Freund, T. und Buzsaki, G. (1998): GABAergic cells are the major postsynaptic targets of mossy fibers in the rat hippocampus, J.Neurosci. (volume 18), issue 9, pp. 3386-3403. URL: PM:9547246

Alle, H. und Geiger, J. R. (2007): GABAergic spill-over transmission onto hippocampal mossy fiber boutons, J.Neurosci. (volume 27), issue 4, pp. 942-950. URL: PM:17251436

Alonso, A. und Llinas, R. R. (1989): Subthreshold Na+-dependent theta-like rhythmicity in stellate cells of entorhinal cortex layer II, Nature (volume 342), issue 6246, pp. 175-177. URL: PM:2812013

Axmacher, N. und Miles, R. (2004): Intrinsic cellular currents and the temporal precision of EPSP-action potential coupling in CA1 pyramidal cells, J.Physiol (volume 555), issue Pt 3, pp. 713-725. URL: PM:14724200

Bean, B. P. (1989): Neurotransmitter inhibition of neuronal calcium currents by changes in channel voltage dependence, Nature (volume 340), issue 6229, pp. 153-156. URL: PM:2567963

Bear, M. F. und Malenka, R. C. (1994): Synaptic plasticity: LTP and LTD, Curr.Opin.Neurobiol. (volume 4), issue 3, pp. 389-399. URL: PM:7919934

Ben Ari, Y. (2002): Excitatory actions of gaba during development: the nature of the nurture, Nat.Rev.Neurosci. (volume 3), issue 9, pp. 728-739. URL: PM:12209121

Bi, G. Q. und Poo, M. M. (1998): Synaptic modifications in cultured hippocampal neurons: dependence on spike timing, synaptic strength, and postsynaptic cell type, J.Neurosci. (volume 18), issue 24, pp. 10464-10472. URL: PM:9852584

Bischofberger, J.; Engel, D.; Li, L.; Geiger, J. R. und Jonas, P. (2006): Patch-clamp recording from mossy fiber terminals in hippocampal slices, Nat.Protoc. (volume 1), issue 4, pp. 2075-2081. URL: PM:17487197

Bischofberger, J.; Geiger, J. R. und Jonas, P. (2002): Timing and efficacy of Ca2+ channel activation in hippocampal mossy fiber boutons, J.Neurosci. (volume 22), issue 24, pp. 10593-10602. URL: PM:12486151

Bland, B. H.; Konopacki, J. und Dyck, R. (2005): Heterogeneity among hippocampal pyramidal neurons revealed by their relation to theta-band oscillation and synchrony, Exp.Neurol. (volume 195), issue 2, pp. 458-474. URL: PM:16023636

Blatow, M.; Caputi, A.; Burnashev, N.; Monyer, H. und Rozov, A. (2003): Ca2+ buffer saturation underlies paired pulse facilitation in calbindin-D28k-containing terminals, Neuron (volume 38), issue 1, pp. 79-88. URL: PM:12691666

Bliss, T. V. und Collingridge, G. L. (1993): A synaptic model of memory: long-term potentiation in the hippocampus, Nature (volume 361), issue 6407, pp. 31-39. URL: PM:8421494

Bliss, T. V. und Lomo, T. (1973): Long-lasting potentiation of synaptic transmission in the dentate area of the anaesthetized rabbit following stimulation of the perforant path, J.Physiol (volume 232), issue 2, pp. 331-356. URL: PM:4727084

Breustedt, J.; Vogt, K. E.; Miller, R. J.; Nicoll, R. A. und Schmitz, D. (2003): Alpha1E-containing Ca2+ channels are involved in synaptic plasticity, Proc.Natl.Acad.Sci.U.S.A (volume 100), issue 21, pp. 12450-12455. URL: PM:14519849

Brown, S. P.; Safo, P. K. und Regehr, W. G. (2004): Endocannabinoids inhibit transmission at granule cell to Purkinje cell synapses by modulating three types of presynaptic calcium channels, J.Neurosci. (volume 24), issue 24, pp. 5623-5631. URL: PM:15201335

Buzsaki, G. (2002): Theta oscillations in the hippocampus, Neuron (volume 33), issue 3, pp. 325-340. URL: PM:11832222

Buzsaki, G. und Czeh, G. (1992): Physiological function of granule cells: a hypothesis, Epilepsy Res.Suppl (volume 7), pp. 281-290. URL: PM:1334667

Castillo, P. E.; Malenka, R. C. und Nicoll, R. A. (1997): Kainate receptors mediate a slow postsynaptic current in hippocampal CA3 neurons, Nature (volume 388), issue 6638, pp. 182-186. URL: PM:9217159

Castillo, P. E.; Weisskopf, M. G. und Nicoll, R. A. (1994): The role of Ca2+ channels in hippocampal mossy fiber synaptic transmission and long-term potentiation, Neuron (volume 12), issue 2, pp. 261-269. URL: PM:8110457

Castro-Alamancos, M. A. und Calcagnotto, M. E. (1999): Presynaptic long-term potentiation in corticothalamic synapses, J.Neurosci. (volume 19), issue 20, pp. 9090-9097. URL: PM:10516326

Catterall, W. A. (2000): Structure and regulation of voltage-gated Ca2+ channels, Annu.Rev.Cell Dev.Biol. (volume 16), pp. 521-555. URL: PM:11031246

Chung, S.; Li, X. und Nelson, S. B. (2002): Short-term depression at thalamocortical synapses contributes to rapid adaptation of cortical sensory responses in vivo, Neuron (volume 34), issue 3, pp. 437-446. URL: PM:11988174

Cunha, R. A.; Sebastiao, A. M. und Ribeiro, J. A. (1998): Inhibition by ATP of hippocampal synaptic transmission requires localized extracellular catabolism by ecto-nucleotidases into adenosine and channeling to adenosine A1 receptors, J.Neurosci. (volume 18), issue 6, pp. 1987-1995. URL: PM:9482785

Dan, Y. und Poo, M. M. (2004): Spike timing-dependent plasticity of neural circuits, Neuron (volume 44), issue 1, pp. 23-30. URL: PM:15450157

Dayan, S. und Abbott, L. F. (2001): Theoretical Neuroscience, 1. edition, The MIT Press.

Dekay, J. G.; Chang, T. C.; Mills, N.; Speed, H. E. und Dobrunz, L. E. (2006): Responses of excitatory hippocampal synapses to natural stimulus patterns reveal a decrease in short-term facilitation and increase in short-term depression during postnatal development, Hippocampus (volume 16), issue 1, pp. 66-79. URL: PM:16261553

Dietrich, D.; Kirschstein, T.; Kukley, M.; Pereverzev, A.; von der, Brelie C.; Schneider, T. und Beck, H. (2003): Functional specialization of presynaptic Cav2.3 Ca2+ channels, Neuron (volume 39), issue 3, pp. 483-496. URL: PM:12895422

Dittman, J. S.; Kreitzer, A. C. und Regehr, W. G. (2000): Interplay between facilitation, depression, and residual calcium at three presynaptic terminals, J.Neurosci. (volume 20), issue 4, pp. 1374-1385. URL: PM:10662828

Dittman, J. S. und Regehr, W. G. (1996): Contributions of calcium-dependent and calcium-independent mechanisms to presynaptic inhibition at a cerebellar synapse, J.Neurosci. (volume 16), issue 5, pp. 1623-1633. URL: PM:8774431

Dobrunz, L. E. und Stevens, C. F. (1997): Heterogeneity of release probability, facilitation, and depletion at central synapses, Neuron (volume 18), issue 6, pp. 995-1008. URL: PM:9208866

Dobrunz, L. E. und Stevens, C. F. (1999): Response of hippocampal synapses to natural stimulation patterns, Neuron (volume 22), issue 1, pp. 157-166. URL: PM:10027298

Dodge, F. A., Jr. und Rahamimoff, R. (1967): On the relationship between calcium concentration and the amplitude of the end-plate potential, J.Physiol (volume 189), issue 2, pp. 90P-92P. URL: PM:6034150

Dunwiddie, T. V. und Masino, S. A. (2001): The role and regulation of adenosine in the central nervous system, Annu.Rev.Neurosci. (volume 24), pp. 31-55. URL: PM:11283304

Ebersolt, C.; Premont, J.; Prochiantz, A.; Perez, M. und Bockaert, J. (1983): Inhibition of brain adenylate cyclase by A1 adenosine receptors: pharmacological characteristics and locations, Brain Res. (volume 267), issue 1, pp. 123-129. URL: PM:6305455

Engel, D. und Jonas, P. (2005): Presynaptic action potential amplification by voltage-gated Na+ channels in hippocampal mossy fiber boutons, Neuron (volume 45), issue 3, pp. 405-417. URL: PM:15694327

Faber, D. S. und Korn, H. (1991): Applicability of the coefficient of variation method for analyzing synaptic plasticity, Biophys.J. (volume 60), issue 5, pp. 1288-1294. URL: PM:1684726

FATT, P. und KATZ, B. (1952): Spontaneous subthreshold activity at motor nerve endings, J.Physiol (volume 117), issue 1, pp. 109-128. URL: PM:14946732

Fedele, D. E.; Gouder, N.; Guttinger, M.; Gabernet, L.; Scheurer, L.; Rulicke, T.; Crestani, F. und Boison, D. (2005): Astrogliosis in epilepsy leads to overexpression of adenosine kinase, resulting in seizure aggravation, Brain (volume 128), issue Pt 10, pp. 2383-2395. URL: PM:15930047

Forsythe, I. D. (1994): Direct patch recording from identified presynaptic terminals mediating glutamatergic EPSCs in the rat CNS, in vitro, J.Physiol (volume 479 (Pt 3)), pp. 381-387. URL: PM:7837096

Fortune, E. S. und Rose, G. J. (2001): Short-term synaptic plasticity as a temporal filter, Trends Neurosci. (volume 24), issue 7, pp. 381-385. URL: PM:11410267

Fredholm, B. B.; IJzerman, A. P.; Jacobson, K. A.; Klotz, K. N. und Linden, J. (2001): International Union of Pharmacology. XXV. Nomenclature and classification of adenosine receptors, Pharmacol.Rev. (volume 53), issue 4, pp. 527-552. URL: PM:11734617

Frerking, M. und Ohliger-Frerking, P. (2006): Functional consequences of presynaptic inhibition during behaviorally relevant activity, J.Neurophysiol. (volume 96), issue 4, pp. 2139-2143. URL: PM:16775209

Fricker, D. und Miles, R. (2000): EPSP amplification and the precision of spike timing in hippocampal neurons, Neuron (volume 28), issue 2, pp. 559-569. URL: PM:11144364

Galarreta, M. und Hestrin, S. (1998): Frequency-dependent synaptic depression and the balance of excitation and inhibition in the neocortex, Nat.Neurosci. (volume 1), issue 7, pp. 587-594. URL: PM:10196566

Gandhi, S. P. und Stevens, C. F. (2003): Three modes of synaptic vesicular recycling revealed by single-vesicle imaging, Nature (volume 423), issue 6940, pp. 607-613. URL: PM:12789331

Gasparini, S.; Kasyanov, A. M.; Pietrobon, D.; Voronin, L. L. und Cherubini, E. (2001): Presynaptic R-type calcium channels contribute to fast excitatory synaptic transmission in the rat hippocampus, J.Neurosci. (volume 21), issue 22, pp. 8715-8721. URL: PM:11698583

Geiger, J. R.; Bischofberger, J.; Vida, I.; Frobe, U.; Pfitzinger, S.; Weber, H. J.; Haverkampf, K. und Jonas, P. (2002): Patch-clamp recording in brain slices with improved slicer technology, Pflugers Arch. (volume 443), issue 3, pp. 491-501. URL: PM:11810221

Geiger, J. R. und Jonas, P. (2000): Dynamic control of presynaptic Ca(2+) inflow by fast-inactivating K(+) channels in hippocampal mossy fiber boutons, Neuron (volume 28), issue 3, pp. 927-939. URL: PM:11163277

Gerstner, W.; Kempter, R.; van Hemmen, J. L. und Wagner, H. (1996): A neuronal learning rule for sub-millisecond temporal coding, Nature (volume 383), issue 6595, pp. 76-81. URL: PM:8779718

Guillery, R. W. (2005): Observations of synaptic structures: origins of the neuron doctrine and its current status, Philos.Trans.R.Soc.Lond B Biol.Sci. (volume 360), issue 1458, pp. 1281-1307. URL: PM:16147523

Gulledge, A. T. und Stuart, G. J. (2003): Excitatory actions of GABA in the cortex, Neuron (volume 37), issue 2, pp. 299-309. URL: PM:12546824

Hallermann, S.; Pawlu, C.; Jonas, P. und Heckmann, M. (2003): A large pool of releasable vesicles in a cortical glutamatergic synapse, Proc.Natl.Acad.Sci.U.S.A (volume 100), issue 15, pp. 8975-8980. URL: PM:12815098

Hanson, J. E. und Jaeger, D. (2002): Short-term plasticity shapes the response to simulated normal and parkinsonian input patterns in the globus pallidus, J.Neurosci. (volume 22), issue 12, pp. 5164-5172. URL: PM:12077211

Harris, E. W. und Cotman, C. W. (1986): Long-term potentiation of guinea pig mossy fiber responses is not blocked by N-methyl D-aspartate antagonists, Neurosci.Lett. (volume 70), issue 1, pp. 132-137. URL: PM:3022192

Harris, K. D.; Henze, D. A.; Hirase, H.; Leinekugel, X.; Dragoi, G.; Czurko, A. und Buzsaki, G. (2002): Spike train dynamics predicts theta-related phase precession in hippocampal pyramidal cells, Nature (volume 417), issue 6890, pp. 738-741. URL: PM:12066184

Henze, D. A.; Urban, N. N. und Barrionuevo, G. (2000): The multifarious hippocampal mossy fiber pathway: a review, Neuroscience (volume 98), issue 3, pp. 407-427. URL: PM:10869836

Henze, D. A.; Wittner, L. und Buzsaki, G. (2002): Single granule cells reliably discharge targets in the hippocampal CA3 network in vivo, Nat.Neurosci. (volume 5), issue 8, pp. 790-795. URL: PM:12118256

Herlitze, S.; Garcia, D. E.; Mackie, K.; Hille, B.; Scheuer, T. und Catterall, W. A. (1996): Modulation of Ca2+ channels by G-protein beta gamma subunits, Nature (volume 380), issue 6571, pp. 258-262. URL: PM:8637576

Hille, B. (2001): Ion Channels of Excitable Membranes, 3rd Edition. edition, Sinauer Associates Inc.,U.S.; Auflage: 3rd (Juli 2001), ISBN: 978-0878933211.

Huang, Y. Y.; Kandel, E. R.; Varshavsky, L.; Brandon, E. P.; Qi, M.; Idzerda, R. L.; McKnight, G. S. und Bourtchouladze, R. (1995): A genetic test of the effects of mutations in PKA on mossy fiber LTP and its relation to spatial and contextual learning, Cell (volume 83), issue 7, pp. 1211-1222. URL: PM:8548807

Huang, Y. Y.; Li, X. C. und Kandel, E. R. (1994): cAMP contributes to mossy fiber LTP by initiating both a covalently mediated early phase and macromolecular synthesis-dependent late phase, Cell (volume 79), issue 1, pp. 69-79. URL: PM:7923379

Ikeda, S. R. und Dunlap, K. (1999): Voltage-dependent modulation of N-type calcium channels: role of G protein subunits, Adv.Second Messenger Phosphoprotein Res. (volume 33), pp. 131-151. URL: PM:10218117

Jeong, H. J.; Jang, I. S.; Nabekura, J. und Akaike, N. (2003): Adenosine A1 receptor-mediated presynaptic inhibition of GABAergic transmission in immature rat hippocampal CA1 neurons, J.Neurophysiol. (volume 89), issue 3, pp. 1214-1222. URL: PM:12626609

Jessell, T. M. und Kandel, E. R. (1993): Synaptic transmission: a bidirectional and self-modifiable form of cell-cell communication, Cell (volume 72 Suppl), pp. 1-30. URL: PM:8381334

Jonas, P.; Major, G. und Sakmann, B. (1993): Quantal components of unitary EPSCs at the mossy fibre synapse on CA3 pyramidal cells of rat hippocampus, J.Physiol (volume 472), pp. 615-663. URL: PM:7908327

Jung, M. W. und McNaughton, B. L. (1993): Spatial selectivity of unit activity in the hippocampal granular layer, Hippocampus (volume 3), issue 2, pp. 165-182. URL: PM:8353604

Kajikawa, Y.; Saitoh, N. und Takahashi, T. (2001): GTP-binding protein beta gamma subunits mediate presynaptic calcium current inhibition by GABA(B) receptor, Proc.Natl.Acad.Sci.U.S.A (volume 98), issue 14, pp. 8054-8058. URL: PM:11416164

Kakegawa, W.; Yamada, N.; Iino, M.; Kameyama, K.; Umeda, T.; Tsuzuki, K. und Ozawa, S. (2002): Postsynaptic expression of a new calcium pathway in hippocampal CA3 neurons and its influence on mossy fiber long-term potentiation, J.Neurosci. (volume 22), issue 11, pp. 4312-4320. URL: PM:12040036

Kamiya, H. und Ozawa, S. (1998): Kainate receptor-mediated inhibition of presynaptic Ca2+ influx and EPSP in area CA1 of the rat hippocampus, J.Physiol (volume 509 (Pt 3)), pp. 833-845. URL: PM:9596803

Kamiya, H. und Ozawa, S. (1999): Dual mechanism for presynaptic modulation by axonal metabotropic glutamate receptor at the mouse mossy fibre-CA3 synapse, J.Physiol (volume 518 (Pt 2)), pp. 497-506. URL: PM:10381595

Kamiya, H. und Yamamoto, C. (1997): Phorbol ester and forskolin suppress the presynaptic inhibitory action of group-II metabotropic glutamate receptor at rat hippocampal mossy fibre synapse, Neuroscience (volume 80), issue 1, pp. 89-94. URL: PM:9252223

Kamondi, A.; Acsady, L.; Wang, X. J. und Buzsaki, G. (1998): Theta oscillations in somata and dendrites of hippocampal pyramidal cells in vivo: activity-dependent phase-precession of action potentials, Hippocampus (volume 8), issue 3, pp. 244-261. URL: PM:9662139

Kepecs, A. und Lisman, J. (2003): Information encoding and computation with spikes and bursts, Network. (volume 14), issue 1, pp. 103-118. URL: PM:12613553

Klyachko, V. A. und Stevens, C. F. (2006a): Excitatory and Feed-Forward Inhibitory Hippocampal Synapses Work Synergistically as an Adaptive Filter of Natural Spike Trains, PLoS.Biol. (volume 4), issue 7, pp. e207. URL: PM:16774451

Klyachko, V. A. und Stevens, C. F. (2006b): Temperature-dependent shift of balance among the components of short-term plasticity in hippocampal synapses, J.Neurosci. (volume 26), issue 26, pp. 6945-6957. URL: PM:16807324

Kobayashi, K.; Manabe, T. und Takahashi, T. (1996): Presynaptic long-term depression at the hippocampal mossy fiber-CA3 synapse, Science (volume 273), issue 5275, pp. 648-650. URL: PM:8662556

Kukley, M.; Schwan, M.; Fredholm, B. B. und Dietrich, D. (2005): The role of extracellular adenosine in regulating mossy fiber synaptic plasticity, J.Neurosci. (volume 25), issue 11, pp. 2832-2837. URL: PM:15772343

Lauri, S. E.; Bortolotto, Z. A.; Bleakman, D.; Ornstein, P. L.; Lodge, D.; Isaac, J. T. und Collingridge, G. L. (2001): A critical role of a facilitatory presynaptic kainate receptor in mossy fiber LTP, Neuron (volume 32), issue 4, pp. 697-709. URL: PM:11719209

Lawrence, J. J. und McBain, C. J. (2003): Interneuron diversity series: containing the detonation--feedforward inhibition in the CA3 hippocampus, Trends Neurosci. (volume 26), issue 11, pp. 631-640. URL: PM:14585604

LeBeau, F. E.; El Manira, A. und Griller, S. (2005): Tuning the network: modulation of neuronal microcircuits in the spinal cord and hippocampus, Trends Neurosci. (volume 28), issue 10, pp. 552-561. URL: PM:16112755

Lee, A. K.; Manns, I. D.; Sakmann, B. und Brecht, M. (2006): Whole-cell recordings in freely moving rats, Neuron (volume 51), issue 4, pp. 399-407. URL: PM:16908406

Lei, S. und McBain, C. J. (2004): Two Loci of expression for long-term depression at hippocampal mossy fiber-interneuron synapses, J.Neurosci. (volume 24), issue 9, pp. 2112-2121. URL: PM:14999062

Lerma, J. (2003): Roles and rules of kainate receptors in synaptic transmission, Nat.Rev.Neurosci. (volume 4), issue 6, pp. 481-495. URL: PM:12778120

Lisman, J. E. (1997): Bursts as a unit of neural information: making unreliable synapses reliable, Trends Neurosci. (volume 20), issue 1, pp. 38-43. URL: PM:9004418

Maccaferri, G.; Toth, K. und McBain, C. J. (1998): Target-specific expression of presynaptic mossy fiber plasticity, Science (volume 279), issue 5355, pp. 1368-1370. URL: PM:9478900

Magee, J. C. (2001): Dendritic mechanisms of phase precession in hippocampal CA1 pyramidal neurons, J.Neurophysiol. (volume 86), issue 1, pp. 528-532. URL: PM:11431530

Malenka, R. C. und Bear, M. F. (2004): LTP and LTD: an embarrassment of riches, Neuron (volume 44), issue 1, pp. 5-21. URL: PM:15450156

Malenka, R. C. und Nicoll, R. A. (1999): Long-term potentiation--a decade of progress?, Science (volume 285), issue 5435, pp. 1870-1874. URL: PM:10489359

Marder, E. und Thirumalai, V. (2002): Cellular, synaptic and network effects of neuromodulation, Neural Netw. (volume 15), issue 4-6, pp. 479-493. URL: PM:12371506

Markram, H.; Lubke, J.; Frotscher, M. und Sakmann, B. (1997): Regulation of synaptic efficacy by coincidence of postsynaptic APs and EPSPs, Science (volume 275), issue 5297, pp. 213-215. URL: PM:8985014

Markram, H. und Tsodyks, M. (1996): Redistribution of synaptic efficacy between neocortical pyramidal neurons, Nature (volume 382), issue 6594, pp. 807-810. URL: PM:8752273

Martin, S. J.; Grimwood, P. D. und Morris, R. G. (2000): Synaptic plasticity and memory: an evaluation of the hypothesis, Annu.Rev.Neurosci. (volume 23), pp. 649-711. URL: PM:10845078

Mehta, M. R.; Lee, A. K. und Wilson, M. A. (2002): Role of experience and oscillations in transforming a rate code into a temporal code, Nature (volume 417), issue 6890, pp. 741-746. URL: PM:12066185

Mehta, M. R.; Quirk, M. C. und Wilson, M. A. (2000): Experience-dependent asymmetric shape of hippocampal receptive fields, Neuron (volume 25), issue 3, pp. 707-715. URL: PM:10774737

Meinrenken, C. J.; Borst, J. G. und Sakmann, B. (2002): Calcium secretion coupling at calyx of held governed by nonuniform channel-vesicle topography, J.Neurosci. (volume 22), issue 5, pp. 1648-1667. URL: PM:11880495

Melamed, O.; Gerstner, W.; Maass, W.; Tsodyks, M. und Markram, H. (2004): Coding and learning of behavioral sequences, Trends Neurosci. (volume 27), issue 1, pp. 11-14. URL: PM:14698603

Miller, V. M. und Best, P. J. (1980): Spatial correlates of hippocampal unit activity are altered by lesions of the fornix and endorhinal cortex, Brain Res. (volume 194), issue 2, pp. 311-323. URL: PM:7388617

Min, M. Y.; Rusakov, D. A. und Kullmann, D. M. (1998): Activation of AMPA, kainate, and metabotropic receptors at hippocampal mossy fiber synapses: role of glutamate diffusion, Neuron (volume 21), issue 3, pp. 561-570. URL: PM:9768842

Mintz, I. M.; Sabatini, B. L. und Regehr, W. G. (1995): Calcium control of transmitter release at a cerebellar synapse, Neuron (volume 15), issue 3, pp. 675-688. URL: PM:7546746

Miyazaki, K.; Ishizuka, T. und Yawo, H. (2005): Synapse-to-synapse variation of calcium channel subtype contributions in large mossy fiber terminals of mouse hippocampus, Neuroscience (volume 136), issue 4, pp. 1003-1014. URL: PM:16226383

Mizumori, S. J.; McNaughton, B. L. und Barnes, C. A. (1989): A comparison of supramammillary and medial septal influences on hippocampal field potentials and single-unit activity, J.Neurophysiol. (volume 61), issue 1, pp. 15-31. URL: PM:2493075

Moore, K. A.; Nicoll, R. A. und Schmitz, D. (2003): Adenosine gates synaptic plasticity at hippocampal mossy fiber synapses, Proc.Natl.Acad.Sci.U.S.A (volume 100), issue 24, pp. 14397-14402. URL: PM:14608033

Mori, M.; Abegg, M. H.; Gahwiler, B. H. und Gerber, U. (2004): A frequency-dependent switch from inhibition to excitation in a hippocampal unitary circuit, Nature (volume 431), issue 7007, pp. 453-456. URL: PM:15386013

Mori-Kawakami, F.; Kobayashi, K. und Takahashi, T. (2003): Developmental decrease in synaptic facilitation at the mouse hippocampal mossy fibre synapse, J.Physiol (volume 553), issue Pt 1, pp. 37-48. URL: PM:12963803

Nicoll, R. A. und Schmitz, D. (2005): Synaptic plasticity at hippocampal mossy fibre synapses, Nat.Rev.Neurosci. (volume 6), issue 11, pp. 863-876. URL: PM:16261180

O'Keefe, J. (1979): A review of the hippocampal place cells, Prog.Neurobiol. (volume 13), issue 4, pp. 419-439. URL: PM:396576

O'Keefe, J. und Dostrovsky, J. (1971): The hippocampus as a spatial map. Preliminary evidence from unit activity in the freely-moving rat, Brain Res. (volume 34), issue 1, pp. 171-175. URL: PM:5124915

O'Keefe, J. und Recce, M. L. (1993): Phase relationship between hippocampal place units and the EEG theta rhythm, Hippocampus (volume 3), issue 3, pp. 317-330. URL: PM:8353611

O'Regan, M. (2005): Adenosine and the regulation of cerebral blood flow, Neurol.Res. (volume 27), issue 2, pp. 175-181. URL: PM:15829181

Patil, P. G.; de Leon, M.; Reed, R. R.; Dubel, S.; Snutch, T. P. und Yue, D. T. (1996): Elementary events underlying voltage-dependent G-protein inhibition of N-type calcium channels, Biophys.J. (volume 71), issue 5, pp. 2509-2521. URL: PM:8913590

Phillis, J. W. und Wu, P. H. (1981): The role of adenosine and its nucleotides in central synaptic transmission, Prog.Neurobiol. (volume 16), issue 3-4, pp. 187-239. URL: PM:6170091

Pinsky, P. F. und Rinzel, J. (1994): Intrinsic and network rhythmogenesis in a reduced Traub model for CA3 neurons, J.Comput.Neurosci. (volume 1), issue 1-2, pp. 39-60. URL: PM:8792224

Porkka-Heiskanen, T.; Alanko, L.; Kalinchuk, A. und Stenberg, D. (2002): Adenosine and sleep, Sleep Med.Rev. (volume 6), issue 4, pp. 321-332. URL: PM:12531135

Porkka-Heiskanen, T.; Strecker, R. E.; Thakkar, M.; Bjorkum, A. A.; Greene, R. W. und McCarley, R. W. (1997): Adenosine: a mediator of the sleep-inducing effects of prolonged wakefulness, Science (volume 276), issue 5316, pp. 1265-1268. URL: PM:9157887

Pouille, F. und Scanziani, M. (2001): Enforcement of temporal fidelity in pyramidal cells by somatic feed-forward inhibition, Science (volume 293), issue 5532, pp. 1159-1163. URL: PM:11498596

Press WH; Flannery BP; Teukolsky SA und Vetterling WT (1992): Numerical Recipes in C: The Art of Scientific Computing, Cambridge University Press, New York.

Proctor, W. R. und Dunwiddie, T. V. (1987): Pre- and postsynaptic actions of adenosine in the in vitro rat hippocampus, Brain Res. (volume 426), issue 1, pp. 187-190. URL: PM:2825915

Qian, J. und Saggau, P. (1999): Modulation of transmitter release by action potential duration at the hippocampal CA3-CA1 synapse, J.Neurophysiol. (volume 81), issue 1, pp. 288-298. URL: PM:9914289

Regehr, W. G.; Delaney, K. R. und Tank, D. W. (1994): The role of presynaptic calcium in short-term enhancement at the hippocampal mossy fiber synapse, J.Neurosci. (volume 14), issue 2, pp. 523-537. URL: PM:8301352

Regehr, W. G. und Tank, D. W. (1991): Selective fura-2 loading of presynaptic terminals and nerve cell processes by local perfusion in mammalian brain slice, J.Neurosci.Methods (volume 37), issue 2, pp. 111-119. URL: PM:1881195

Reymann, K. G. und Frey, J. U. (2007): The late maintenance of hippocampal LTP: requirements, phases, 'synaptic tagging', 'late-associativity' and implications, Neuropharmacology (volume 52), issue 1, pp. 24-40. URL: PM:16919684

Rollenhagen, A. und Lubke, J. H. (2006): The morphology of excitatory central synapses: from structure to function, Cell Tissue Res. (volume 326), issue 2, pp. 221-237. URL: PM:16932936

Ruiz, A.; Fabian-Fine, R.; Scott, R.; Walker, M. C.; Rusakov, D. A. und Kullmann, D. M. (2003): GABAA receptors at hippocampal mossy fibers, Neuron (volume 39), issue 6, pp. 961-973. URL: PM:12971896

Rumpel, S.; LeDoux, J.; Zador, A. und Malinow, R. (2005): Postsynaptic receptor trafficking underlying a form of associative learning, Science (volume 308), issue 5718, pp. 83-88. URL: PM:15746389

Sabatini, B. L. und Regehr, W. G. (1997): Control of neurotransmitter release by presynaptic waveform at the granule cell to Purkinje cell synapse, J.Neurosci. (volume 17), issue 10, pp. 3425-3435. URL: PM:9133368

Sajikumar, S. und Frey, J. U. (2004): Late-associativity, synaptic tagging, and the role of dopamine during LTP and LTD, Neurobiol.Learn.Mem. (volume 82), issue 1, pp. 12-25. URL: PM:15183167

Salin, P. A.; Malenka, R. C. und Nicoll, R. A. (1996a): Cyclic AMP mediates a presynaptic form of LTP at cerebellar parallel fiber synapses, Neuron (volume 16), issue 4, pp. 797-803. URL: PM:8607997

Salin, P. A.; Scanziani, M.; Malenka, R. C. und Nicoll, R. A. (1996b): Distinct short-term plasticity at two excitatory synapses in the hippocampus, Proc.Natl.Acad.Sci.U.S.A (volume 93), issue 23, pp. 13304-13309. URL: PM:8917586

Sanabria, E. R.; Wozniak, K. M.; Slusher, B. S. und Keller, A. (2004): GCP II (NAALADase) inhibition suppresses mossy fiber-CA3 synaptic neurotransmission by a presynaptic mechanism, J.Neurophysiol. (volume 91), issue 1, pp. 182-193. URL: PM:12917384

Sara, Y.; Virmani, T.; Deak, F.; Liu, X. und Kavalali, E. T. (2005): An isolated pool of vesicles recycles at rest and drives spontaneous neurotransmission, Neuron (volume 45), issue 4, pp. 563-573. URL: PM:15721242

Scanziani, M.; Capogna, M.; Gahwiler, B. H. und Thompson, S. M. (1992): Presynaptic inhibition of miniature excitatory synaptic currents by baclofen and adenosine in the hippocampus, Neuron (volume 9), issue 5, pp. 919-927. URL: PM:1358131

Schmitz, D.; Mellor, J.; Breustedt, J. und Nicoll, R. A. (2003): Presynaptic kainate receptors impart an associative property to hippocampal mossy fiber long-term potentiation, Nat.Neurosci. (volume 6), issue 10, pp. 1058-1063. URL: PM:12947409

Schmitz, D.; Mellor, J. und Nicoll, R. A. (2001): Presynaptic kainate receptor mediation of frequency facilitation at hippocampal mossy fiber synapses, Science (volume 291), issue 5510, pp. 1972-1976. URL: PM:11239159

Scholz, K. P. und Miller, R. J. (1992): Inhibition of quantal transmitter release in the absence of calcium influx by a G protein-linked adenosine receptor at hippocampal synapses, Neuron (volume 8), issue 6, pp. 1139-1150. URL: PM:1351733

Sebastiao, A. M.; Cunha, R. A.; Cascalheira, J. F. und Ribeiro, J. A. (1999): Adenine nucleotides as inhibitors of synaptic transmission: role of localised ectonucleotidases, Prog.Brain Res. (volume 120), pp. 183-192. URL: PM:10550997

Selig, D. K.; Nicoll, R. A. und Malenka, R. C. (1999): Hippocampal long-term potentiation preserves the fidelity of postsynaptic responses to presynaptic bursts, J.Neurosci. (volume 19), issue 4, pp. 1236-1246. URL: PM:9952401

Sen, K.; Jorge-Rivera, J. C.; Marder, E. und Abbott, L. F. (1996): Decoding synapses, J.Neurosci. (volume 16), issue 19, pp. 6307-6318. URL: PM:8815910

Shepherd, G. M. und Erulkar, S. D. (1997): Centenary of the synapse: from Sherrington to the molecular biology of the synapse and beyond, Trends Neurosci. (volume 20), issue 9, pp. 385-392. URL: PM:9292963

Sherrington, C. S. (1897): The central nervous system, A text-book of physiology , 7th edition. edition, London: McMillan.

Skaggs, W. E.; McNaughton, B. L.; Wilson, M. A. und Barnes, C. A. (1996): Theta phase precession in hippocampal neuronal populations and the compression of temporal sequences, Hippocampus (volume 6), issue 2, pp. 149-172. URL: PM:8797016

Takahashi, T.; Kajikawa, Y. und Tsujimoto, T. (1998): G-Protein-coupled modulation of presynaptic calcium currents and transmitter release by a GABAB receptor, J.Neurosci. (volume 18), issue 9, pp. 3138-3146. URL: PM:9547222

Taschenberger, H.; Scheuss, V. und Neher, E. (2005): Release kinetics, quantal parameters and their modulation during short-term depression at a developing synapse in the rat CNS, J.Physiol (volume 568), issue Pt 2, pp. 513-537. URL: PM:16096340

Tong, G.; Malenka, R. C. und Nicoll, R. A. (1996): Long-term potentiation in cultures of single hippocampal granule cells: a presynaptic form of plasticity, Neuron (volume 16), issue 6, pp. 1147-1157. URL: PM:8663991

Toth, K. und McBain, C. J. (2000): Target-specific expression of pre- and postsynaptic mechanisms, J.Physiol (volume 525 Pt 1), pp. 41-51. URL: PM:10811723

Toth, K.; Suares, G.; Lawrence, J. J.; Philips-Tansey, E. und McBain, C. J. (2000): Differential mechanisms of transmission at three types of mossy fiber synapse, J.Neurosci. (volume 20), issue 22, pp. 8279-8289. URL: PM:11069934

Trussell, L. O. und Jackson, M. B. (1985): Adenosine-activated potassium conductance in cultured striatal neurons, Proc.Natl.Acad.Sci.U.S.A (volume 82), issue 14, pp. 4857-4861. URL: PM:2991897

Tsodyks, M. V. und Markram, H. (1997): The neural code between neocortical pyramidal neurons depends on neurotransmitter release probability, Proc.Natl.Acad.Sci.U.S.A (volume 94), issue 2, pp. 719-723. URL: PM:9012851

Tsodyks, M. V.; Skaggs, W. E.; Sejnowski, T. J. und McNaughton, B. L. (1996): Population dynamics and theta rhythm phase precession of hippocampal place cell firing: a spiking neuron model, Hippocampus (volume 6), issue 3, pp. 271-280. URL: PM:8841826

Tzounopoulos, T.; Janz, R.; Sudhof, T. C.; Nicoll, R. A. und Malenka, R. C. (1998): A role for cAMP in long-term depression at hippocampal mossy fiber synapses, Neuron (volume 21), issue 4, pp. 837-845. URL: PM:9808469

Umemiya, M. und Berger, A. J. (1994): Activation of adenosine A1 and A2 receptors differentially modulates calcium channels and glycinergic synaptic transmission in rat brainstem, Neuron (volume 13), issue 6, pp. 1439-1446. URL: PM:7993635

Urban, N. N.; Henze, D. A. und Barrionuevo, G. (2001): Revisiting the role of the hippocampal mossy fiber synapse, Hippocampus (volume 11), issue 4, pp. 408-417. URL: PM:11530845

van Calker, D.; Muller, M. und Hamprecht, B. (1978): Adenosine inhibits the accumulation of cyclic AMP in cultured brain cells, Nature (volume 276), issue 5690, pp. 839-841. URL: PM:214714

Varela, J. A.; Sen, K.; Gibson, J.; Fost, J.; Abbott, L. F. und Nelson, S. B. (1997): A quantitative description of short-term plasticity at excitatory synapses in layer 2/3 of rat primary visual cortex, J.Neurosci. (volume 17), issue 20, pp. 7926-7940. URL: PM:9315911

Wang, C. T.; Lu, J. C.; Bai, J.; Chang, P. Y.; Martin, T. F.; Chapman, E. R. und Jackson, M. B. (2003): Different domains of synaptotagmin control the choice between kiss-and-run and full fusion, Nature (volume 424), issue 6951, pp. 943-947. URL: PM:12931189

Weisskopf, M. G. und Nicoll, R. A. (1995): Presynaptic changes during mossy fibre LTP revealed by NMDA receptor-mediated synaptic responses, Nature (volume 376), issue 6537, pp. 256-259. URL: PM:7617037

Wu, L. G. und Saggau, P. (1997): Presynaptic inhibition of elicited neurotransmitter release, Trends Neurosci. (volume 20), issue 5, pp. 204-212. URL: PM:9141196

Xiang, Z. und Brown, T. H. (1998): Complex synaptic current waveforms evoked in hippocampal pyramidal neurons by extracellular stimulation of dentate gyrus, J.Neurophysiol. (volume 79), issue 5, pp. 2475-2484. URL: PM:9582221

Xu, J. und Wu, L. G. (2005): The decrease in the presynaptic calcium current is a major cause of short-term depression at a calyx-type synapse, Neuron (volume 46), issue 4, pp. 633-645. URL: PM:15944131

Yamamoto, C.; Higashima, M.; Sawada, S. und Kamiya, H. (1991): Quantal components of the synaptic potential induced in hippocampal neurons by activation of granule cells, and the effect of 2-amino-4-phosphonobutyric acid, Hippocampus (volume 1), issue 1, pp. 93-106. URL: PM:1669346

Yawo, H. und Chuhma, N. (1993): Preferential inhibition of omega-conotoxin-sensitive presynaptic Ca2+ channels by adenosine autoreceptors, Nature (volume 365), issue 6443, pp. 256-258. URL: PM:8396730

Yeckel, M. F.; Kapur, A. und Johnston, D. (1999): Multiple forms of LTP in hippocampal CA3 neurons use a common postsynaptic mechanism, Nat.Neurosci. (volume 2), issue 7, pp. 625-633. URL: PM:10404192

Yokoi, M.; Kobayashi, K.; Manabe, T.; Takahashi, T.; Sakaguchi, I.; Katsuura, G.; Shigemoto, R.; Ohishi, H.; Nomura, S.; Nakamura, K.; Nakao, K.; Katsuki, M. und Nakanishi, S. (1996): Impairment of hippocampal mossy fiber LTD in mice lacking mGluR2, Science (volume 273), issue 5275, pp. 645-647. URL: PM:8662555

Yoshino, M.; Sawada, S.; Yamamoto, C. und Kamiya, H. (1996): A metabotropic glutamate receptor agonist DCG-IV suppresses synaptic transmission at mossy fiber pathway of the guinea pig hippocampus, Neurosci.Lett. (volume 207), issue 1, pp. 70-72. URL: PM:8710213

Zalutsky, R. A. und Nicoll, R. A. (1990): Comparison of two forms of long-term potentiation in single hippocampal neurons, Science (volume 248), issue 4963, pp. 1619-1624. URL: PM:2114039

Zimmermann, H. und Braun, N. (1999): Ecto-nucleotidases--molecular structures, catalytic properties, and functional roles in the nervous system, Prog.Brain Res. (volume 120), pp. 371-385. URL: PM:10551012

Zucker, R. S. und Regehr, W. G. (2002): Short-term synaptic plasticity, Annu.Rev.Physiol (volume 64), pp. 355-405. URL: PM:11826273